The role of ROR alpha and CD34 in mucosal inflammation and fibrosis

by

Bernard Clement Lo

B.Sc., The University of British Columbia, 2010

A THESIS SUBMITTED IN PARTIAL FULFILLMENT OF

THE REQUIREMENTS FOR THE DEGREE OF

DOCTOR OF PHILOSOPHY

in

The Faculty of Graduate and Postdoctoral Studies

(Experimental Medicine)

THE UNIVERSITY OF BRITISH COLUMBIA

(Vancouver)

July 2017

Abstract

Fibrosis is the result of dysregulated tissue regeneration and is characterized by excessive accumulation of matrix proteins that become detrimental to tissue function. Type 2 immunity has long been associated with fibrotic scarring because of its role in wound healing and parasite-initiated tissue remodeling. Our objective was to examine two components of this inflammatory pathway that could potentially be modulated to limit fibrosis, namely RORα, a nuclear receptor required for ILC2 development, and CD34, a sialomucin involved in trafficking of eosinophils and mast cells to peripheral tissues.

Using a model of infection-induced chronic gut inflammation, we demonstrate that *Rora*-deficient mice are protected from fibrosis; infected intestinal tissues displayed diminished pathology and attenuated collagen deposition. Although *Rora* is known for its role in ILC2s, we found that *Salmonella*-induced fibrosis was independent of eosinophils, STAT6 signaling and Th2 cytokines arguing that ILC2s are dispensable in this disease model. Instead, we observed reduced levels of ILC3- and T cell-derived IL-17A and IL-22 in infected tissues. Furthermore, using $Rora^{sg/sg}/Rag1^{-/-}$ bone marrow chimeric mice, we found that restoring ILC function was sufficient to re-establish IL-17A and IL-22 production and a profibrotic phenotype. Our findings suggest that RORα-dependent ILC3 functions are pivotal in mediating gut fibrosis and they offer an avenue for therapeutic intervention in Crohn's-like diseases.

CD34 has been shown to drive lung inflammation and colitis by coordinating immune cell recruitment. However CD34 is also expressed by multiple non-hematopoietic subsets including endothelial and mesenchymal cells. To assess CD34 function in pulmonary repair, we induced lung injury by bleomycin administration. We found that $Cd34^{-/-}$ mice displayed severe weight loss and early mortality compared to WT controls. CD34-deficient animals developed severe interstitial edema and endothelial delamination, indicating impaired endothelial function. Chimeric $Cd34^{-/-}$ mice reconstituted with WT hematopoietic cells exhibited early mortality compared to WT mice reconstituted with $Cd34^{-/-}$ cells thus confirming this to be a non-hematopoietic defect. Lastly, CD34-deficient mice were more sensitive to lung damage caused by influenza infection, displaying greater weight loss and more extensive pulmonary

remodeling. These results suggest that CD34 plays a protective role in maintaining vascular integrity in response to lung damage.

Lay Summary

Tissue fibrosis defined by excessive scarring is the end result of dysregulated regeneration and chronic inflammation. Fibrotic degeneration can affect all organs and account for nearly half of all deaths in the developed world. In Crohn's disease, fibrotic strictures lead to bowel obstruction – a condition with no effective therapeutic options. Using an experimental mouse model of Inflammatory Bowel Disease, we find that deletion of ROR alpha protects animals from developing intestinal fibrosis. This effect is due to an inability of a subset of innate immune cells to produce soluble factors which promote disease. Survival during tissue injury requires a coordinated program of damage limitation and repair; we find that CD34 is required for maintaining blood vessel integrity in response to acute lung injury and influenza infection. In summary, the work presented in this thesis describes inflammatory and vascular processes that may be modulated to promote tissue regeneration while limiting fibrosis.

Preface

A version of chapter 2 has been published: Lo, B.C., Gold, M.J., Hughes, M.R., Antignano, F., Valdez, Y., Zaph, C., Harder, K.W., McNagny, K.M. (2016) The orphan nuclear receptor RORa and group 3 innate lymphoid cells drive fibrosis in a mouse model of Crohn's disease. *Science Immunology* (1) 3: e8864.

I designed and conducted the majority of the experiments, and co-wrote the manuscript with Dr. K. McNagny. Dr. M. Gold provided assistance with flow cytometry experiments and generated bone marrow transplant animals. Dr. M. Hughes maintained animal colonies and generated bone marrow transplant animals. Dr. F. Antignano and Dr. Y. Valdez provided intellectual content. Dr. C. Zaph and Dr. K. Harder edited the manuscript and provided valuable reagents. Dr. K.M. McNagny directed the research.

A version of chapter 3 has been submitted for peer review: Lo, B.C., Gold, M.J., Scheer, S., Hughes, M.R., DeBruin, E.J., Chu, F.S.F., Walker, D.C., Blanchet, M.-R., Perona-Wright, G., Zaph, C., McNagny, K. Loss of vascular CD34 results in increased sensitivity to lung injury.

I designed and conducted the majority of the experiments, and co-wrote the manuscript with Dr. K. McNagny. Dr. M. Gold provided assistance with experiments related to flow cytometry and respiratory mechanics, and generated bone marrow transplant animals. Dr. S. Scheer performed influenza infection experiments. Dr. M. Hughes maintained animal colonies, generated bone marrow transplant animals. Dr. E. DeBruin provided intellectual content. F. Chu prepared tissue sections and performed electron micrograph image acquisition and analysis. Dr. D. Walker analyzed electron micrographs and provided intellectual content. Dr. M.-R. Blanchet provided intellectual content. Dr. G. Perona-Wright edited the manuscript and provided valuable reagents. Dr. C. Zaph provided valuable reagents. Dr. K. McNagny directed the research.

All animal experiments presented in this thesis were performed in accordance with the UBC animal care guidelines; certificate numbers include A13-0078, A11-0096, and A11-0347.

Table of Contents

List of Figures

List of Abbreviations

APC	Antigen presenting cell
BASC	Bronchoalveolar stem cell
BAL	Bronchoalveolar lavage
BCR	B cell receptor
BLM	Bleomycin
BMT	Bone marrow transplant
CBA	Cytometric bead array
CD	Crohn's disease
CFU	Colony forming unity
ChILP	Common helper-like innate lymphoid progenitor
CILP	Common innate lymphoid progenitor
CLP	Common lymphoid progenitor
CTGF	Connective tissue growth factor
CTL	Cytotoxic T cell
DAPI	4',6-Diamidnino-2-phenylindole
DC	Dendritic cell
DSS	Dextran sodium sulfate
ECM	Extracellular matrix
ELISA	Enzyme linked immunosorbent assay
e.t.	Endotracheally
FAP	Fibroadipogenic progenitor
GALT	Gut-associated lymphoid tissue
GI	Gastrointestinal
GM-CSF	Granulocyte-macrophage colony-stimulating factor
GWAS	Genome-wide association studies
H&E	Hematoxylin and eosin
HDM	House dust mite
HEV	High endothelial venules
HSC	Hematopoietic stem cell

IBD	Inflammatory bowel disease
ID2	Inhibitor of DNA binding 2
IGF	Insulin growth factor
i.v.	Intravenous
IFN	Interferon
IPF	Idiopathic pulmonary fibrosis
Ig	Immunoglobulin
ILC	Innate lymphoid cell
KLRG	Killer cell lectlin-like receptor subfamily G member
Krt	Keratin
LBD	Ligand binding domain
Lin	Lineage
LN	Lymph node
LTi	Lymphoid tissue inducer
M	Microfold
MCP	Monocyte chemoattractant protein
MHC	Major histocompatibility complex
MT	Masson's Tricrhome
NG2	Neural glial antigen 2
NK	Natural killer
NOD	Nucleotide-binding oligomerization domain-containing protein
PAMP	Pathogen associated molecular pattern
PBS	Phosphate buffered saline
PDGF	Platelet derived growth factor
PLZF	Promyelocytic leukemia zinc finger
PMA	Phorbol 12-myristate 13-acetate
PRR	Pattern recognition receptor
qPCR	Quantitative PCR
RAG	Recombination activating gene
Reg	Regenerating islet-derived protein
ROR	Retinoic acid receptor-related orphan receptor

RORE	ROR response element
SMA	Smooth muscle actin
STAT	Signal transducer and activator of transcription
TCR	T cell receptor
TEM	Transmission electron microscopy
TGF	Tumor growth factor
Th	T helper
TLR	Toll-like receptor
Treg	Regulatory T cell
TNF	Tumor necrosis factor
UC	Ulcerative colitis
UIP	Usual interstitial penumonia
WT	Wildtype

Acknowledgements

I am sincerely grateful to my supervisor Dr. K. McNagny for his mentorship and encouragement. I would also like to thank my supervisory committee members, Drs. F. Rossi, M. Underhill, and B. Vallance, for their time and guidance. Many thanks to Dr. M. Hughes, Dr. M. Gold, Dr. M. Lopez, Dr. E. Debruin, K. Snyder, D. Canals, J. Cait, I. Refeali, Dr. F. Antignano, Dr. S. Scheer, Dr. H. S. Seo, Dr. H. Soliman, F. Chu, Dr. D. Walker, Dr. G. Perona-Wright, Dr. Colby Zaph, Dr. K. Harder, Dr. Y. Valdez, Dr. H. Yu, I. Barta, T. Murakami, M. Williams, R. Dhesi, L. Rollins, A. Johnson, J. Wong, R. Vander werff, H. Younesy, K. Ranta, W. Yuan, M. Prychyna, M. Cowan, Dr. N. Ford, A. Wong, Dr. G. Sun, M. Harkness, Dr. D. Martin and Dr. W. Kum.

This thesis is dedicated to my parents.

Chapter 1.

Introduction

1.1 The immune system

Immunity represents the complex network of effector cells and processes that protect our bodies from infectious agents. They function co-operatively to orchestrate context appropriate responses that can be broadly characterized as innate or adaptive. Innate immune responses are the first line of defense against pathogens; it is mediated by a physical barrier and leukocytes, which include macrophages, dendritic cells, neutrophils, eosinophils, basophils and mast cells (*1*). Innate immunity relies on germline encoded pattern recognition receptors (PRRs) which recognize simple molecular signatures known as pathogen-associated molecular patterns (PAMPs); these are unique to microorganisms and not found on host cells, invariant within broad microbial classes, and are essential for the microorganism's survival (*1, 2*). In response to PRR activation, innate immune cells limit the infection by phagocytizing and eliminating the pathogen, producing signals to amplify the immune responses, and directing the adaptive immune cells (*1, 2*).

Adaptive immunity involves antigen specific T-cell and B-cell receptors (TCR, BCR); these receptors are encoded by genes assembled by recombination activating gene (RAG)-mediated somatic recombination, which produces a diverse repertoire of antigen-specific receptors (*3*). While B cell immunoglobulin-type BCRs recognize intact antigens, TCRs recognize short peptide fragments of antigen presented by major histocompatibility complex (HMC) molecule-bound peptides presented on antigen presenting cells (APCs) (*4*). T cells are responsible for effector cell functions and can be

classified as cytotoxic T cells (CTL), which directly eliminate infected cells, and T helper (Th) cells, which produce signals that amplify specific immune responses and activate other effector cell types (*5*). In contrast, B cells are responsible for humoural immunity; upon BCR activation, B cells differentiate into plasma cells, which produce antibodies specific to the antigen recognized by the BCR (*6*).

Until recently, natural killer (NK) and lymphoid tissue inducer (LTi) cells were the only recognized common lymphoid progenitor (CLP)-derived cells that lack antigen receptors; it is now clear that these cells are members of a broader family of innate lymphoid cells (ILCs) that respond rapidly to stress signals following tissue injury or infection by producing cytokines classically associated with $CD4^+$ Th cells (*7*). ILCs together with invariant NKT, γδ T cells, and memory T cells are categorized as tissue-resident lymphocytes that can populate non-lymphoid tissues such as barrier surfaces where they are maintained locally; they function as sentinel cells responding quickly to infection or damage to preserve tissue integrity (*8, 9*).

The majority of cells involved in immunity arise from hematopoietic stem cells (HSCs) of the bone marrow (BM). However, some myeloid lineage subsets, including microglia, Langerhans cells, Kupffer cells, and alveolar macrophages, arise independently from the yolk sac prior to the emergence of fetal liver HSCs and colonize peripheral tissues before birth (*10, 11*). These tissue-resident myeloid cells originate from an erythro-myeloid progenitor and are self-sustained and can renew independently of BM-derived hematopoiesis (*10*).

1.2 Immunity at barrier surfaces

Mucosal tissues such as the gastrointestinal and respiratory tracts are in direct contact with the external environment and are therefore continuously exposed to potentially harmful agents. Moreover, these barrier surfaces are colonized by diverse commensal microbial communities termed microbiota that exist symbiotically with the host. The regulation of immune responses at barrier sites are complex due to the nature of maintaining host tolerance to benign or innocuous microbes and antigens while also retaining the capacity to effectively coordinate effector responses to eliminate invading pathogens. Perturbations in this balance have been associated with numerous inflammatory diseases or increased susceptibility to infections.

In the intestinal tract, the epithelia constitutes the interface between host and the external environment (*12*). The single layered mucosal epithelium is critical for maintaining the barrier that separates pathogenic and commensal microbes from the lamina propria; this is bolstered by epithelial cell secretion of broad-spectrum anti-microbial peptides while specialized epithelial cells (termed goblet cells) produce mucins that make up the mucus layer lining the apical surface (*12*). Furthermore, epithelial microfold (M) cells that are associated with gut-associated lymphoid tissues (GALTs) can sample microbes and antigens of the lumen and deliver them to dendritic cells (DCs) for antigen presentation at sites of immune induction (*12*). DCs can also acquire antigen by directly sampling luminal contents through projections that penetrate the epithelial layer (*13*). Like GALTs (which include the Peyer's patches, cecal patch, and lymphoid follicles), mesenteric lymph nodes (mLNs) are organized structures that compartmentalize lymphocyte subsets and regulate their exposure to luminal contents

(*14*). Tolerogenic DCs present in lymphoid structures can interact with lymphocytes to promote the differentiation of FoxP3$^+$ Tregs in the presence of TGF-β and retinoic acid to maintain a non-inflammatory state (*15*). Under homeostatic conditions, these IL-10$^+$ Th cells are highly enriched in GALTs suggesting that T cell mediated immunosuppression is the default pathway at steady state (*16*). Antigen-experienced Th1 and Th17 cells may also be detected in the intestinal lamina propria while Th2 cells are rare or nonexistent (*17*). RORγt$^+$ T cells and ILC3s are important sources of IL-22, which promotes the production of epithelium-derived antimicrobial peptides and supports barrier integrity (*12*). Plasma cell-derived IgA also plays an important role in the containment of the microbiota and maintenance of intestinal homeostasis (*18*).

Following infection, host immunity is initiated by the activation of PRRs (such as cell surface bound toll-like receptors and cytosolic NOD-like receptors) and chemokine and pro-inflammatory cytokine release. Macrophages, dendritic cells, neutrophils, eosinophils and basophils are recruited to the site of infection and function in concert with ILCs and the cells of the adaptive immune system to mount an immune response. ILCs respond rapidly to danger signals elaborated by epithelial, stromal, and myeloid cells while CD4$^+$ Th cell activation is initiated by TCR ligation and subsequent responses dictated by the cytokine profile of the microenvironment (**Fig. 1.1**) (*19*). ILCs, in particular, can influence the adaptive immune response directly through the production of soluble factors and contact-dependent interactions or indirectly though the modulation of other accessory cells (*20*). For example, antigen-presenting ILC3s can induce apoptosis of commensal-specific effector CD4$^+$ Th cells to limit dysregulated T-cell-mediated pathologies (*21*). In lung allergen recall responses, ILC2s are required for the stimulation

of DCs and the subsequent recruitment of Th2 memory cells (*22*). Alternatively, it has been proposed that $CD4^+$ Th cells may function as antigen-specific sensors that can activate ILCs, which in turn direct the inflammatory milieu (*19*).

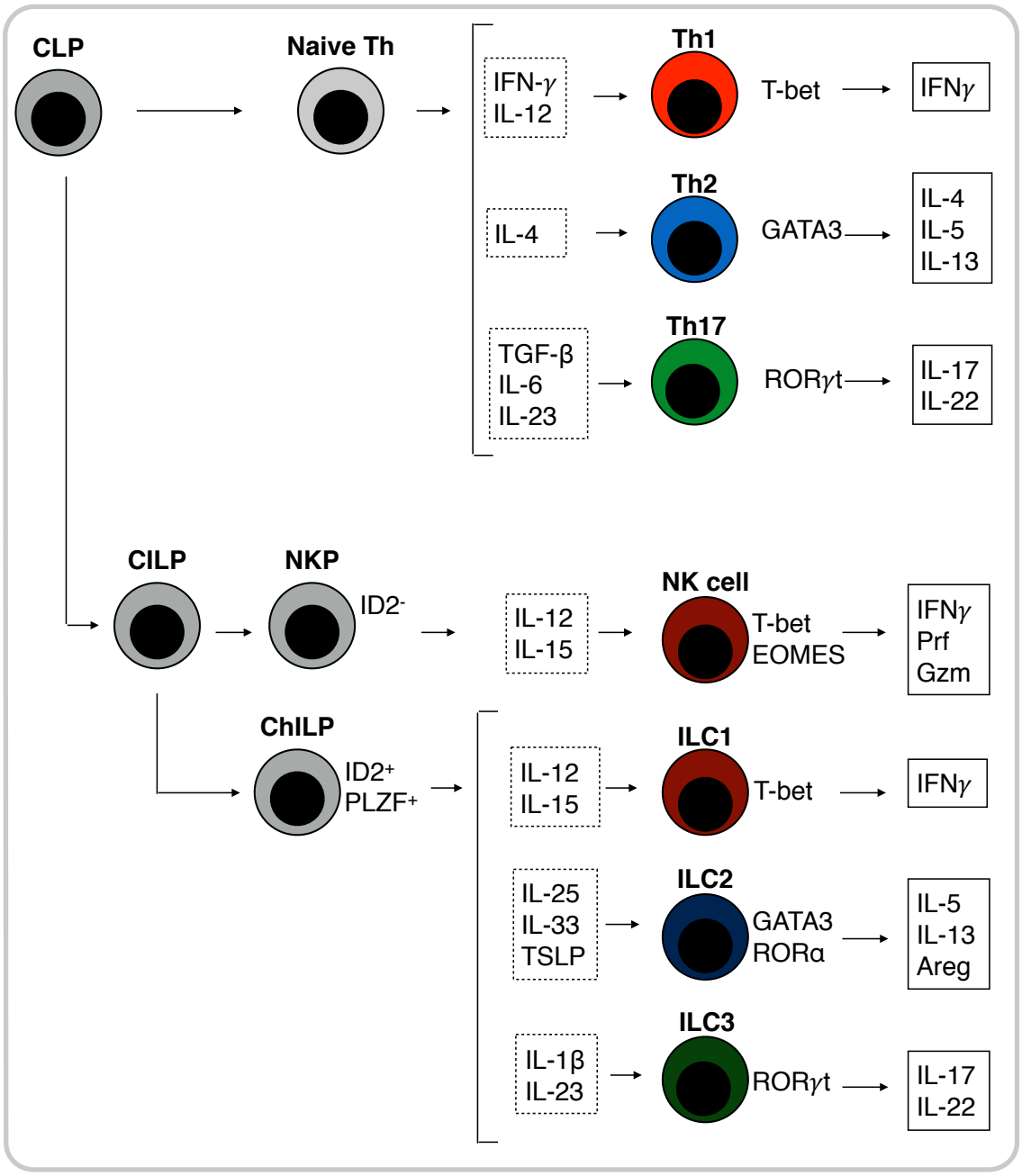

Figure 1.1. Development and classification of lymphocyte subsets. Bone marrow-derived common lymphoid progenitors (CLPs) give rise to T and B cell precursors, NK precursors (NKPs), and helper-like ILC precursors (ChILPs) (*7, 19*). T cell precursors migrate to the thymus where they undergo selection and subsequent priming in secondary lymphoid tissues whereby recognition of an antigen presented via peptide-MHC complex by APCs and polarizing cytokines direct differentiation; lineage maintenance is reinforced by expression of key transcription factors as T cells acquire the ability to

produce signature cytokines (*5*). The majority of ILCs originate from $ID2^+$ $PLFZ^+$ ChILPs; in contrast, LTi cells are derived from a distinct $ID2^+$ $PLZF^-$ progenitor population (*23*). NKP and ChILP lineage commitment is not completely understood although various suppression pathways of T and B cell-promoting programs mediated by ID2, NFIL3, and GATA3 have been proposed (*24-26*). ILCs are highly enriched in peripheral tissues and have the capacity to produce cytokines in response to their local microenvironmental cues, and together with $CD4^+$ Th cells, co-ordinate context appropriate responses. Type 1 immune cells are involved in the protection against intracellular pathogens and anti-tumour immunity. IL-12 derived from antigen presenting DCs direct the development of Th1 cells while NK and ILC1s can rapidly secrete IFNγ in response to IL-12 and IL-18 (*27, 28*). Type 2 immunity is critical for the expulsion of extracellular parasites such as Helminth infections, but are also involved in asthma and other allergic diseases. Type 2 immune responses are initiated at barrier sites where parasites or allergens can trigger the innate cell release of alarmins including TSLP, IL-25, and IL-33 (*29*). ILC2s respond directly to these factors, while DCs present antigen and secrete cytokines that direct Th2 cell differentiation (*20, 29, 30*). Th2- or ILC2-dervied cytokines have several effects. IL-4 can promote B cell class switching to IgE production; IgE immune complexes can activate mast cells by inducing crosslinking of Fc receptors (FcεR1) causing degranulation and the release of proteases and soluble factors. In addition, IL-5 and IL-13 promote eosinophilia, mucus production, goblet cell hyperplasia, and smooth muscle contraction (*29*). Finally, Th17 cells and ILC3s are critical for host defense responses against extracellular bacterial pathogens such as *Citrobacter rodentium* and *Klebsiella pneumoniae*, or fungi including *Candida albicans*; Th17 cells and ILC3s are also important regulators of tissue homeostasis (*31*). Th17 differentiation involves IL-6, TGF-β1, and IL-23 while ILC3s can respond to phagocytic cell derived IL-1β and IL-23 (*20, 31*). Th17 cell and ILC3 cytokines including IL-17, IL-22, and GM-CSF are involved in the recruitment of innate effector cells, secretion of antimicrobial peptides, or maintenance of mucosal barrier (*20*).

1.3 Inflammatory bowel disease

Ulcerative colitis (UC) and Crohn's disease (CD) are the two major forms of IBD and are characterized as chronic and relapsing inflammatory disorders of the gastrointestinal tract (*32, 33*). These disorders have a major impact on the quality of life of patients; symptoms of IBD include abdominal pain, diarrhea, nausea, weight loss, fever, and fatigue (*34*). Recent studies have identified genetic and environmental factors that contribute to disease pathogenesis; intriguingly, based on the genetic loci linked to disease, the high risk factors appear to be linked to genes that alter integrity of the epithelial barrier, likely resulting in the translocation or oversampling of luminal antigens (*35*). The consequences of these polymorphisms are thought to initiate an aberrant inflammatory response to the commensal flora mediated by intestinal immune cells (*35*). Features of IBD-associated complications may extend to sites beyond the GI tract affecting various organs including joints, skin, and liver (*32, 33*). Hallmarks of UC include severe and diffuse inflammation typically localized in the colon (*32*). Disease pathology affects the mucosa and submucosa of the bowel resulting in superficial mucosal ulcerations (*32*). In contrast, CD can affect any part of the GI tract although evidence of disease is commonly found in the colon and distal ileum (*33*). Moreover, the inflammation in CD is transmural, affecting all layers of the bowel wall (*33*).

As stated above, functionally, the IBD susceptibility genes that have been identified suggest that dysregulation of the epithelial barrier or immunity are critical contributors to disease progression (*36*). Mutations in nucleotide oligomerization domain 2 (NOD2) found to be associated with increased susceptibility to CD; this highlights a link between altered innate immune detection of bacterial components and the disease (*37*). More recent genome-wide association studies (GWAS) have revealed additional

pathways potentially involved in the pathogenesis of IBD including genetic variations in: *STAT1*-, *NKX2-3*-, *IL2RA*-, and *IL23R*-dependent pathways linked to adaptive immunity, *MUC1*, *MUC19*, and *PTGER4* in intestinal barrier maintenance, and *ATG16L*-mediated autophagy (*38-40*). While these population-based genetics studies have enhanced our understanding of IBD, susceptibility alleles alone are likely insufficient to solely initiate and/or sustain chronic disease (*34*). Other environmental factors including alterations in gut microbiome composition and a reduction in diversity have been associated with intestinal inflammation; however, it is unclear whether gut dysbiosis precedes or is the consequence of dysregulated immune responses (*34*).

1.4 Mouse models of IBD

Although the etiology of IBD remains unclear, our understanding of the pathogenesis of the disease has been greatly enhanced by experimental mouse models of intestinal inflammation (*41, 42*). These models individually do not fully represent the complexity of the human disease, but they are valuable for elucidating pathophysiological pathways that could be relevant to IBD and validating possible therapeutic strategies (*41, 42*). These mouse models typically rely on the initiation of inflammation by chemical induction or infection, immune cell transfer, or genetic manipulation; moreover these strategies often involve perturbations in epithelial integrity or modulation of innate or adaptive immunity (**Table 1.1**) (*41*).

Table 1.1. A brief summary of mouse models of intestinal inflammation.

Model	*Description*
Dextran sodium sulfate (DSS)	Induces damage to gut epithelia leading to increased permeability of barrier and over-exposure to commensal bacteria. Results in acute colitis with UC-like features that is largely independent of adaptive immunity; chronic exposure to DSS can lead to fibrosis. (*43-45*)
Trinitrobenzene sulfonic acid (TNBS)	Renders gut antigens immunogenic, also requires ethanol for the disruption of epithelial barrier. $CD4^+$ T cells play a key role in chronic immunopathology; sustained exposure to TNBS results in defined fibrotic features that resemble CD. (*44, 46*)
Oxazolone	Causes severe weight loss, diarrhea, and loss of goblet cells; pathology is associated with Th2 cytokines as inhibition of IL-4 and IL-13 improves disease outcomes. (*44*)
Citrobacter rodentium	Oral infection results in acute and mild colitis of the colon and cecum; associated with crypt hyperplasia and loss of goblet cells. ILC3s are essential in providing host protection in the absence of functional adaptive immune cells. (*42, 47, 48*)
Salmonella Typhimurium	Treatment with streptomycin before oral infection enhances intestinal colonization resulting in severe cecitis. Infection with *S.* Typhimurium SL1344 leads to inflammation, neutrophil influx, tissue edema and high mortality rates in genetically susceptible host strains such as C57BL/6 mice. Host protection is also mediated by IFNγ producing ILCs. Infection by the Δ*aroA* mutant vaccine strain results in chronic Th1/Th17-mediated fibrosis. (*49-53*)
Adherent-invasive *Eschericia coli*	Chronic infection with AIEC induces inflammation of the ileum and colon, and the upregulation of pro-fibrotic cytokines and collagen production in the gut; $CD8^+$ T cells enhance pathogen clearance and resolution of fibrosis. (*54*)

Model	*Description*
Helicobacter hepaticus	Induces IL-23-mediated innate colitis that is IL-17- and IFNγ-dependent. *H. hepaticus* infection also drives Th1 dependent colitis in *Il10*$^{-/-}$ mice, or may be used in conjunction with 2-azoxymethane (AOM) to induce colon cancer. (*55-57*)
T cell transfer	Adoptive transfer of CD45RB^{high} T cells into immunocompromised (including *Rag1*$^{-/-}$) hosts leads to wasting disease and colitis. Pathology is the result of donor-derived T cell immunity against host antigens and commensal microbiota in the absence of Treg cells. (*58-60*)
Anti-CD40 antibody	Treatment with agonistic antibodies against CD40 (expressed by DCs) in *Rag1*$^{-/-}$ mice results in IL-12 and IL-23 driven colitis; ILC3s and GM-CSF can also promote pathology in this model by the recruitment of myeloid cells. (*48, 61*)
Il10$^{-/-}$	Genetic ablation of the immunosuppressive cytokine IL-10 results in chronic enterocolitis; pathology is microbiota driven and the consequence of an unrestrained Th1 response. (*62-64*)
TGF-β1 gene transfer	Rectal administration of adenoviral vector of biologically active TGF-β1 leads to colonic inflammation, myofibroblast activation, and severe fibrosis. (*65*)

1.5 *Salmonella*-driven intestinal inflammation

Salmonella enterica serovars are intestinal pathogens that can infect humans and mice; after ingestion, *Salmonella* colonize the gut by direct invasion of epithelia, M cells, or antigen presenting cells (*66*). Unlike infection by *Citrobacter rodentium*, a non-invasive mouse pathogen belonging to the class of attaching and effacing (A/E) bacteria, mice infected orally with *S.* Typhimurium results in the colonization primarily of systemic sites such as the spleen and mesenteric lymph nodes with relatively low

abundance in the GI tract (*66*). However, pretreatment of mice with streptomycin enhances the efficiency of *Salmonella* colonization of the gut by diminishing the host protective effects of the normal microbiota (*49*). Pathological features of this model include the disruption or ulceration of the epithelial barrier, granulocyte recruitment, and severe edema (*49*). Alternatively, infection with the vaccine grade *S.* Typhimurium Δ*aroA* mutant, which has a defect in the biosynthesis of aromatic amino acids, leads to chronic infection of the cecum and colon that persists up to day 40 after infection (*51*). This leads to a Th1 and Th17 inflammatory response, extensive tissue remodeling, and collagen deposition. Tissue pathology is associated with elevated levels of pro-fibrotic factor such as TGF-β1, CTGF, and IGF (*51*). The transmural fibrotic scarring reported in this model is reminiscent of stricture formations often observed in CD. Importantly this *S.* Tymphimurium Δ*aroA* infection model is a useful system for the study of fibrotic responses in mutant mice maintained on a C57/BL6 background. The C57/BL6 strain is extremely sensitive to *S.* Typhiumurim SL1344 infection due to a loss-of-function mutation in the gene encoding the natural resistance-associated macrophage protein (NRAMP)-1 (*50, 52*). Thus the attenuated Δ*aroA* mutant permits persistent infection without the C57/BL6 host death associated with the SL1344 strain.

1.6 Fibrosis as a complication of IBD

A major complication of CD is the dysregulated and excessive deposition of extracellular matrix (ECM) including collagen throughout all layers of the mucosal tissue (*33, 67*). Although the GI tract has a relatively high capacity for regeneration, fibrotic scarring can arise due to unresolved wound healing responses that are associated with

chronic and severe inflammation (**Fig. 1.2**) (*68, 69*). In CD, this results in deleterious effects on tissue architecture leading to significant organ impairment (*69, 70*). The transmural nature of the inflammation observed in CD ultimately precedes the thickening of the bowel wall associated with symptomatic stenosis or stricture formation (*69*). About a third of CD patients require intestinal resection for this complication (*70*). There are no effective anti-fibrotic therapies in IBD and, unfortunately, the use of immunosuppresants such as azathioprine or anti-TNFα biologics have no impact or only modestly reduce the requirement of surgical interventions for fibrosis (*67, 71*). Type I collagen is the primary ECM component in normal intestinal tissue while strictured tissues have an increase in total collagen as well as elevated percentages of types III and V collagen (*67*).

While fibrosis is thought be the consequence of chronic inflammation, the origins of the matrix producing cells have been the subject of extensive controversy. The prevailing view is that cells of mesenchymal origin such as fibroblasts and pericytes are the primary cellular sources of ECM in fibrotic scarring (*69, 72*). However, in response to pro-inflammatory cytokines and TGF-β1, there are reports that epithelial or endothelial cells may undergo transdifferentiation to become fibroblast-like ECM producing cells (*73, 74*). Moreover, studies have also suggested that $CD45^+$ BM-derived circulating cells, termed fibrocytes, may also contribute to matrix deposition.

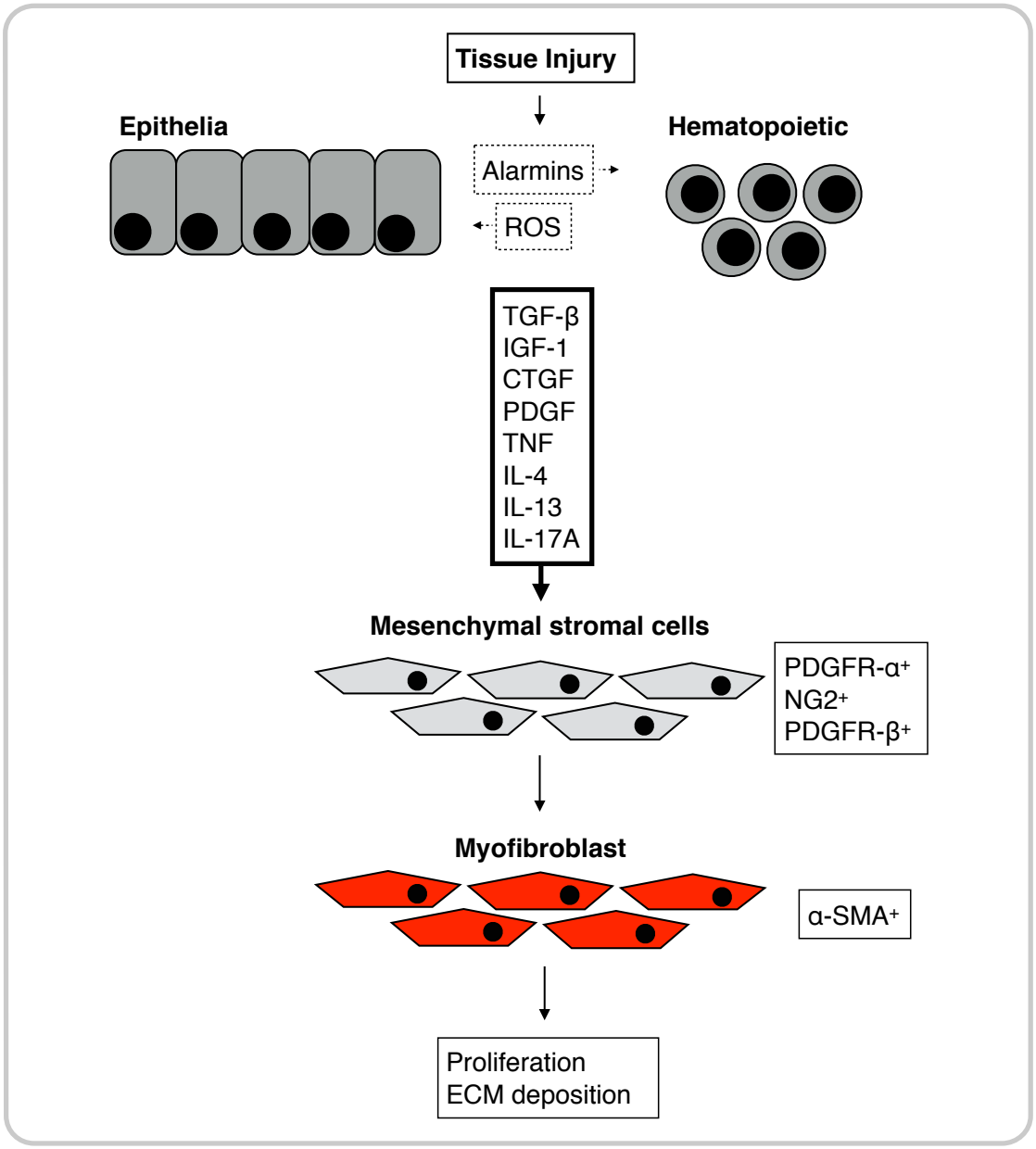

Figure 1.2. Cellular and molecular factors in tissue fibrosis. Fibrosis is often viewed as the consequence of dysregulated regeneration following tissue injury. When epithelial or endothelial cells are damaged by infection or irritants, platelets are activated and soluble factors are released, which initiate an inflammatory response; if unresolved, functional cells are replaced with excessive scar tissue eventually leading to organ failure (*72, 75*). At the center of this degenerative process are myofibroblasts: the primary ECM-producing cell type (*75*). Myofibroblasts are derived mainly from a population of tissue-resident mesenchymal cells that include PDGFRα^{+} fibroblasts and NG2^{+}

PDGFRβ^{+} pericytes (*76*). Myofibroblasts can be activated by multiple soluble factors derived from epithelila, endothelia, or hematopoietic cells after tissue injury and sustained during chronic inflammation (*77*). For instance, TGF-β1 is a potent pro-fibrotic factor in multiple organs by promoting the differentiation of MSCs to ECM-producing myofibroblasts (*78*). TGFβ-1 is produced by multiple cell types including alternatively activated macrophages, eosinophils, platelets and epithelial cells (*78*). TNFα can also promote fibrosis indirectly by inducing epithelial cell death or by augmenting the activity of reactive oxygen species (ROS)-producing myeloid cells (*79*); this cytokine can also directly activate myofibroblast cells (*72*). Type 2 immune cytokines derived from Th2 cells, ILC2s, and eosinophils are also linked fibrogenesis; specifically, IL-13 can drive myofibroblast proliferation and matrix synthesis (*78*). Finally, IL-17A also possesses pro-fibrotic activity by promoting neutrophilic infiltration, which induces tissue injury, or by directly acting on fibroblasts to produce collagen (*78, 80*).

1.7 Idiopathic pulmonary fibrosis

Idiopathic pulmonary fibrosis (IPF) is a chronic, degenerative, and often lethal disease of unknown etiology. It is characterized by features of usual interstitial pneumonia (UIP) which includes the heterogeneous appearance of fibrotic scarring and "honeycomb" patterns in affected tissues (*81*). Although a dysregulated immunological component has been associated with the progression of IPF, the use of broad-spectrum immunosuppressants including corticosteroids is often ineffective (*82*). More recently, the pathogenesis of IPF is thought to be the consequence of perturbations in repair processes of the epithelium; this may be triggered by repeated injury and cellular stress responses of the alveolar epithelium or dysregulated interplay between epithelium and the underlying stromal cells resulting in fibroproliferative responses (*68, 81*). The critical environmental risk factors of IPF are cigarette smoke and exposure to irritants such as

metal and wood dust; in some instances, chronic viral infections may contribute to IPF (*81*). There are no genetic factors consistently linked to IPF; however mutations in the genes encoding surfactant protein C, which is expressed exclusively by type II pneumocytes, and mucin 5B, expressed by large airway epithelia, are linked to some familial cases of IPF (*83, 84*).

Many animal models of lung injury and fibrosis have been developed to study the progression of fibrotic degeneration with the aim of identifying critical molecular and cellular pathways likely involved in IPF (*85*). Although they have been utilized in the identification and validation of potential therapeutic targets, there are serious limitations to these models: in particular, the dissimilarity in the development of the human disease which may require up to two decades to develop in contrast to the more immediate induction of fibrotic scarring in animals (*86, 87*). Moreover, unlike in IPF where the pathology is progressive and thought to be irreversible, in several animal models, tissue scarring is either self-limiting or may resolve after the removal of the causative agent (*86, 87*).

Bleomycin exposure is a commonly used and well-characterized mouse model of pulmonary fibrosis (*85*). Originally purified from *Streptomyces verticillatus*, bleomcyin possesses anti-neoplastic properties but also causes damage to alveolar cell types and capillary endothelial cells (*68, 88*). Lung injury initiates an acute inflammatory response that once resolved, progresses to fibroblast proliferation and matrix deposition culminating in a maximal fibrotic response approximately 21 days after bleomycin-induced injury (*85*). Histopathological features of bleomycin-induced lung fibrosis that resemble IPF include matrix deposition in the interstitium and intra-alveolar space,

variable inflammation in the parenchyma, epithelial injury, and disruption of the basal lamina (*68, 89, 90*).

1.8 Retinoic acid receptor-related orphan receptors in immunity

Retinoic acid receptor-related orphan receptors (RORs) are a family of ligand-dependent, steroid hormone type transcription factors that regulate gene expression by binding to ROR response elements (ROREs) in the regulatory regions of target genes (*91*). These nuclear receptors are critical for processes related to immunity (**Fig. 1.3**), development, metabolism, and the circadian rhythm (*91*). In hematopoiesis, RORγt is required for the development of the Th17 lineage (*92*). In addition, RORγt null mice also lack ILC3s including LTi cells resulting in a defect in the formation of lymph nodes, lymphoid follicles, and Peyer's patches (*93-95*). RORα also plays an important role in Th17 cell differentiation through synergistic mechanisms with RORγt; naïve T cells lacking both RORγt and RORα display a more striking defect in Th17 differentiation than RORγt deletion alone (*96*). Moreover, in Th17 cells, RORs bind to ROREs in regulatory regions of Th17 signature genes (*Il17a*, *Il17f*, *Il23r*) and thereby promote their expression (*97*). The reciprocal relationship between Th17 and Tregs is illustrated by the ability of FoxP3 to interact with RORγt or RORα and limit their transcriptional activity in a TGF-β dose dependent manner (*98, 99*). RORγt is also expressed by a subset of microbiota-induced $FoxP3^{+}$ Tregs and is required for the suppression of Th2 driven pathologies (*100*).

Early mouse models of ILC2 deficiency relied on a spontaneous mutation in *Rora* resulting in a truncated non-functional protein that lacks the C-terminal ligand-binding

domain (*101, 102*). Termed Staggerer mice, these *Rora*$^{sg/sg}$ mutants are runted and have an ataxic gait and shortened lifespan primarily due to defects in neural development; RORα is required for the survival and maturation of Purkinje neurons of the cerebellum (*103*). Although the *Rora* transcript is detectable in all three ILC subsets, its deletion in hematopoiesis results in the selective depletion of ILC2s (*101, 102*). This selective defect in the hematopoietic compartment leads to several functional consequences: RORα-deficient bone marrow chimeras have impaired immunity to parasitic helminth infection and are protected from pathologies associated with papain- and HDM-induced allergic lung inflammation (*101, 102, 104*).

The IL-23/IL-17 immune pathway comprised of RORγt-expressing CD4$^+$ Th17, γδ T cells, NKTs, and ILCs have been implicated in the pathogenesis of several immune disorders including IBD. In GWAS, polymorphisms in *IL23R* are associated with increased susceptibility to Crohn's disease, while IL-17A levels are elevated in the intestinal mucosa and feces of patients with active CD (*105-107*). Moreover, IL-23 responsive ILC3s are enriched in the intestines of CD patients (*108*). Given these observations, the suppression of the IL-23/IL-17 immune axis has been investigated extensively in the development of therapies for IBD. The use of IL-23-specific antibodies has shown promise in patients with Crohn's disease (*109*); however, trials investigating antibodies targeting IL-17A were terminated due to a lack of effectiveness and an increase in susceptibility to infections in some patients (*110*). Despite this setback, IL-17A suppression has demonstrated efficacy in the treatment of psoriasis, rheumatoid arthritis, uveitis, and spondylitis (*111, 112*). Alternatively, targeting transcription factors required for IL-17$^+$ inflammatory cells has also been proposed; RORs are suitable for

pharmacological modulation as they possess a ligand-binding domain that can be targeted with various small-molecular weight inhibitors (*113*). An early example of this strategy was the development of SR1001, an inverse agonist selectively targeting Rorγt and RORα (*114*). SR1001 selectively binds to the LBD of Rorγt and RORα resulting in the inhibition of their transcriptional activity; this inhibitor was effective in suppressing Th17 differentiation and could protect animals from developing pathological features of experimental autoimmune encephalomyelitis (*114*).

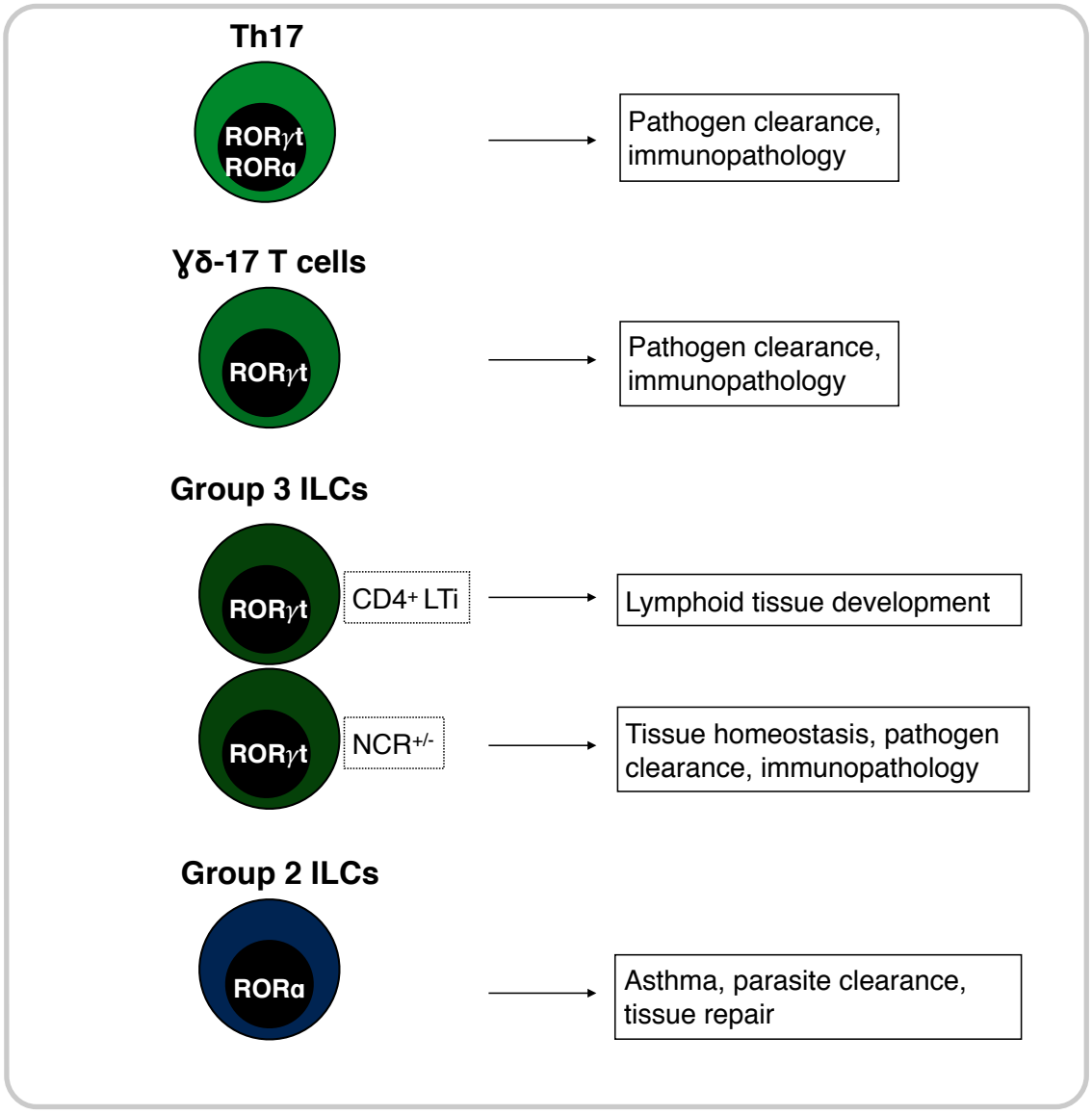

Figure 1.3. Overview of RORγt and RORα requirement in lymphoid cell lineages. Adapted from Cook et al. (*91*). RORγt is required for Th17 differentiation, IL-17-producing γδ T cells, and ILC3s including LTi cells. RORα is known to promote Th17 differentiation in concert with RORγt and is also required for ILC2 development.

1.9 CD34-family of sialomucins

CD34 is a founding member of a family of cell surface sialomucins that includes podocalyxin and endoglycan (*115*). CD34 is commonly used clinically as a marker for

the enrichment of hematopoietic progenitor or stem cells for bone marrow transplantation (*116*). More recently its use as a progenitor cell marker has been extended to various non-hematopoietic tissue specific stem-like precursor cells including muscle satellite cells, epidermal progenitors, corneal keratocytes, vascular endothelial progenitors and pulmonary epithelial stem cells (*117, 118*). CD34-family proteins have unique and some overlapping expression in multiple cell types. Like CD34, podocalyxin is expressed by a subset of primitive HSCs and vascular endothelia; in addition, podocalyxin was originally described as an important marker for kidney glomerular epithelia (podocytes) and is required for normal kidney development (*115*). Podocalyxin upregulation has also been implicated in a number of malignancies including breast cancer, leukemia and pancreatic cancer (*115*). Podocalyxin expression in breast cancer is associated with tumour aggressiveness and poor patient prognosis (*119*). This oncoantigen was recently validated as a viable target for breast cancer immunotherapy; treatment with podocalyxin-specific antibodies can suppress tumour formation and metastasis in xenograft models (*120*).

Several cellular functions of CD34-related proteins have been proposed including promoting cell proliferation and blocking cell differentiation of progenitor cells, context-specific enhancement or inhibition of cell adhesion, and cell morphogenesis, chemotaxis and asymmetric cell division (*121*). An example of CD34-mediated cell adhesion was demonstrated by its expression in specialized lymphoid high endothelial venules (HEVs). On these cells it is modified with a unique post-translational glycosylation that enables CD34 to act as a ligand for L-selectin during the recruitment of lymphocytes to the peripheral lymph nodes (*122*). However, this Sialyl-Lewis X modification is extremely

rare and unique to HEVs; more recent functional studies would suggest that in most tissues CD34 functions as an anti-adhesive molecule (*115*). For instance, the deletion of CD34 from mast cells results in an increase in homotypic cell aggregation - an effect, which can be reversed by ectopic CD34 expression (*123*). Moreover, *Cd34*$^{-/-}$ mice are resistant to a number of experimental Th2- or Th17-biased inflammatory diseases of the mucosa including OVA- or SR antigen-induced lung inflammation and DDS-mediated colitis; this protection phenotype is the consequence of defective eosinophil, mast cell, and dendritic cell trafficking in the absence of functional CD34 resulting in an attenuated inflammatory response (*124-126*).

1.10 Thesis hypothesis and summary

There is compelling evidence that type 2 immune responses defined by the production of IL-4, IL-5, and IL-13 are critical promoters of tissue fibrosis (*77*). Th2 immunity and accessory cells such as eosinophils, mast cells, and alternatively activated macrophages have long been associated with wound healing responses or host immunity against parasitic helminth infections such as *Schistosoma mansoni*, which can induce liver fibrosis (*77, 127*). It has also been noted that in the context of host defense strategies against infectious pathogens, fibrosis is the pathological outcome of dysregulated tolerance responses (*128*). IL-13, in particular, has been linked with fibrotic scarring in several experimental animal models including radiation- or chemical-induced lung fibrosis in rodents (*129*), IBD-related intestinal fibrosis (*130*), and dermatitis-mediated skin fibrosis (*131*). Moreover, Th2-associated cytokines are linked to the development of fibrosis and airway remodeling in response to chronic lung inflammation

in cases of asthma or IPF (*132-134*). In addition to $CD4^+$ Th2 cells, ILC2s are another critical source of IL-13 in the induction of pulmonary fibrosis and the depletion of ILC2s is sufficient to protect mice from inflammation-induced ECM lung deposition (*135*). Although Crohn's disease is thought to be primarily Th17 driven, IL-13 producing lymphocytes have been reported to be highly enriched in intestinal strictures of patients; moreover IL-13 can alter MMP activity in fibroblasts leading to attenuated matrix degradation resulting in excessive ECM accumulation (*33, 136*). Mechanistically, IL-13 promotes fibrosis through the induction of TGF-β; however in some cases the pro-fibrotic activity of IL-13 may be independent of TGF-β signaling (*137, 138*). IL-13/IL13Rα1 signaling can also drive the proliferation of fibroblasts and ECM-synthesis (*136, 139, 140*). Therefore, the suppression of Th2 immune responses by antibody neutralization of IL-13 or IL-5 or the inhibition of cellular sources of these cytokines may be exploited in the treatment of fibrotic diseases (*78*).

On the basis of these observations, we hypothesized that ILC2s and hematopoietic CD34 are important contributors to fibrotic development in mucosal tissues by promoting type 2 immunity; ILC2s and CD34 are of particular interest as they represent potential therapeutic targets for immunomodulation. To address these hypotheses, we examined mutant mouse strains that either lack ILC2s ($Rora^{sg/sg}$ BMT) or the CD34 molecule ($Cd34^{-/-}$) in experimental models of tissue injury and fibrosis (*101, 102, 141, 142*).

Although we find that $Rora^{sg/sg}$ BMT mice are protected from infection-induced intestinal fibrosis, the disease was largely independent of type 2 immune cytokines, eosinophils and STAT6 signaling (a downstream signaling modulator of IL-13R) which suggests that ILC2s may be dispensable in this model. Given that ROR-type

transcription factors are known to be required for the maintenance of the Th17 cell lineage, we examined the expression levels of IL-17A and IL-22 in *Rora*$^{sg/sg}$ BMT mice. We found a clear reduction in IL-17A and IL-22 in infected tissues of *Rora*$^{sg/sg}$ BMT mice; RORα-deficient ILC3s and T cells exhibited defects in cytokine expression. Moreover, the restoration of functional innate cells in *Rora*$^{sg/sg}$ BMT animals reestablished a fibrotic phenotype following infection; this suggests that RORα-dependent ILC3s are important contributors to intestinal fibrosis in this experimental model of intestinal fibrosis.

Contrary to my original hypothesis, *Cd34*$^{-/-}$ mice did not exhibit significant resistance to *Salmonella*-induced fibrosis. *Cd34*$^{-/-}$ mice were, however, extremely sensitive to bleomycin-induced lung injury displaying greater weight loss and higher rates of mortality. Although, eosinophil recruitment to the lungs was attenuated during the acute phases of lung damage in the absence of CD34, these cell types are sparse in this model representing only a small percentage of total airway inflammatory infiltrates. However, we found clear evidence of more severe interstitial edema in injured-lung tissues by electron microscopic analysis. Moreover, using bone marrow chimeric mice, this sensitivity to lung injury was found to be the result of *Cd34* deletion in non-hematopoietic cells. In aggregate, our data provide support for the hypothesis that CD34 is required for the maintenance of vascular integrity in response to acute lung injury and that, in its absence, mice suffer from pathology associated with increased vascular leak.

Chapter 2.

Orphan nuclear receptor RORα-dependent immunity in *Salmonella*-induced intestinal fibrosis

2.1 Introduction

Fibrosis is the pathological deposition of extracellular matrix (ECM) associated with persistent inflammation. The contribution of the hematopoietic system to this process has been widely investigated and numerous leukocyte subsets are implicated in driving fibrotic remodeling including M2 macrophages, neutrophils, eosinophils, mast cells and lymphocytes (*70, 72*). In particular, type 2 immune responses have long been associated with tissue fibrosis and IL-4 and IL-13 signaling has been shown to drive tissue remodeling and ECM deposition in the liver in response to *Schistosoma mansoni* infection (*143*). In mucosal tissues both $CD4^+$ T helper 2 (Th2) and Th17 cells have been linked to the development of tissue fibrosis. For example, in a mouse model of chronic gut inflammation and fibrosis, an overlapping production of IL-13 and IL-17A coincides with the appearance of fibrotic tissue, which suggests the pathology may be driven by a mixed Th2 and Th17 response (*144*).

Innate lymphoid cells (ILCs) are a recently identified subset of leukocytes and a prominent source of cytokines with profiles similar to those of T helper cells, yet these cells lack antigen-specific receptors and their temporal production of cytokines precedes adaptive immune responses. ILCs can be classified based on their transcript and cytokine profiles; for instance, group 2 ILCs (ILC2s) are GATA3- and RORα-dependent and produce IL-5 and IL-13 while group 3 ILCs (ILC3s) express RORγt and are a source of

IL-17A and IL-22. ILCs have broad functions in host defense responses against pathogens, maintenance of tissue homeostasis, and pathologies such as allergic asthma and colitis (*20*). Recently, ILC2s were shown to have the capacity to drive excessive lung collagen deposition; likewise, analyses of idiopathic pulmonary fibrosis patient bronchoalveolar lavage fluid (BAL) revealed an expansion of ILC2s, providing correlative evidence that ILCs may be pathogenic in fibrotic remodeling (*135*). Despite their pathogenic role in these models, ILC2s have also been shown to play a critical role in tissue repair. For example, in mouse models of lung influenza infection (*145*) and DSS-induced colitis (*146*) ILC2s aid tissue repair through their production of amphiregulin. Similarly, ILC3s in the gut demonstrate protective or pathogenic roles depending on context. ILC3s are necessary for pathogen clearance (*95, 147*) and gut tissue repair following chemotherapy-induced injury (*148*). This is likely through IL-22-dependent activation of epithelial progenitors (*148*), but ILC3s can also promote intestinal tumor formation in a chronic inflammatory setting (*57*). In summary, there are data to support both beneficial and pathogenic roles for ILC2s and ILC3s in tissue remodeling.

Crohn's disease (CD) is primarily characterized as a Th17-driven disease (*33*), and distinct IL-23-dependent ILCs that produce IL-17A and IL-22 are also elevated in CD patient samples (*108, 149*) arguing for a role for Th17 cytokines. Conversely, other studies have suggested that ILC2s and eosinophils are contributing factors to CD progression through an IL-13 dependent accumulation of matrix-producing fibroblasts (*136, 150*). Thus, there is evidence to support both Th2 and Th17 responses in the

pathology of CD. However, the direct involvement of ILCs in driving excessive tissue remodeling and ultimately fibrosis in the gut remains unclear.

RORα is a transcription factor known to regulate ILC2 development. It is closely related to RORγt, which is a critical regulator of Th17 and ILC3 subsets including lymphoid tissue-inducer cells (*92, 151, 152*). Moreover, in the Th17 lineage, RORγt and RORα are co-expressed and function synergistically for lineage maintenance and cytokine production (*96*). Previously we showed that *Rora*$^{sg/sg}$ bone marrow transplant (BMT) chimeric mice provide a suitable model of ILC2 deficiency as they selectively lack ILC2s while other leukocyte lineages, including other ILCs, are present at steady state (*102*). Furthermore, *Rora*$^{sg/sg}$ BMT animals are protected from type 2 immune lung pathology (*102, 153, 154*). We used a similar strategy to evaluate the role of ILC2s in a *Salmonella*-induced model of gut fibrosis. Strikingly, we show that RORα is required for a fibrotic response. Surprisingly, this is not through regulation of ILC2-dependent production of type 2 cytokines, but rather through a previously unrecognized role for RORα in the production of cytokines from ILC3s. We also find that restoration of ILCs in *Rora*$^{sg/sg}$ BMT mice is sufficient to reestablish susceptibility to fibrotic disease. These data provide evidence that ILC3s contribute to fibrosis, and offer RORα as a new therapeutic target for fibrotic tissue remodeling.

2.2 Materials and Methods

2.2.1 Mice

C57BL/6J, B6.SJL-Ptprc^{a}Pepc^{b}/BoyJ (CD45.1), B6.C3(Cg)-*Rora*^{sg}/J (*Rora*$^{sg/sg}$), C.129S1(B6)-*Gata1*^{tm6Sho}/J (ΔdblGATA), C.129S2-*Stat6*^{tm1Gru}/J (*Stat6*$^{-/-}$), and B6.129S7-*Rag1*^{tm1Mom}/J (*Rag1*$^{-/-}$) mice were maintained in a specific pathogen-free environment at the Biomedical Research Centre (UBC). BM chimeras were generated by lethally irradiating and reconstituting CD45.1 animals with two million BM cells isolated from WT or *Rora*$^{sg/sg}$ littermates. For *Rag1*$^{-/-}$ co-transplant experiments, WT or *Rora*$^{sg/sg}$ BM cells were mixed 1:1 with *Rag1*$^{-/-}$ BM cells for reconstitution. Animals were used at least 8 weeks after transplantation. All experiments performed were approved by the UBC Animal Care Committee.

2.2.2 Infection model

Mice were treated with 20 mg of streptomycin by oral gavage 24 hours prior to oral infection with 3 X 10^6 *Salmonella* Typhimurium Δ*aroA* CFU in 100 μL PBS. At various time points, tissues were collected and homogenized in sterile PBS; serial dilutions of the homogenates were plated on LB agar plates (100 μg/mL streptomycin) for bacterial enumeration. For cytokine neutralizing experiments, mice were injected intraperitoneally with 200 μg of antibodies against IL-17A (Janssen, CNTO 8096), 200 μg of antibodies against IL-22 (Genentech, 8E11) or their respective isotype controls (Janssen, CNTO 2407; Genentech, GP120:9709) three times per week beginning at 7 days after infection, and sacrificed at day 21 pi for tissue collection.

2.2.3 Histology and immunohistochemistry

Formalin fixed and paraffin embedded tissues were cut into 5-μm sections for Masson's trichrome (MT) staining. Cecal pathology assessed by scoring the lumen, surface epithelium, mucosa, and submucosa as described previously (*51*). For immunostaining, tissue sections were deparaffinized, rehydrated, and underwent antigen retrieval; antibodies against type 1 collagen (ABcam), type 3 collagen (Fitzgerald), vimentin (ABcam), and desmin (Santa Cruz) were used, followed by incubation with Alexa Fluor-conjugated secondary antibodies (Life Technologies). Sections were then mounted using ProLong Gold Antifade with DAPI (Life Technologies). Optical z-stack images were captured on a Leica SP5X confocal microscope and analyzed using ImageJ.

2.2.4 Quantitative RT-PCR

Total RNA was extracted from the terminal ends of cecal tissue using Trizol (Invitrogen) was reverse transcribed with a high-capacity cDNA RT kit (Thermo). Quantitative real-time PCR was performed using SYBR green chemistry (KAPA) and gene-specific primer pairs (Appendix 1) on an AB7900 RT-PCR system.

2.2.5 Cytokine detection

Concentrations of TNF, IL-6, MCP-1, IFN-γ, IL-12p70, IL-10, and IL-17A in cecal homogenates were determined using a cytometric bead array (BD Biosciences); TGF-β1 and IL-22 levels were determined by plate ELISA kits (eBiosciences) according to manufacturer's instructions.

2.2.6 Immune analysis and flow cytometry

Mesenteric lymph nodes were excised and passed through a 70-μm filter to generate single cell suspensions. Leukocytes were isolated from ceca by flushing luminal contents, mincing and incubating tissues in 1.5 U/mL collagenase D and 2.4 U/mL dispase II (Roche) for 30 minutes at 37˚C with gentle rotation; samples were then passed through a 70 μm filter and hematopoietic cells were enriched by Percoll (GE) separation. Cells were restimulated using 50 ng/mL PMA and 750 ng/mL ionomycin (Sigma) in the presence of brefeldin A (eBiosciences) for 4 hours. For *ex vivo* stimulation experiments, leukocytes were purified from the lamina propria of naïve small intestines and cultured in the presence of 20 ng/mL IL-2, IL-1b, and IL-23 (eBiosciences) for 2 hours followed by the addition of 50 ng/mL PMA, 750 ng/mL ionomycin, and 3 ug/mL brefeldin A (eBiosciences) for 3 hours. Samples were then incubated with 5 μg/mL anti-CD16/32 (2.4G2, in house) to block non-specific antibody binding. Fluorescence-conjugated antibodies to CD45.2 (104), CD8 (53.67), CD11b (M1/70), CD11c (N418), CD19 (1D3), NK1.1 (PK136), Gr1 (RB6-8C5), Ter119, CD3e (145-2C11), CD90.2 (30-H12), KLRG1 (2F1), Sca-1 (D7), IL-17A (eBio17B7), and IL-22 (1H8PWSR) were used. A fixation and permeabilization buffer set (eBiosciences) was used for intracellular cytokine staining and a fixable viability dye (eBiosciences) was used for dead cell exclusion. Data was acquired on a BD LSRII, and analyzed using FlowJo.

2.2.7 RNA sequencing

ILC3s were sorted directly into TRIzol LS reagent (Thermo) for RNA isolation. ILC3 RNA sample quality was assessed using the Agilent 2100 Bioanalyzer to check for RNA integrity; qualifying samples were then prepared following the standard protocol for the TruSeq stranded mRNA library kit (Illumina) on the Neoprep Library System (Illumina). Sequencing was performed on the Illumina NextSeq 500 with Paired End 75bp x 75 base pair reads. De-multiplexed read sequences were then aligned to the *Mus musculus* mm10 reference sequence using TopHat2 splice junction mapper and differential expression assessed using Cuffdiff through bioinformatics applications available on Basespace.

2.2.8 Statistical analysis

Results are presented as mean +/- SEM; statistical significance was determined by unpaired Student's *t* test.

2.3 Results

2.3.1 *Salmonella*-induced gut pathology is dependent on hematopoietic expression of RORα

We generated *Rora*$^{sg/sg}$ BMT mice and evaluated how they respond to infection with the Δ*aroA* strain of *Salmonella* Typhimurium, which induces robust ECM deposition in the cecum (*51*). We found no differences in pathogen burdens in the ceca or spleens of WT BMT and *Rora*$^{sg/sg}$ BMT mice at days 7, 21, and 35 postinfection (pi),

indicating that *Rora* is dispensable for *Salmonella* clearance (Fig. 2.1A). In addition, we found similar degrees of mucosal thickening, edema, and inflammatory infiltrates in these animals at day 7 pi (Fig. 2.1B). In contrast, at 21 days pi, during peak fibrosis, we observed pronounced epithelial cell hyperplasia and pathological remodeling of normal tissue architecture, including disruption and thickening of the basal lamina in WT BMT ceca, whereas we found a striking attenuation in collagen deposition and dampened immunopathology in cecal sections of $Rora^{sg/sg}$ BMT mice. Similarly, by day 35 pi, much of the pathology and inflammation was resolved in $Rora^{sg/sg}$ BMT mice, with mucosa thickness returning to levels similar to uninfected samples (albeit with some residual collagen in the submucosal regions) (Fig. 2.1B). Conversely, WT BMT cecal sections revealed persistent tissue inflammation and lymphoid cell aggregates at this time point (Fig. 2.1B, C).

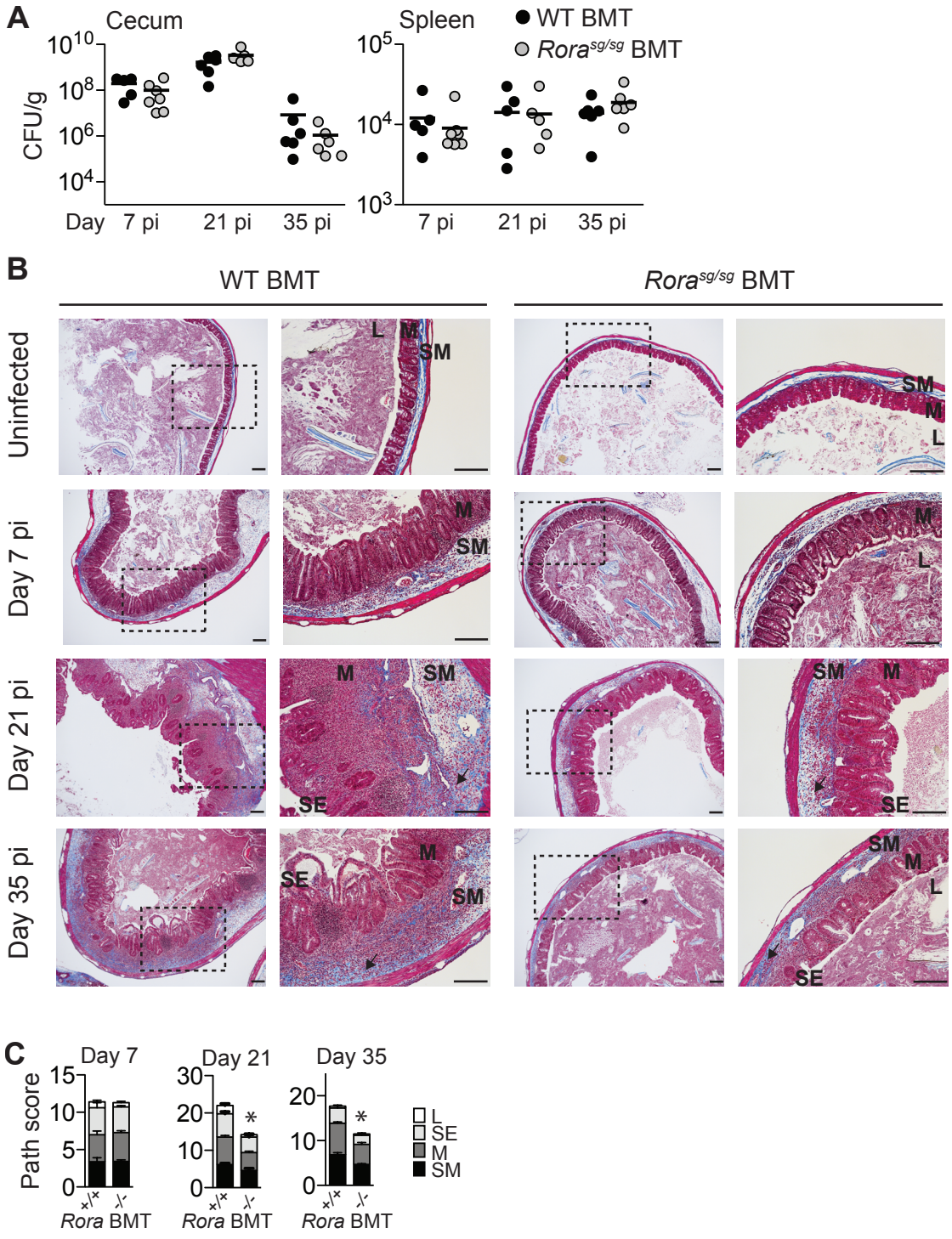

Figure 2.1. Hematopoietic expression of *Rora* mediates *S.* Typhimurium Δ*aroA* driven cecal immunopathology and fibrosis. WT and *Rora*$^{sg/sg}$ BMT mice were infected with *Salmonella* and sacrificed 7, 21, and 35 days pi. (A) *Salmonella* colonization of ceca and spleens of infected animals. CFU, colony-forming unit. (B)

Masson's trichrome (MT)-stained cecal tissue sections. L, lumen; SE, surface epithelium; M, mucosa; SM, submucosa. Arrowheads indicate submucosal collagen accumulation visualized by blue staining. Scale bar, 200 μm. (C) Pathology scores of the luminal, epithelial, mucosal, and submucosal subsections of cecal tissue. *, $p < 0.05$, (n=5-7 per group).

In evaluating cytokine production, we found *Tnfa* and *Il6* transcripts were present at similar levels at day 7 pi, but were significantly reduced in *Rora*$^{sg/sg}$ BMT cecal samples at the day 21 and 35 time points (Fig. 2.2A). Consistent with these mRNA results, quantification of cytokines in cecal homogenates revealed significantly less TNF, IL-6, MCP-1, and IL-10 (but comparable levels of IL-12p70 and IFN-γ) in *Rora*$^{sg/sg}$ BMT samples when compared with their WT BMT counterparts at day 21 pi (Fig. 2.2B). In summary we found that the deletion of *Rora* lead to attenuated inflammatory responses associated with fibrosis and these correlated with a more rapid resolution of immunopathology and tissue architecture during the late phases of chronic *Salmonella* infection.

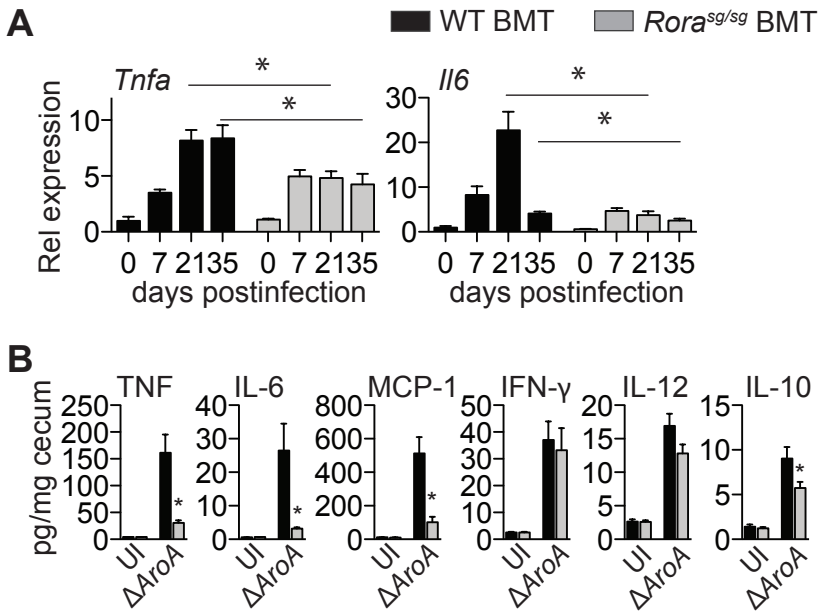

Figure 2.2. Attenuated inflammation in infected *Rora*$^{sg/sg}$ cecal tissues. (A) Transcript levels of pro-inflammatory cytokines *Tnfa* and *Il6* in ceca normalized to *Gapdh*. (B) Protein levels of TNF, IL-6, MCP-1, IFN-γ, IL-12p70, and IL-10 in naïve and 21 days pi cecal homogenates as determined by cytometric bead array (CBA) normalized to total tissue protein. *, $p < 0.05$ (n=5-6 per group; or pooled from 2 independent experiments, n= 11, 12). Significance determined by unpaired student's t test.

2.3.2 Fibrosis is attenuated in *Rora*$^{sg/sg}$ BMT mice during chronic infection

Consistent with a role for RORα in driving fibrosis we found significantly reduced levels of *Col1a2* and *Tgfb1* transcripts and TGF-β1 protein in *Rora*$^{sg/sg}$ BMT ceca at days 21 and 35 pi (Fig. 2.3A, B).

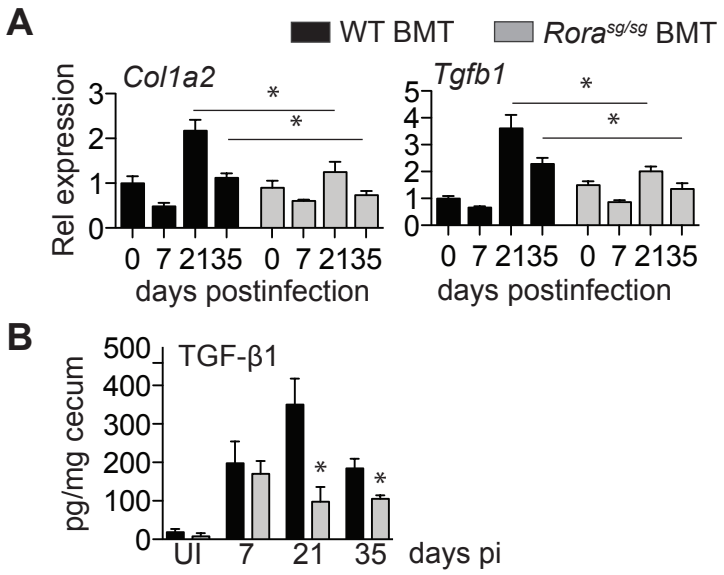

Figure 2.3. Reduced collagen and TGF-β1 levels in cecal tissue of infected *Rora*$^{sg/sg}$ BMT animals. (A) Cecal transcript levels of *Col1a2* and *Tgfb1* normalized to *Gapdh*. (B) TGF-β1 protein levels of cecal homogenates normalized to total protein. *, $p < 0.05$ (n=5-7 per group). Significance determined by unpaired student's t test.

Immunofluorescent staining for type 1 collagen (Col1) in WT BMT tissues indicated that the most pronounced collagen deposition occurs in the submucosal (SM) region of the cecum, with more modest accumulation in the mucosa, 21 and 35 days pi; strikingly, there was less SM Col1 staining in the *Rora*$^{sg/sg}$ BMT ceca at days 21 and 35 pi (Fig. 2.4A). Next, we visualized fibroblast accumulation at day 21 pi by staining for the common fibroblast markers vimentin and desmin (*51*). We found substantial accumulation of vimentin and desmin positive cells across the mucosal and SM regions of WT BMT ceca; desmin staining was particularly enriched within the basal lamina which appeared thicker in WT than in *Rora*$^{sg/sg}$ BMT samples (Fig. 2.4B). Taken together our results indicate that, by all criteria, *Rora*$^{sg/sg}$ BMT animals were protected from intestinal fibrosis with reduced collagen and fibroblast accumulation in the cecum.

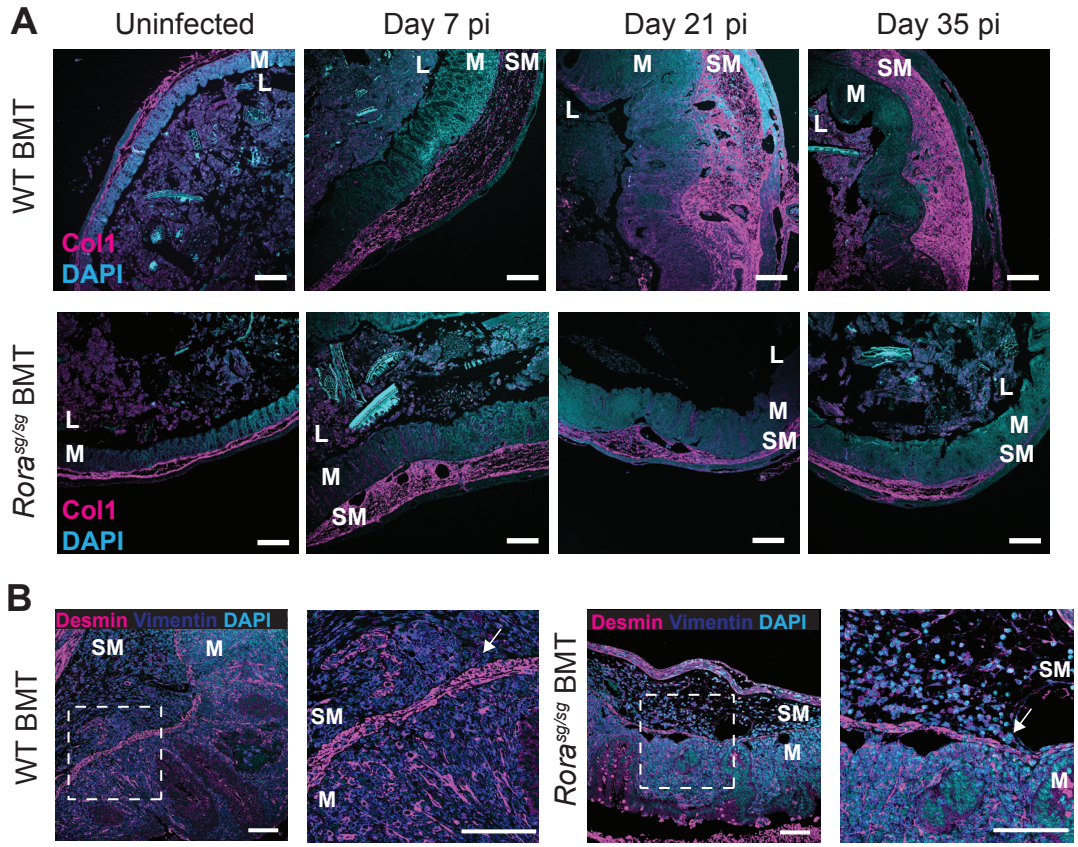

Figure 2.4. Attenuated collagen deposition and reduced fibroblast cell numbers in cecal tissue of chronically infected *Rora*$^{sg/sg}$ BMT animals. (A) Immunofluorescence images of cecal sections stained for type 1 collagen (Col1, magenta) and nuclei (DAPI, cyan). Scale bar, 100 μm. (B) Desmin (magenta), vimentin (blue), and nuclear (DAPI, cyan) staining for fibroblasts in cecal tissues 21 days pi. Arrowheads indicate desmin^{+} staining in the basal lamina. Scale bar, 100 μm.

2.3.3 Eosinophils and STAT6 signaling are dispensable in *Salmonella* induced fibrosis

Chronic *Salmonella* infection is known to induce a Th1/Th17 response (*51*), but the contribution of type 2 immune cell cytokines in this model has not been thoroughly addressed. In our cytokine analysis, however, we found that IL-5 and IL-13 transcript

levels in fibrotic WT BMT cecal tissues were similar to infected tissues of *Rora*$^{sg/sg}$ BMT animals, and importantly, were reduced or unaltered when compared with uninfected samples (Fig. 2.5).

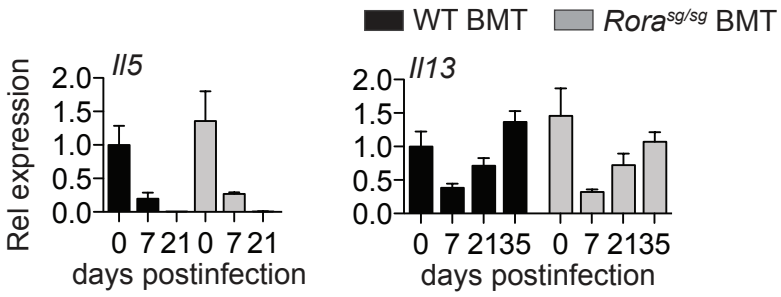

Figure 2.5. Assessment of *Il5* and *Il13* transcript levels in WT and *Rora*$^{sg/sg}$ gut tissues at various time points postinfection.

To further rule out a role of Th2 immunity in *Salmonella* induced fibrosis, infections were performed in eosinophil-deficient ΔdblGATA mice. These studies revealed similar pathogen burdens in the cecum and spleen (Fig. 2.6A) as well as comparable evidence of pathology in MT-stained cecal sections of infected animals (Fig. 2.6B, C). Transcript quantification also revealed similar levels of *Col1a2*, *Tnfa*, and *Il6* in the eosinophil-deficient tissues, although *Tgfb1* and *Epx* transcripts were significantly reduced (Fig. 2.6D). We conclude that eosinophils are dispensable in this model.

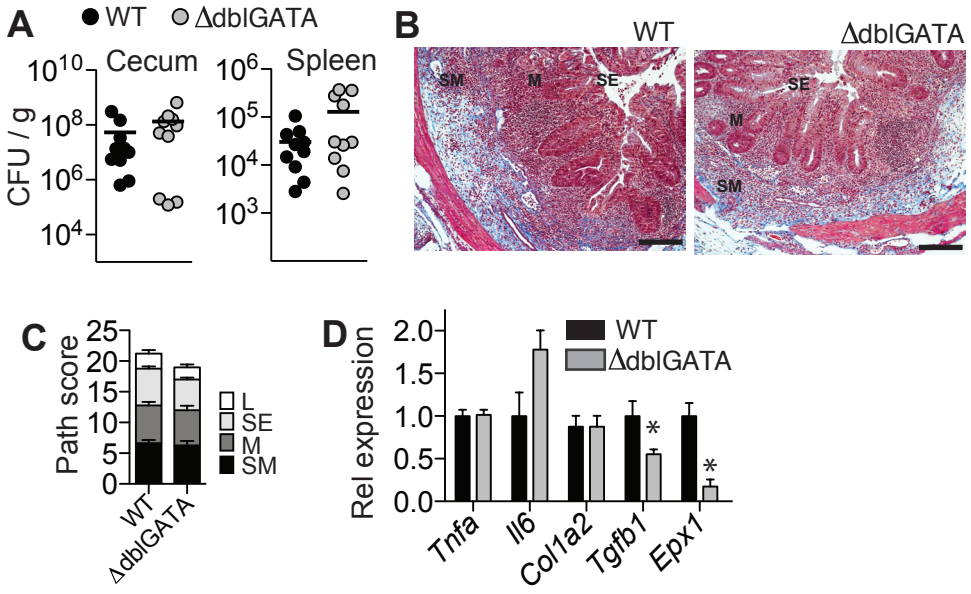

Figure 2.6. Eosinophils are dispensable in *S.* Typhimurium Δ*aroA*-dependent gut inflammation and fibrosis. (A-D) Eosinophil deficient ΔdblGATA and their respective WT controls were infected with *Salmonella* and sacrificed 21 days pi. (A) Cecal and splenic *Salmonella* burdens of infected animals (n=10 per group; data from two independent experiments). (B) MT-stained cecal sections and (C) their corresponding pathology scores. (D) Transcript levels of *Tnfa, Il6, Col1a2, Tgfb1,* and *Epx* of infected cecal tissues normalized to *Gapdh*. *, $p < 0.05$ (n=5 per group). Significance determined by unpaired student's t test.

In many examples of fibrosis, STAT6 plays an essential role as a transcriptional mediator of downstream IL-4/IL-13 receptor signaling involved in the propagation of other type 2 immune cells (*72*). Following infection with *Salmonella*, we found that *Stat6*$^{-/-}$ and WT animals exhibited similar pathogen burdens in the cecum and the spleen (Fig. 2.7A) and displayed a similar degree of pathology in the cecum (Fig. 2.7B, C). Furthermore, we observed comparable levels of *Col1a2*, *Tgfb1*, *Tnfa*, and *Il6* expression in both WT and *Stat6*$^{-/-}$ cecal tissues (Fig. 2D). In aggregate, our data indicate that

STAT6 in Th2 effector function signaling are dispensable for *Salmonella*-induced gut fibrosis.

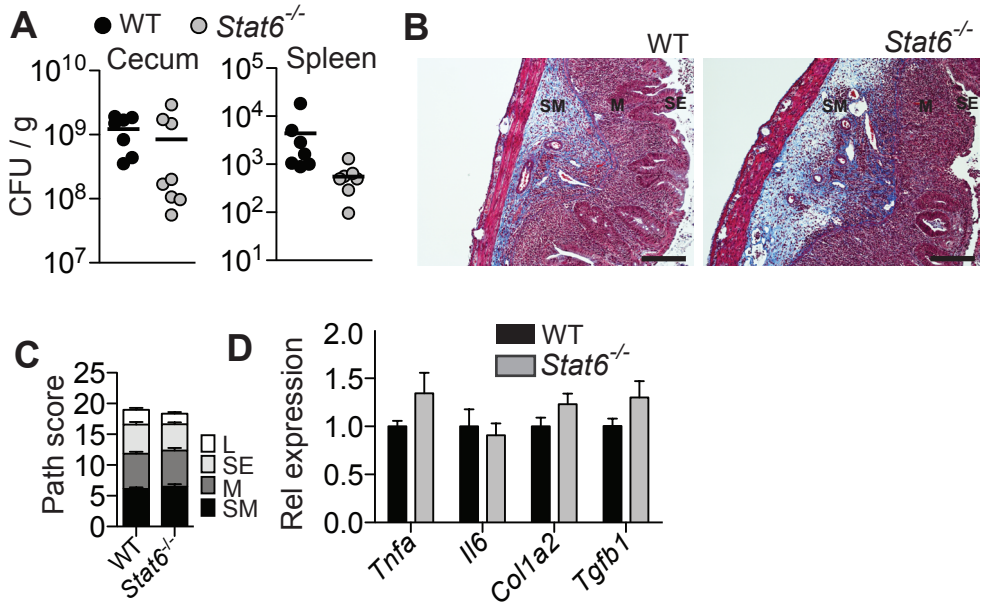

Figure 2.7. STAT6 signaling is dispensable in *S.* Typhimurium Δ*aroA*-dependent gut inflammation and fibrosis. (A) Pathogen burdens of *Salmonella* infected ceca and spleens of infected *Stat6*$^{-/-}$ and WT animals (n=7, 8; data from single experiment). (B) MT-stained infected cecal tissues and (C) their corresponding pathological scores. (D) Transcript levels of *Tnfa, Il6*, *Col1a2*, and *Tgfb1* of *Salmonella* infected ceca normalized to *Gapdh*. Scale bar, 200 μm.

2.3.4 RORα mediates IL-17A and IL-22 production in chronic gut inflammation and fibrosis

Although *Rorα*$^{sg/sg}$ BMT mice are known to have a profound defect in ILC2 development (*101, 102*), one previous study indicated that RORα is also required by Th17 cells for normal cytokine production (*96*). In addition, although *Rorα*$^{sg/sg}$ BMT animals have normal ILC3 numbers in the small intestine and mesenteric lymph nodes

(mLNs) at steady state (*102*), several studies have detected high *Rora* transcript levels in gut ILC3s (*155, 156*) or ILC3-like subsets (*94, 157*). Despite these observations, the importance of RORα expression in regulating ILC3s in the context of inflammatory diseases is unknown. We therefore evaluated Th17 and ILC3 associated cytokines in infected *Rora*$^{sg/sg}$ BMT ceca. These mice exhibited a decrease in cecal *Il17a* and *Il22* transcripts at days 21 and 35, and a corresponding reduction in IL-17A and IL-22 protein in cecal homogenates (Fig. 2.A, B). Consistent with this observation, we previously reported significantly reduced levels of IL-17A in the lungs of *Rora*$^{sg/sg}$ BMT mice in both Ova- and HDM-induced models of allergic disease (*153*). We conclude that Th17-biased immune responses are highly attenuated in RORα-deficient mice.

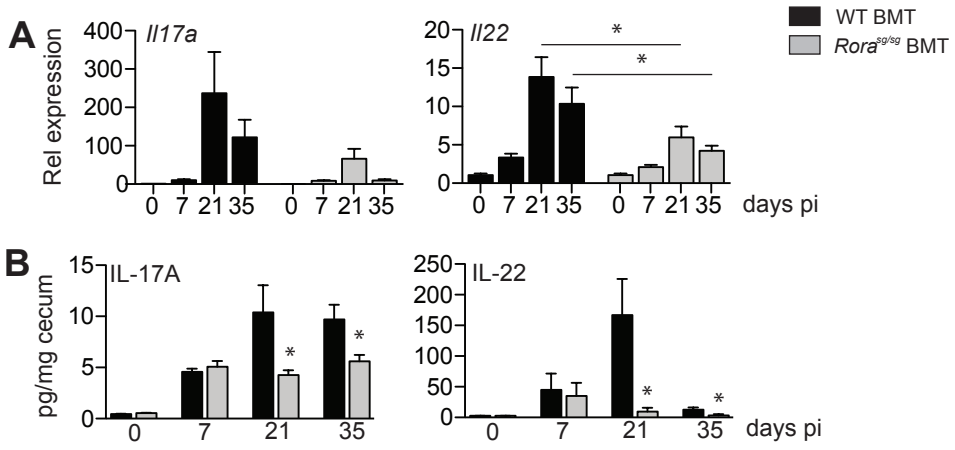

Figure 2.8. Reduced IL-17A and IL-22 levels in cecal tissue of infected *Rora*$^{sg/sg}$ BMT animals. (A) Transcripts of *Il17a* and *Il22* in WT and *Rora*$^{sg/sg}$ BMT ceca normalized to *Gapdh*. (B) Protein levels of IL-17A and IL-22 in cecal homogenates normalized to total protein. *, $p < 0.05$ (n=5-7 per group). Significance determined by unpaired student's t test.

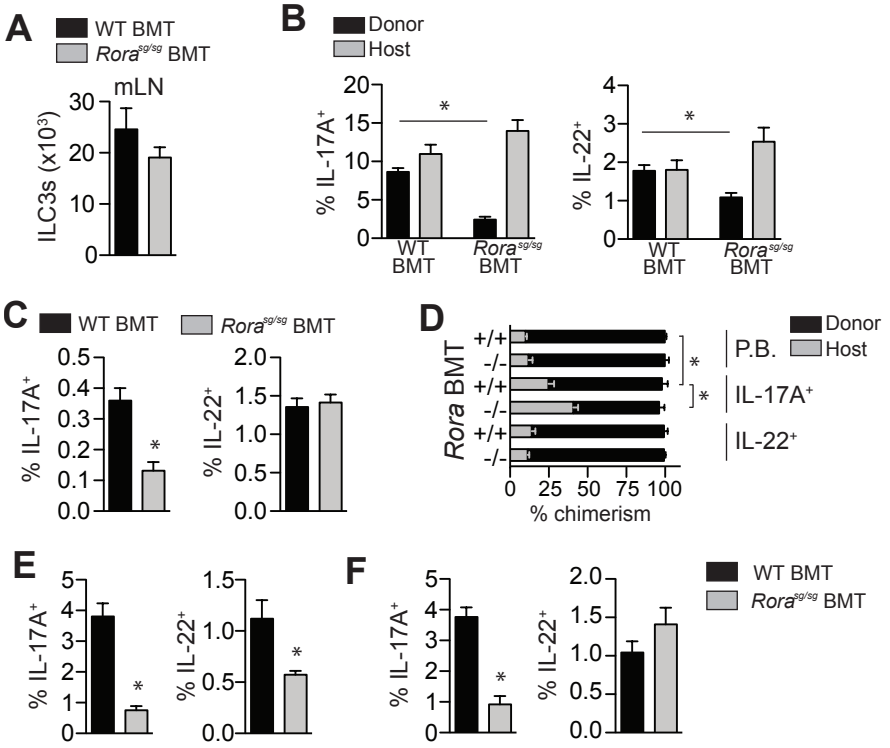

Figure 2.9. ILC3 production of IL-17A and IL-22 is *Rora* dependent in response to chronic *Salmonella* infection. (A) Total ILC3s ($CD45^+$ Lin^{neg} $CD90^{high}$ $KLRG1^{neg}$) per mLN 21 days pi. (B-D) Intracellular staining of IL-17A and IL-22 of mLN leukocyte subsets following restimulation with PMA, ionomycin, and BFA. Donor versus recipient hematopoietic cells determined by expression of congenic CD45. Percentages of $IL\text{-}17A^+$ and $IL\text{-}22^+$ mLN ILC3s (B) and $CD3e^+$ lymphocytes (C). (D) Comparison of peripheral blood chimerism with percent contribution of total $IL\text{-}17A^+$ or $IL22^+$ events from BM-donor derived versus radio-resistant recipient hematopoietic cells. Percentages of $IL\text{-}17A^+$ and $IL\text{-}22^+$ cecal ILC3s (E) and $CD3e^+$ lymphocytes (F). *, $p < 0.05$ (n=5-7 per group). Significance determined by unpaired student's t test. Significance determined by unpaired Student's *t* test.

Next, we characterized IL-17A- and IL-22-producing mLN populations by flow cytometry (Appendix 2). Total mLN ILC3 numbers were comparable in WT and *Rora*$^{sg/sg}$

BMT mLNs at 21 days pi (Fig 2.9A). Intriguingly, despite their normal frequency, we found highly attenuated IL-17A and IL-22 production in ILC3s of *Rorα*$^{sg/sg}$ BMT mice (Fig. 2.10B). This was further supported by evaluation of residual, radio-resistant WT ILC3 present in the mLN of *Rora*$^{sg/sg}$ BMT chimeric mice. These cells represented roughly 10% of the mLN ILC3 as determined by allotype marker staining and produced normal levels of IL-17A and IL-22 (Fig. 2.9B). This suggests that defective cytokine production by *Rora*$^{sg/sg}$ ILC3s is cell-intrinsic and independent of potential alterations in the composition of the inflammatory environment. Consistent with previous characterization of RORα in Th17 cells (*96*), *Rora*$^{sg/sg}$ CD3^{+} T cells isolated from mLNs of infected animals had reduced IL-17A but unaltered IL-22 production compared to WT T cells (Fig. 2.9C).

Peripheral blood analyses of BM chimeras revealed approximately 90% donor-derived CD45.2^{+} cells, and 10% CD45.1^{+} radio-resistant host-derived cells (Fig. 2.9D). More selective analyses of IL-17A^{+} mLN cells in WT BMT mice revealed 73% IL-17A^{+} cell chimerism suggesting there was a subset of tissue-specific, radio-resistant IL-17A-producing cells (Fig. 2.9D). Interestingly, these cells were more frequent in *Rora*$^{sg/sg}$ BMT chimeras, with only 55% of total IL-17A^{+} cells originating from donor BM cells. Host and donor contributions to IL-22^{+} cells in both WT and *Rora*$^{sg/sg}$ BMT mice overlapped with their respective peripheral blood chimerism indicating a lack of IL-22^{+} cell enrichment in the tissue-resident, radio-resistant population (Fig. 2.9D). Consistent with mLN cell analyses, ILC3s isolated from the ceca of *Rora*$^{sg/sg}$ BMT mice had reduced IL-17A and IL-22 production compared with WT BMT ILC3s (Fig. 2.9E); RORα-deficient cecal CD3^{+} T-cells also displayed attenuated IL-17A but normal IL-22

expression (Fig. 2.9F). In summary, we conclude that there is a clear defect in cytokine production by Th17 and ILC3 cells in *Rora*$^{sg/sg}$ BMT mice.

2.3.5 *Salmonella*-induced gut fibrosis is dependent on *Rora*$^{+}$ ILC3

To further evaluate the ILC- versus T cell-dependent contributions to fibrosis in our experimental model, we generated mixed BM chimeras by reconstituting lethally irradiated mice with equal numbers of BM cells from *Rag1*$^{-/-}$ mice combined with either WT or *Rora*$^{sg/sg}$ BM cells. The rationale was that co-transplanting *Rag1*$^{-/-}$ and *Rora*$^{sg/sg}$ BM cells would restore normal ILC3s (*Rag1*$^{-/-}$-derived) without altering the *Rora*$^{sg/sg}$–derived T cell compartment. At 21 days pi we found cecal and splenic *Salmonella* burdens in these mice were similar (Fig. 2.10A). MT-stained cecal tissues from these *Rag1*$^{-/-}$/*Rora*$^{sg/sg}$ BMT animals revealed immunopathology and fibrosis comparable to *Rag1*$^{-/-}$/WT BMT animals (Fig. 2.10B), including a similar degree of epithelial cell hyperplasia, inflammatory infiltrates, and collagen deposition in the submucosal regions, which was represented in the pathology scores (Fig. 2.10C). Further, we found similar transcript levels of *Col1a2, Tgfb1, Tnfa and Il6* in infected ceca of *Rag1*$^{-/-}$/WT and *Rag1*$^{-/-}$/*Rora*$^{sg/sg}$ BMT animals (Fig. 2.10D). Quantification of IL-17A and IL-22 in cecal homogenates indicated that these cytokines are restored to comparable levels in *Rag1*$^{-/-}$/WT BMT and of *Rag1*$^{-/-}$/*Rora*$^{sg/sg}$ BMT samples (Fig. 2.10E). In summary, these data argue that *Rora*-expressing ILC3s are sufficient to cause fibrosis.

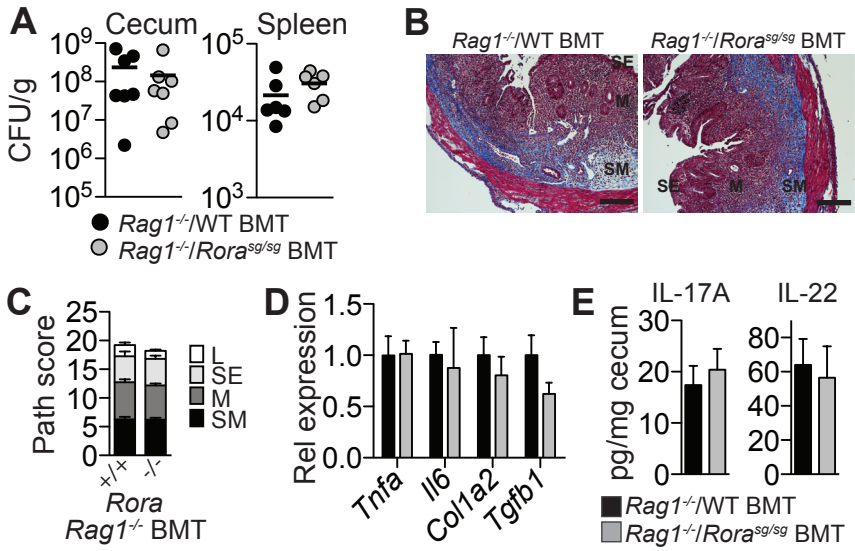

Figure 2.10. Restoring the innate cell compartment in *Rora*$^{sg/sg}$ BMT mice is sufficient to cause fibrosis. *S.* Typhimurium Δ*aroA* infection of *Rag1*$^{-/-}$/WT and *Rag1*$^{-/-}$/*Rora*$^{sg/sg}$ mixed BMT chimeras. (A) Bacterial counts of ceca and spleens 21 days pi. (B) MT-stained cecal tissue with (C) corresponding pathology scores. (D) Relative mRNA expression of *Tnfa, Il6, Col1a2*, and *Tgfb1* in infected ceca normalized to *Gapdh*. (E) IL-17A and IL-22 protein quantification in cecal homogenates. Representative data from two independent experiments (n = 5 or 7 per experiment). Scale bar, 200 μm.

2.3.6 RORα preserves ILC3 lineage identity

To gain further mechanistic insights into the role of RORα in ILC3 behavior, we isolated bulk populations of ILC3s from the mesenteric lymph nodes of WT and *Rora*$^{sg/sg}$ hematopoietic chimeric animals 21 days after *Salmonella* infection (during peak inflammation and fibrotic remodeling) and performed whole transcriptome sequencing analysis. We found a striking reduction in the expression levels of a number of ILC3-defining transcripts (*156*) including *Rorc*, and the cytokine-encoding transcripts *Il22* and *Tnf* (Fig 2.11). Furthermore, we found a substantial reduction in the expression of a number of critical cytokine receptor genes that would allow ILC3 cells to respond to their

local inflammatory milieu including receptors for IL-1β, IL-23, and IL-17. Therefore, these data would suggest that loss of RORα leads to a lesion upstream of cytokine production in ILC3s. Consistent with the down regulation of the *Rorc*, we observed an increase in the majority of transcripts uniquely associated with the "ex-Rorγt" ILC3 subset (*156*); these cells displayed an increased expression of T-bet and a reduced capacity to produce IL-17A and IL-22 (*53, 158*). This functional ILC plasticity is modulated by environmental cues and the contrasting gradient expression of T-bet and Rorγt (*53, 158*). These results indicate that RORα plays a role in preserving functional ILC3 in a chronic inflammatory setting.

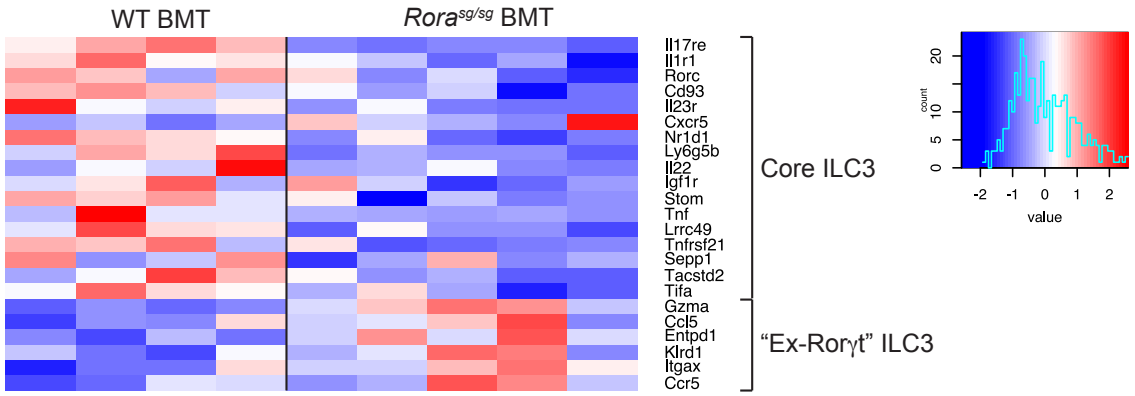

Figure 2.11. RNA-seq analysis of WT and *Rora*$^{sg/sg}$ ILC3s. Heat map ranking significantly ($P < 0.05$) altered core ILC3 and ex-Rorgt ILC3 gene signatures described previously (*156*). ILC3s defined by CD45.2$^+$ Lineage$^-$ CD90$^+$ KLRG1$^-$ were isolated from the mesenteric lymph nodes of WT BMT and *Rora*$^{sg/sg}$ BMT mice 21 days after *Salmonella* infection; each column represents an individual animal (n = 4, 5).

Next, we assessed RORα-dependent functions in integrating defined ILC3-activating signals for cytokine production. We purified leukocytes from the lamina propria of the small intestines of WT and *Rora*$^{sg/sg}$ chimeric mice and cultured them in the presence of IL-1β, IL-23, and IL-2. Consistent with the transcriptome analysis, we found

a reduction in Rorγt-expressing cells in the bulk sorted *Rora*$^{sg/sg}$ ILC3 population. Moreover, *Rora*$^{sg/sg}$ ILC3s displayed a striking defect in IL-17A expression, which suggests that they are unresponsive to IL-1β, IL-23, and IL-2 stimulation likely due to attenuated receptor expression.

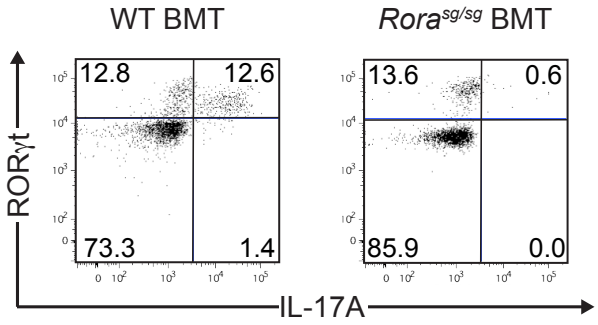

Figure 2.12. RORγt and IL-17A expression in WT and *Rora*$^{sg/sg}$ ILC3s. Cells were isolated from the small intestine lamina propria and stimulated *ex vivo* in the presence of 20 ng/mL IL-2, IL-1b, and IL-23. ILC3s (CD45^{+} Lineage^{-} CD90^{+} KLRG1^{-}) were sorted by flow cytometry and analyzed for RORγt and IL-17A expression.

2.3.7 IL-17A and IL-22 neutralization in chronic *Salmonella* infection

To determine the functions of ILC3- and Th17-derived cytokines in experimental intestinal fibrosis, we treated *Salmonella*-infected mice with neutralizing antibodies against IL-17A or IL-22. Although we found that the *Salmonella* burdens in the spleens and the ceca of isotype control and anti-IL-17A treated mice were unaltered (Fig. 2.13A), we observed reduced pathology in the ceca of animals treated with antibodies against Il-17A (Fig. 2.13B) as MT-stained cecal sections exhibited an attenuation in epithelial remodeling and fibrotic scarring (Fig. 2.13C). Moreover, IL-17A neutralization resulted

in a decrease in SM collagen accumulation (Fig. 2.13D). Our results indicate fibrosis during the late phases of chronic *Salmonella* infection is IL-17A dependent.

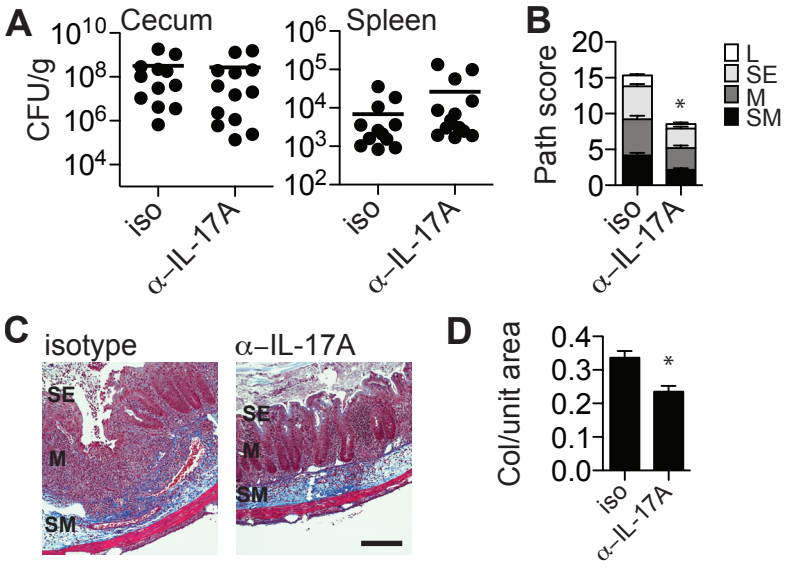

Figure 2.13. Neutralizing antibodies against IL-17A attenuates fibrosis following *Salmonella* infection. Isotype control (iso) or neutralizing antibodies against IL-17A (α-IL-17A) were administered intraperitoneally to infected mice and sacrificed at day 21. (A) *Salmonella* counts in ceca and spleens. (B-C) Cecal pathology scores and MT-stained tissue sections. L, lumen; SE, surface epithelium; M, mucosa; SM, submucosa.. Scale bar, 200 μm. (D) Quantification of submucosal collagen surface area normalized to total tissue surface area. *, $p < 0.05$ (n=12, 13 per group, results from two independent experiments). Significance determined by unpaired Student's *t* test.

We found that treatment with neutralizing antibodies against IL-22 did not alter *Salmonella* loads in the ceca or spleens of infected animals (Fig. 2.14A) although epithelial derived antimicrobial lectins regenerating islet-derived protein 3 (Reg3)β and Reg3γ were reduced (Fig. 2.14B). In examining tissue pathology, we found that IL-22

suppression resulted in disrupted epithelial cell organization within the mucosa and surface epithelial barrier (Fig. 2.14C, D).

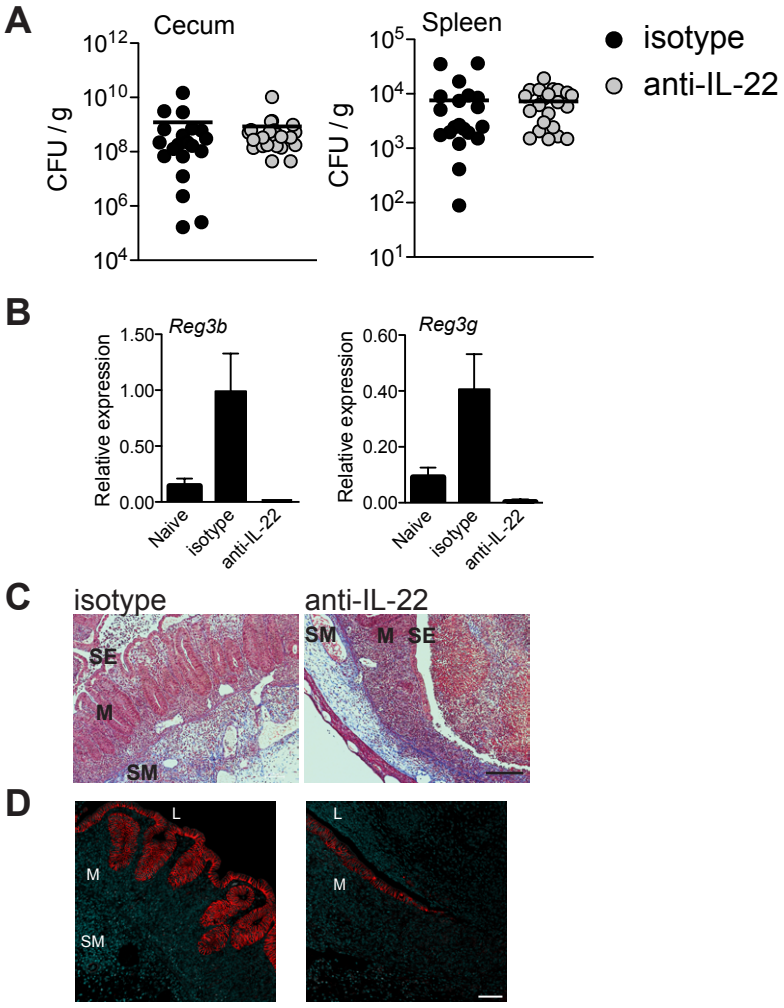

Figure 2.14. Antibody suppression of IL-22 results in disrupted epithelial barrier maintenance following *Salmonella* infection. Isotype control or neutralizing antibodies against IL-22 were administered intraperitoneally to infected mice and sacrificed at day 21. (A) *Salmonella* counts in ceca and spleens (n=20, 24, results pooled from 3 independent experiments). (B) Transcript levels of IL-22 dependent anti-microbial peptides *Reg3b* and *Reg3g* (n = 6 per group). (C) MT-stained tissue sections. L, lumen; SE, surface epithelium; M, mucosa; SM, submucosa. Scale bar, 200 μm. (D) Visualization of epithelial cells in chronically infected cecal sections by β-catenin (red) immunofluorescent staining and nuclei (cyan). Scale bar, 75 μm.

2.4 Discussion

This report provides important insights into *Rora*-dependent immune function and Crohn's-like fibrotic disease. Using a model of *Salmonella* induced intestinal fibrosis, we found that hematopoietic deletion of *Rora* protected animals from fibrogenesis in the gut. Assessment of tissue pathology and cytokine analysis during the pre-fibrotic phase at day 7 pi suggests early inflammatory responses were comparable in WT and $Rora^{sg/sg}$ BMT animals. Furthermore, *Salmonella* burdens in the gut and spleen during initial colonization were unaltered by hematopoietic *Rora* expression. These observations suggest that RORα does not influence initial inflammatory responses, or the host's ability to clear the infection, but rather plays a specific role in generating a pro-fibrotic response in the gut during late stages of chronic *Salmonella* infection. The apparent disconnect between bacterial colonization and the severity of fibrosis is consistent with previous reports which demonstrate that intestinal fibrosis does not require the presence of *Salmonella* as a persistent inflammatory stimulus (*159, 160*). Instead, the pathology becomes self-propagating and is largely irrespective of interventions that attempt to reduce pathogen burdens or repress early inflammatory responses.

Although gut fibrosis that develops following chronic *Salmonella* infection strongly correlates with a Th17 response (*51*), we initially sought to examine the contributions of type 2 immune cell-associated cytokines in fibrosis. This is relevant for several reasons. First, in a mouse model of TNBS-induced colitis, peak IL-4 and IL-13 cytokine levels were reported during the late phases of inflammation and were associated with tissue remodeling and fibrosis (*144*). Second, ILC2s are well known to recruit eosinophils by their secretion of IL-5 (*161*); eosinophilia has been linked previously to

stricture complications in CD patients and IL-13 has been reported to promote gut fibroblast activation (*150*). Therefore, while it is likely ILC2s are irrelevant during the early phase of *Salmonella* infection, their role in downstream fibrotic remodeling has not been thoroughly investigated. While we observed a profound attenuation in collagen deposition in infected *Rora*$^{sg/sg}$ BMT ILC2 deficient animals, IL-13 and IL-5 levels were not markedly altered in fibrotic gut tissue when compared to uninfected controls. In support of these observations, we found that fibrosis is not diminished in cecal tissues of infected ΔdblGATA or *Stat6*$^{-/-}$ mice, which suggests that eosinophils and STAT6 signaling as mediators of Th2 effector cell functions are dispensable for *Salmonella*-induced fibrosis. Theses findings argue strongly for a Th2/ILC2-independent role for RORα in fibrosis. In examining other eosinophil derived factors previously implicated in IBD, the reduction in *Epx1* was fully expected since infected ΔdblGATA mice lack eosinophils and therefore, this selective marker. Eosinophils are also a well-known source of TGF-β1 and therefore it is perhaps not surprising that its production is lower in these animals. The fact that loss of eosinophils as a source of TGF-β1 has no effect on the fibrotic outcome, however, is intriguing. One could argue that the residual levels of TGF-β1 we observed in the eosinophil-deficient mice was necessary but not sufficient to induce fibrosis and that a second signal was required. Based on our antibody suppression experiments we would argue that IL-17A is one such factor and a critical driver of fibrotic disease.

Consistent with a previous report identifying RORα as an important transcriptional mediator of Th17 cell cytokine production (*96*), we found that IL-17A and IL-22 levels were diminished in infected cecal tissue of *Rora*$^{sg/sg}$ BMT mice compared

with WT samples. Interestingly, normal IL-17A and IL-22 production by ILC3s was *Rora* dependent while IL-17A expression by T cells was also impaired in *Salmonella*-infected *Rora*$^{sg/sg}$ BMT animals. This defect in cytokine production by RORα-deficient ILC3s and Th17 cells was further illustrated by a ~50% increase in the relative proportion of radio-resistant, host-derived IL-17^{+} cell numbers in mLNs of *Rora*$^{sg/sg}$ BMT animals when compared to WT controls. The persistence of WT radio-resistant subsets represents a caveat in our BMT model. However, despite the presence of a larger relative population of IL-17A producing radio-resistant host-derived cells, the cumulative effect of deleting *Rora* in donor cells was sufficient to attenuate the fibrotic phenotype. To delineate the contributions of ILC3s and Th17 cells to the phenotype in our disease model, we restored WT innate cells by co-transplanting mixed *Rag1*$^{-/-}$ and *Rora*$^{sg/sg}$ BM cells into recipient animals. Following *Salmonella* infection, these mice developed fibrotic disease in the gut and had IL-17A and IL-22 levels similar to their *Rag1*$^{-/-}$/WT BMT counterparts. These data demonstrates that ILC3s are sufficient to cause fibrosis, but does not formally rule out an additional role of Th17 cells. New technological approaches to selectively deplete ILC3s or ablate *Rora* in ILC3s would be necessary to definitively address this question.

While we have shown that antibody mediated neutralization of IL-17A protected against fibrosis in a *Salmonella*-induced model, the clinical importance of these findings may be questioned since anti-IL-17A antibody treatment failed as a therapy in a clinical trial of Crohn's disease patients due to lack of efficacy and adverse side effects (*162*). However, Crohn's disease manifests itself in many ways and fibrosis is only detected in a subset of these patients. Importantly, patients with "stricture causing obstructive

symptoms" were excluded from this clinical trial. With this in mind, we would argue that the effects of anti-IL-17A on stricture formation and maintenance in humans remain an open question and that further study is justified.

Although RORα and RORγt are related members of a subfamily of nuclear orphan receptors, each possess distinct and some overlapping functions in hematopoietic development. Unlike *Rorc* deletion, which ablates ILC3s and Th17 cells, the effect of *Rora* deletion on these subsets appears to be far more subtle and limited to an attenuation of cytokine production. There has been strong interest in developing RORγt inhibitors as a therapy for Th17- or ILC3- mediated disorders (*114, 163, 164*). However, there are some concerns with this strategy as $ROR\gamma t^{+}$ regulatory T cells were found to be critical in limiting disease severity in experimental colitis (*100, 165*). Moreover, RORγt regulates thymocyte differentiation and aged $Rorc^{-/-}$ mice exhibit a very high frequency of T cell lymphoma (*166*). Our findings argue that RORα may serve as a more attractive therapeutic target for Crohn's disease associated fibrosis and that development of selective inhibitors of RORα (that spare RORγt) is warranted.

Chapter 3.

Loss of vascular CD34 results in increased sensitivity to lung injury

3.1 Introduction

Although the adult lung has a robust capacity to regenerate following acute injury, dysregulation of normal wound healing processes leads to fibrosis and loss of organ function. These observations have prompted extensive studies into the identification of lung progenitor populations capable of facilitating lung repair (*68, 167*). The cell surface sialomucin CD34 is a widely used marker for the enrichment of primitive multipotent hematopoietic cells for bone marrow (BM) transplantation (*168, 169*). More recently, its utility as a marker for progenitor cells has been extended to non-hematopoietic subsets including muscle satellite cells (*118*), hair follicle stem cells (*117*), multipotent stromal cells (*170, 171*), bronchoalveolar stem cells (BASCs) (*172, 173*) and lung-resident endothelial progenitors (*174*). Since CD34 is highly expressed by multiple progenitor populations and downregulated in differentiated states, it has been hypothesized that CD34 may play a role in cycling of undifferentiated precursors (*115*), but functional studies instead suggest that CD34 is an important regulator of cell adhesion and chemotaxis. In lymphoid tissues, a distinct glycoform of CD34 is expressed by high endothelial venules (HEVs) and serves as a ligand for L-selectin on lymphocytes thereby mediating naïve cell recruitment to lymph nodes (*122*). While this suggests that CD34 can, in some cases, facilitate adhesion, this glycoform of CD34 is exquisitely specific to rare HEVs and, thus, is unlikely to promote adhesion in other tissues. We and others have noted that CD34 is also expressed by a number of more mature hematopoietic

subsets including eosinophils (*125, 126*), mast cells (*123, 125, 175*), dendritic cell (DC) precursors (*124*), fibrocytes, and circulating endothelial progenitors (*176, 177*). Intriguingly, deletion of CD34 in mast cells results in homotypic aggregation suggesting an alternate role as a blocker of adhesion (*123*). We have also noted impaired chemokine-dependent migration of DCs and eosinophils arguing for a role in facilitating cell mobility and chemotaxis (*124, 125*). Consistent with these observations, *Cd34*$^{-/-}$ mice are resistant to a variety of mucosal inflammatory diseases (allergic lung inflammation, hypersensitivity pneumonitis, and colitis) due to defective inflammatory cell recruitment to peripheral tissues (*124-126, 178*). While this suggests an important role for CD34 in inflammatory cell trafficking, its function on non-hematopoietic cells and structural cells during tissue remodeling remains unknown.

Because CD34 is expressed by a variety of cells thought to mediate lung regeneration (epithelial, vascular and stromal cells) we have now investigated its function in two models of lung injury. Bleomycin (BLM) exposure results in damage to pneumocytes and endothelia and is characterized by an inflammatory phase and vascular leakage followed by the accumulation of extracellular matrix (ECM) in the parenchyma resulting in abnormal alveolar architecture and compromised function (*68, 85, 179*). Based on the well-documented contribution of chronic inflammation to dysregulated tissue repair, we speculated that *Cd34*$^{-/-}$ mice would be protected from the development of fibrosis. Surprisingly, we found instead that *Cd34*$^{-/-}$ mice were extremely sensitive to BLM-induced damage and exhibited a higher incidence of morbidity and mortality than their wild type counterparts. Ultrastructure analyses of BLM-treated *Cd34*$^{-/-}$ mice revealed severe interstitial edema in the alveolar walls and delamination of endothelial

cells from the basal lamina. Similar experiments with BM chimeric mice indicate that sensitivity to BLM was due to the selective loss of CD34 on non-hematopoietic cells. While *Cd34*$^{-/-}$ mice were equally adept at controlling influenza infection, they exhibited more pronounced evidence of epithelial remodeling. In aggregate, these studies argue that, in contrast to its pathological role in facilitating hematopoietic cell recruitment to sites of inflammation on endothelial cells, CD34 plays a protective role in maintaining vascular integrity and basal lamina adhesion and thereby facilitates tissue repair.

3.2 Materials and Methods

3.2.1 Mice and bone marrow transplants

C57BL/6J (WT), *Cd34*$^{-/-}$, B6.SJL-Ptprc^{a}Pepc^{b}/BoyJ (CD45.1), and B6.129S4-Pdgfra$^{tm11(EGFP)Sor}$/J (PDGFRα ^{EGFP}) mice were maintained under specific pathogen-free conditions at the Biomedical Research Centre (UBC). Chimeric mice were generated by transplanting 10^7 nucleated BM cells isolated from mice expressing CD45.2 (WT or *Cd34*$^{-/-}$) or CD45.1 intravenously (i.v.) into lethally irradiated (11-12 Gy) CD45.1 or CD45.2 recipients. All procedures were approved by the Animal Care Committee of the University of British Columbia and conducted under guidelines for conducting ethical animal research provided by the Canadian Council on Animal Care.

3.2.2 Lung injury models

Mice were challenged with bleomycin (BLM) (PPC, ON, Canada) endotracheally (e.t.) at a dose of 2.5 or 5.0 U/kg, or i.v. at a dose of 1.6 U/mouse. Static lung elastance

was measured by performing volume-regulated perturbations on anesthetized and tracheotomized mice using a flexiVent apparatus (SCIREQ, QC, Canada) (*180*). For the lung infection model, mice were infected intranasally with 2.90 x 10^3 50% egg infective dose (EID_{50}) of influenza A/strain PR8 (H1N1).

3.2.3 Histology and immunohistochemistry

Formalin-fixed and paraffin-embedded lung tissues were cut into 5 μm sections for Masson's trichrome or hematoxylin and eosin staining. For immunostaining, lung sections underwent antigen retrieval and were stained using antibodies against CD34 (RAM34) (eBiosciences), podocalyxin (AF1556) (R&D Systems), GFP (ab13970) (Abcam), vimentin (ab92547) (Abcam), surfactant protein C (Millipore), E-cadherin (36/E-cad) (BD Biosciences), and keratin 5 (Poly9059) (Biolegend). Sections were then incubated with AlexaFluor-conjugated secondary antibodies and mounted using Prolong Gold Antifade with DAPI (Life Technologies). Optical z-stack images were captured on a Leica SP5X confocal microscope and morphometric analysis was performed using ImageJ.

3.2.4 Transmission electron microscopy

Animals were euthanized by intraperitoneal injection of avertin and lungs were fixed in 2.5% glutaraldehyde in 0.1 M cacodylate buffer. Tissues were processed for sectioning as described previously (*181*) and imaged using a FEI Tecnai 12 Transmission Electron Microscope.

3.2.5 Flow cytometry analysis

Bronchoalveolar lavage fluid (BALF) was collected by three consecutive tracheal instillations and aspirations of 1 mL phosphate buffered saline (PBS). For analysis of lung cells, tissues were digested with collagenase D (1.5 U/mL) and dispase II (2.4 U/mL) (Roche) for 30 minutes. Samples were then incubated with anti-CD16/32 (2.4G2) to block nonspecific antibody binding. Fluorescence-conjugated antibodies to CD45 (I3/2), CD11c (N418), CD3e (145-2C11), CD8 (53.67), CD4 (GK1.5), B220 (RA3-6B2), Ly6B (7/4) (Abcam), SiglecF (E50-2440) (eBiosciences), CD34 (RAM34) (eBiosciences), CD31 (390) (eBiosciences), PDGFRα (APA5) (eBiosciences), Sca1 (D7) (eBiosciences), and EpCAM (G8.8) (eBiosciences) were used. For the EdU uptake experiments, mice were given 1 mg EdU daily by intraperitoneal injections over the disease course; EdU detection was performed using the Click-IT assay kit (Life Technologies). Data was acquired on a BD LSRII and analyzed with FlowJo Software. All antibodies were generated in-house (UBC AbLab) unless otherwise indicated.

3.2.6 Quantitative RT-PCR

Total RNA was isolated from lung tissues using TRIzol (Life Technologies) and reverse transcribed with a high-capacity complementary DNA reverse transcription (RT) kit (Thermo). Gene expression was assessed on an AB7900 RT-PCR system (Applied Biosystems) by quantitative real-time polymerase chain reaction (PCR) using SYBR Green chemistry (KAPA) and gene specific primer pairs (Appendix 1).

3.2.7 Statistics

Survival data are presented as Kaplan-Meier curves and analyzed with a log rank test. All other results are expressed as mean values +/- standard error of mean (SEM) and compared using unpaired Student's *t* test.

3.3 Results

3.3.1 Early mortality but unaltered fibrosis in *Cd34*$^{-/-}$ mice following BLM challenge

To assess the role of CD34 in acute lung injury and fibrosis, *Cd34*$^{-/-}$ and WT control mice were treated endotracheally with a single dose of BLM. Strikingly, after administration of 5.0 U/kg or 2.5 U/kg of BLM (e.t.), *Cd34*$^{-/-}$ mice showed a significant dose-dependent increased frequency of mortality compared with WT controls (Fig 3.1A, B). Nearly all mortality in *Cd34*$^{-/-}$ mice at the 2.5 U/kg BLM dose occurred prior to day 10. Since the onset of fibrosis in this model is known to occur at approximately two weeks following tracheal administration of BLM (*85*), these data suggest that early morbidity was associated with the acute exudative phase of the disease and independent of fibrosis. To further corroborate *Cd34*$^{-/-}$ mouse sensitivity to BLM in a systemic treatment regime, we assessed animal response following intravenous administration of 1.6 U/mouse BLM. Again, *Cd34*$^{-/-}$ mice experienced significantly greater weight loss than WT controls with nearly all *Cd34*$^{-/-}$ animals reaching their humane endpoint by day 6 (Fig 3.1C). In summary, we conclude that CD34 plays a protective role in lung injury prior to the development of fibrosis.

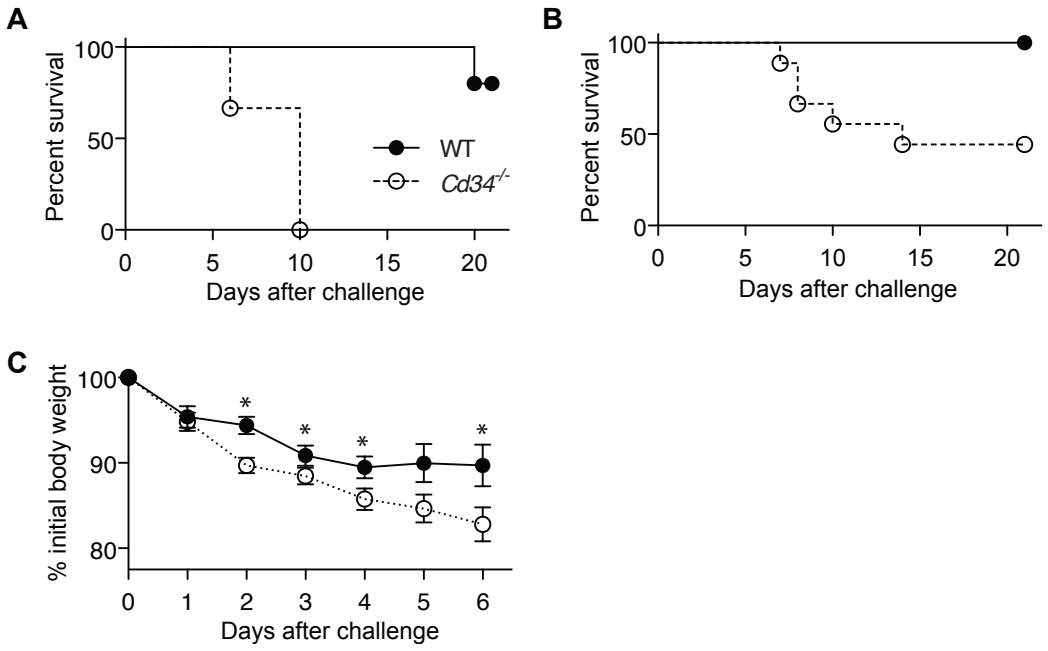

Figure 3.1. BLM-treated *Cd34*$^{-/-}$ mice have increased incidence of mortality and weight loss. Mortality rates of WT and *Cd34*$^{-/-}$ mice challenged with single dose of (A) 5.0 U/kg or (B) 2.5 U/kg BLM (e.t.). (A) $P < 0.001$ (n=3 or 5 per group). Data are from a single experiment. (B) $P < 0.02$ (n=8 or 9 per group). One of two independent experiments. Significance determined by log-rank test. (C) Weight loss of WT and *Cd34*$^{-/-}$ mice following treatment of 1.6 U/mouse BLM (i.v.). *$P < 0.05$ (n=7-9 per group). Plots shown are representative of two independent experiments.

Although there was a clear increase in early mortality in *Cd34*$^{-/-}$ mice, sufficient numbers of these mice tolerated the lower dose of BLM to permit the evaluation of lung fibrosis 21 days after treatment. Quantitative analyses of Masson's trichrome stained lung sections revealed similar degrees of fibrotic remodeling in WT and *Cd34*$^{-/-}$ animals (Fig. 3.2A, B). Employing airway perturbation maneuvers, we found that static elastance was similar in BLM-treated WT and *Cd34*$^{-/-}$ animals suggesting that loss of CD34 did not alter this functional outcome of fibrosis (Fig. 3.2C). To eliminate the possibility of a biased assessment of fibrosis selectively in mice that survived initial lung damage, we

also evaluated WT and *Cd34*$^{-/-}$ mice after endotracheal treatment with a lower BLM dose (1.25 U/kg) to ensure 100% survival by day 18 post-treatment. Again, no significant differences in fibrotic indices were observed between WT and *Cd34*$^{-/-}$ animals (Appendix 3). We conclude that loss of CD34 exacerbates the early phase of BLM-induced injury but has no effect on the later fibrotic responses.

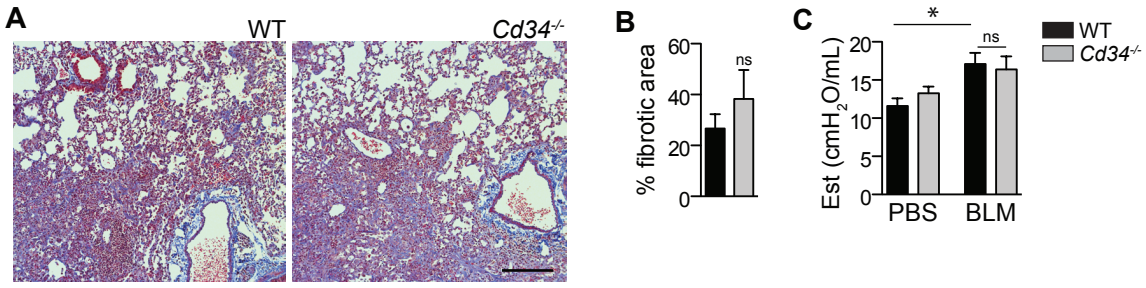

Figure 3.2. BLM-treated *Cd34*$^{-/-}$ mice have comparable fibrotic responses to WT mice. (A) Representative Masson's trichrome-stained lung sections of WT and *Cd34*$^{-/-}$ mice 21 days after BLM treatment (2.5 U/kg). Scale bar = 200 μm. (B) Percent fibrotic area determined by quantifying area of fibrotic lesions normalized to total tissue area. (C) Static elastance (Est) measurements of PBS and BLM-treated WT and *Cd34*$^{-/-}$ mice. *$P <$ 0.05.

3.3.2 CD34 does not significantly alter acute lung inflammation in response to BLM

Because we have previously observed attenuated allergic inflammatory responses in the lungs of *Cd34*$^{-/-}$ mice (*124, 125*), we evaluated whether the acute inflammation that occurs immediately after BLM-treatment was altered by loss of CD34. We observed similar levels of transcripts for pro-inflammatory cytokines tumor necrosis factor alpha (*Tnfa*) and interleukin 6 (*Il6*) in damaged lung tissue of *Cd34*$^{-/-}$ and WT animals 3 and 6 days after damage (Fig. 3.3A). Total numbers of CD45^{+} infiltrating leukocytes in the

BALF were similar in both WT and *Cd34*$^{-/-}$ mice three and six days after BLM-induced damage (Fig 3.3B). Differential analyses revealed equivalent frequencies of macrophage, neutrophil, and lymphocyte subsets (Fig 3.3C). The only significant alteration was a decrease in the frequency of infiltrating eosinophils (representing <3% of the infiltrate in WT mice and <1% in *Cd34*$^{-/-}$ mice) six days after BLM challenge (Fig. 3.3C). This likely reflects a previously documented role of CD34 in the recruitment of eosinophils to the lung (*125, 141*). In summary, because of the similar degree of acute inflammation, we conclude that differences in infiltrating inflammatory cells is unlikely to account for the increased mortality in BLM-treated *Cd34*$^{-/-}$ mice.

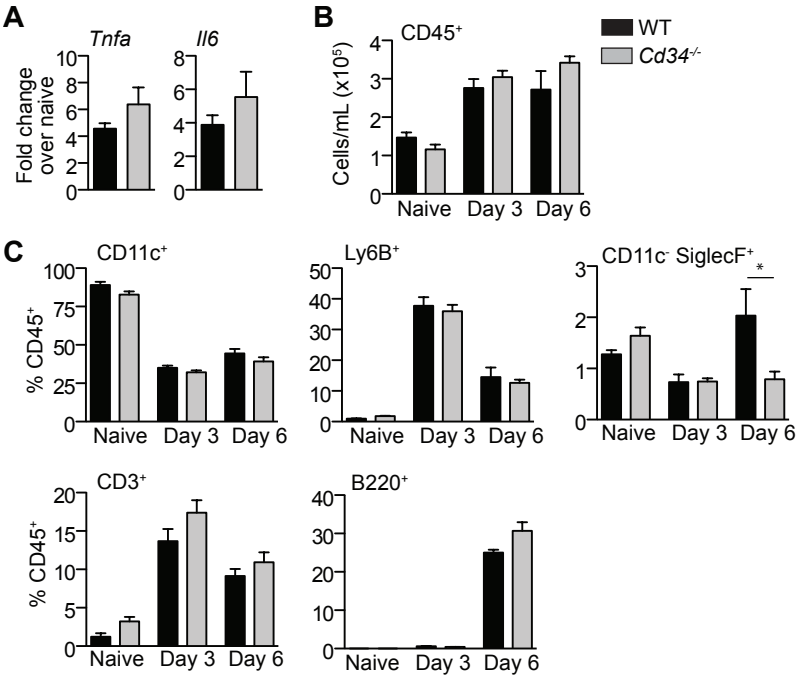

Figure 3.3. BLM-induced acute lung inflammatory response is comparable in *Cd34*$^{-/-}$ and WT mice. (A) Enumeration of total CD45^{+} hematopoietic cells in the BALF of mice treated with PBS (naïve) or BLM (mice were sacrificed and tissues harvested Day 3 or 6 post-treatment as indicated). (B) Differential analysis of infiltrating leukocyte subsets in

the BALF by flow cytometry using the surface markers $CD11c^+$ (myeloid cells), $Ly6B^+$ (7/4) (neutrophils), $CD11c^-$ $SiglecF^+$ (eosinophils), $CD3e^+$ (T lymphocytes), and $B220^+$ (B lymphocytes). (C) Relative expression (R.E.) of *Il6* and *Tnfa* in lung tissues of WT and *Cd34*$^{-/-}$ mice 6 days after BLM challenge; R.E. is normalized to *Gapdh* and shown as fold change over naïve samples. $*P > 0.05$ (n=4-7); representative data from two independent experiments. Significance was determined by unpaired Student's *t* test.

3.3.3 Severe interstitial edema in BLM-treated *Cd34*$^{-/-}$ mice

Morbidity within the first week of BLM treatment can also be attributed to exacerbated exudative responses during acute lung injury; such pathological features include disruption of endothelial and epithelial barriers resulting in leakage of circulatory contents into the interstitium and edema (*179, 182*). We have previously demonstrated increased vascular leak in lungs of *Cd34*$^{-/-}$ animals in a model of occupational asthma (*124*). To further evaluate CD34 function in the maintenance of vascular integrity, we analyzed WT and *Cd34*$^{-/-}$ lungs at the ultrastructure level by TEM before and after BLM treatment. In PBS-treated WT and *Cd34*$^{-/-}$ lungs, TEM evaluation did not reveal profound differences in the structure or localization of interstitial collagen and elastin, alterations in capillary endothelial or type I epithelial tight junctions, or cell-basal lamina interactions (Appendix 4). In contrast, six days after BLM challenge, we detected hypertrophy of type 1 pneumocytes in both WT and *Cd34*$^{-/-}$ lung sections, which was indicative of injury (Fig. 3.4A-F). Strikingly, BLM-treated *Cd34*$^{-/-}$ lung specimens exhibited extensive edema within the interstitium and delamination of the endothelia as evidenced by the exposed interstitial collagen and the disruption in the epithelial and capillary endothelial basal lamina interactions. Thus, the ultrastructure data suggests that CD34 plays a role in maintaining appropriate structural integrity of the alveolar wall in

response to acute damage.

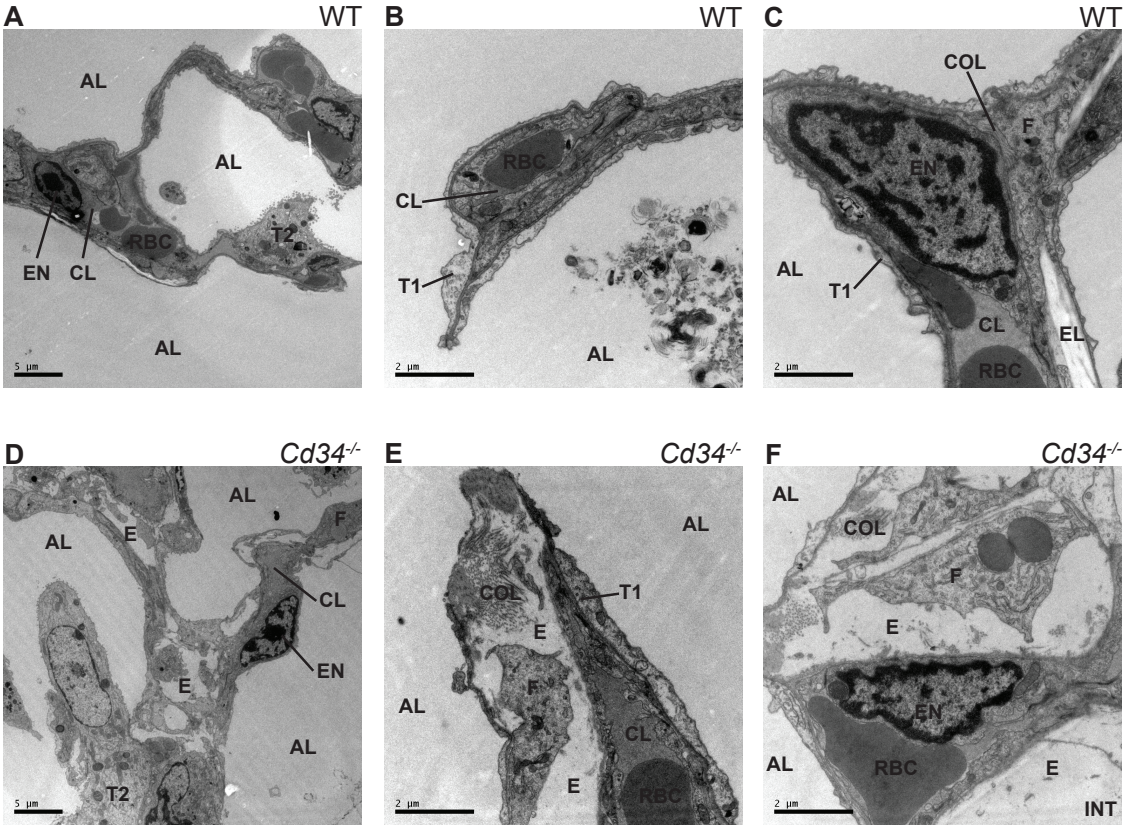

Figure 3.4. Lung tissue ultrastructure reveals severe interstitial edema in BLM-challenged *Cd34*$^{-/-}$ mice. Transmission electron micrographs of (A-C) WT and (D-F) *Cd34*$^{-/-}$ lung 6 days after BLM-induced lung injury. Images shown are representative of at least 50 fields of view per sample. Lung specimens were sampled from four mice per genotype. AL, alveolus; EN, endothelial cell; F, fibroblast; T1, type 1 alevolar epithelial cell (AEC); T2, type 2 AEC; CL, capillary lumen; RBC, erythrocyte; COL, collagen; EL, elastin; INT, interstitium; E, edema.

3.3.4 CD34 is expressed by endothelia and resident mesenchymal subsets, but not by epithelia in normal mouse lung

While previous work has suggested that, in the lung, CD34 is expressed primarily by endothelial and mesenchymal cells, there are conflicting reports regarding the

expression of CD34 on lung epithelial progenitors (*172, 183, 184*). To address this issue, we performed immunohistochemical analyses with monoclonal antibodies against CD34 and used *Cd34*$^{-/-}$ lung samples as negative controls. CD34^{+} cells were detected in nearly all compartments of the lung except large airway epithelia, with minimal background in knockout-control sections (Appendix 5). From the analysis of confocal *z* stack images, we found that CD34 was expressed by podocalyxin^{+} vascular endothelial cells in addition to PDGFRα^{+} and vimentin^{+} fibrobroblast subsets (Fig. 3.5A, B). Co-staining with antibodies against E-cadherin (E-cad) and surfactant protein C (SfpC) indicate that CD34 is not expressed by epithelial cells in the distal airways or the bronchoalveolar duct junctions where CD34-expressing epithelial progenitors were previously reported (Fig. 3.5C) (*172*). These observations were consistent with flow cytometric data, which showed that CD34^{+} cells co-stain with the endothelial specific antigen CD31 as well as the majority of PDGFRα^{+} mesenchymal progenitors enriched by Sca1^{+} selection. Moreover, we found a lack of CD34 expression in sorted EpCAM^{+} epithelial cells (Fig. 3.5D).

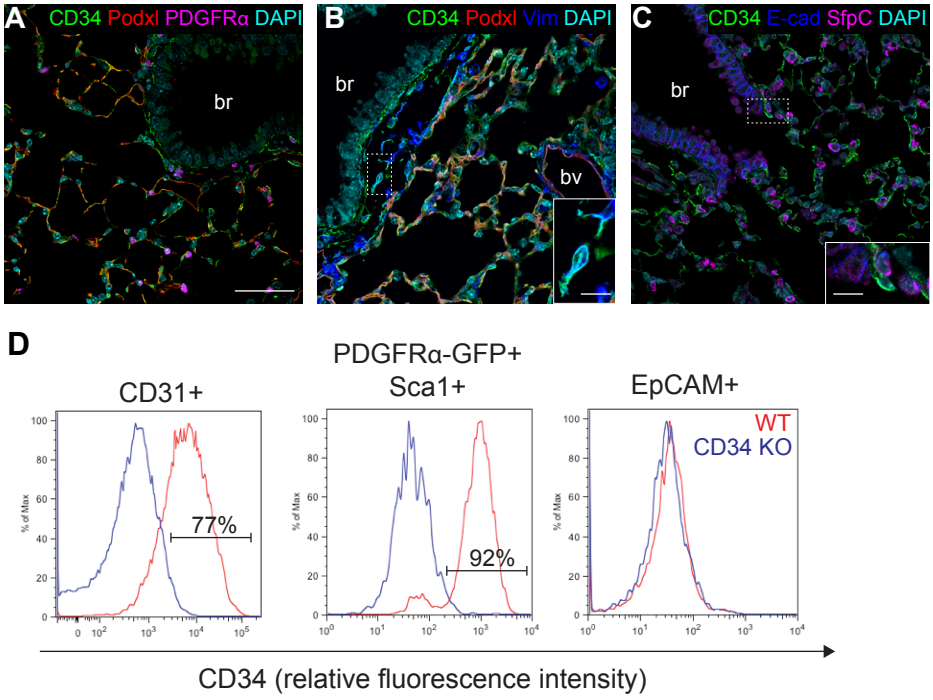

Figure 3.5. CD34 is expressed by vascular endothelia and mesenchymal subsets but not epithelial cells in naïve mouse lung. (A-C) Confocal images from z stacks demonstrating CD34 co-expression with podocalyxin (Podxl)$^+$ endothelial cells and (A) PDGFRα$^+$ and (B) vimentin$^+$ fibroblasts. (C) E-cadherin (E-cad)$^+$ and surfactant protein C (Sfpc)$^+$ epithelial cells do not express CD34; inset displays higher magnification of a bronchoalveolar duct junction (BADJ). Scale bars = 50 μm and inset scale bar = 10 μm. (D) Histograms represent relative fluorescence intensity of a CD34 specific antibody to cellular subsets gated for CD31$^+$ endothelia, PDGFRα$^+$ Sca1$^+$ fibroadipogenic progenitors (FAPs), or EpCam$^+$ epithelial cells. Bv, blood vessel; br, bronchiole.

PDGFRα$^+$ cells have previously been described in the adult mouse tibia as stromal cells that support muscle regeneration and have been termed fibro/adipogenic progenitor cells (FAPs) (*185*). Pulmonary fibroblasts represent a heterogeneous population; recent studies indicate that lung PDGFRα$^+$ cells consist of desmin$^+$ lipofibroblasts that support type 2 pneumocyte maintenance in alveolosphere cultures and proliferate in response to BLM treatment (*90, 186*). However, we saw equivalent

expansion and proliferation of this lung FAP population in WT and *Cd34*$^{-/-}$ mice, analyzed six days following bleomycin damage (Fig 3.6). We conclude that CD34 is not expressed by lung epithelial progenitors and, although it is expressed by FAPs, loss of CD34 has no effect on the proliferative response of these cells or their ability to produce matrix in late stage disease.

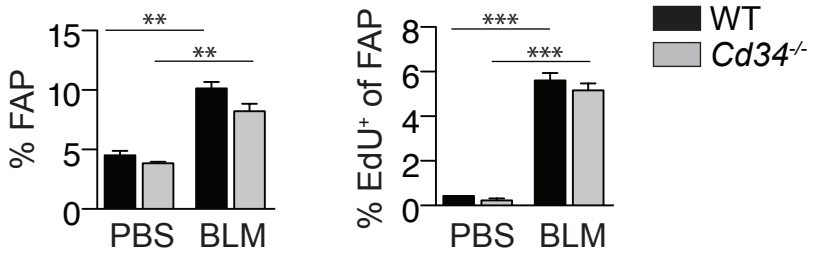

Figure 3.6. Analysis of *Cd34*$^{-/-}$ FAP proliferation in response to acute bleomycin-induced lung injury. Flow cytometric analysis of FAP percentages in the lineage negative (CD45^{-}, CD31^{-}) fraction of naïve mice (PBS) and in mice six days after BLM treatment (e.t.) (BLM). Quantification of EdU uptake indicates lung FAP proliferation in response to BLM-induced injury. $^{**}P < 0.01$; $^{***}P < 0.001$ (n = 5 or 6 per group). Significance was determined by unpaired Student's t test.

3.3.5 Early mortality in BLM-treated *Cd34*$^{-/-}$ mice is independent of its expression by hematopoietic cells

Previously, we have observed increased vascular leakage in *Cd34*$^{-/-}$ mice during autoimmune arthritis (*187*) and, thus, we hypothesize that this vascular cell intrinsic function of CD34 could contribute to the early mortality phenotype observed in the current study. To conclusively exclude the possibility that this enhanced mortality reflects a defective hematopoietic function for CD34, we generated BM chimeric mice with selective loss of CD34 in either the hematopoietic or non-hematopoietic

compartments. Following BLM challenge by endotracheal or intravenous treatment, lethally irradiated *Cd34*$^{-/-}$ mice transplanted with WT BM exhibited a significantly higher incidence of mortality and weight loss compared with the WT control recipients (Fig. 3.7A, B). Conversely, lethally irradiated WT CD45.1 animals transplanted with either *Cd34*$^{-/-}$ or WT BM and subsequently challenged with BLM displayed no significant differences in mortality rate or weight loss (Fig. 3.7C, D). These data suggest that the selective loss of CD34 from non-hematopoietic tissues contributes to increased sensitivity to BLM challenge.

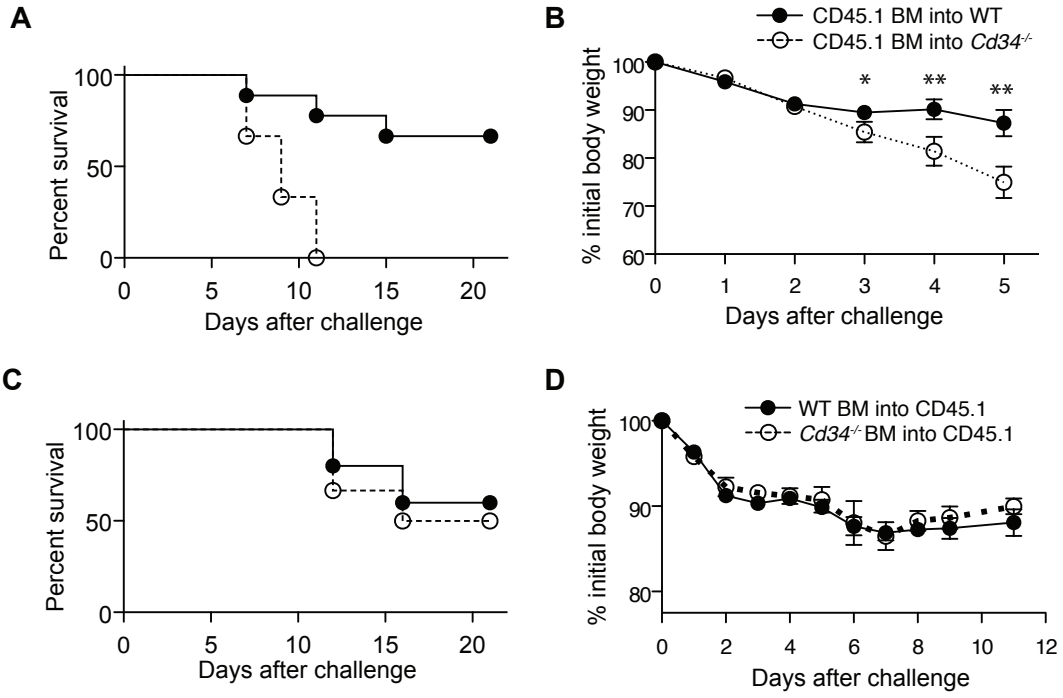

Figure 3.7. Loss of CD34 in non-hematopoietic tissues results in increased sensitivity to BLM challenge. (A) Survival curves of lethally irradiated WT or *Cd34*$^{-/-}$ mice reconstituted with CD45.1 bone marrow (BM) treated with 2.5 U/kg BLM (e.t.). *P > 0.02 (n= 6-9 per group). (B) Weight loss of lethally-irradiated WT or *Cd34*$^{-/-}$ mice reconstituted with CD45.1 BM challenged with 1.6 U/mouse BLM (i.v.) . *P > 0.05; **P > 0.01 (n=5-7 per group). (C) Survival curves of lethally-irradiated CD45.1 mice reconstituted with WT or *Cd34*$^{-/-}$ BM treated with 2.5 U/kg BLM (e.t.) (n= 5-6 per

group). (D) Weight loss of lethally-irradiated CD45.1 mice reconstituted with WT or *Cd34*$^{-/-}$ BM challenged with 1.6 U/mouse BLM (i.v.) (n=6 per group).

3.3.6 Loss of CD34 results in increased influenza infection-induced tissue remodeling

Next, we investigated whether CD34-deficiency alters responses to H1N1 influenza infection that, like BLM, induces extensive damage in the bronchioles and alveolar regions (*68*). Following intranasal infection, *Cd34*$^{-/-}$ mice displayed significantly greater weight loss than WT animals over the disease course (Fig. 3.8A). Again, the overall inflammatory responses were similar in *Cd34*$^{-/-}$ and WT animals as the total numbers of hematopoietic infiltrates in the airways were comparable at days 7 and 12 post-infection (Fig. 3.8B). Moreover, differential analyses indicate that myeloid, neutrophil, eosinophil, and lymphocyte subsets were unaltered due to loss of CD34 (Fig. 3.8C).

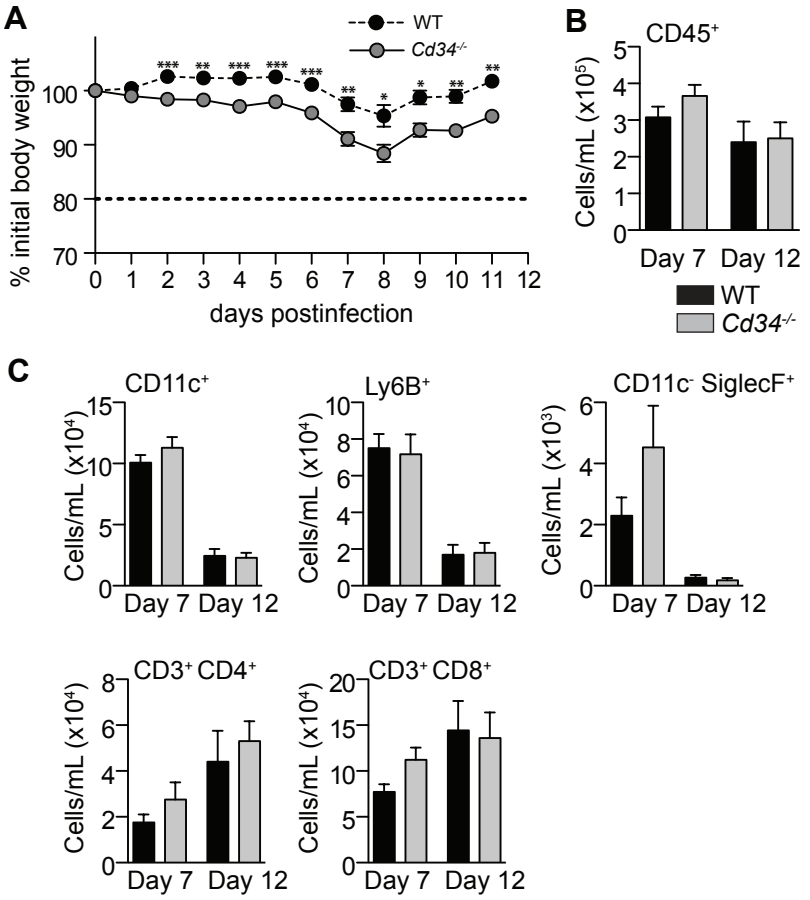

Figure 3.8. *Cd34*$^{-/-}$ mice display increased weight loss but comparable lung inflammation following influenza infection. (A) Weight loss of WT and *Cd34*$^{-/-}$ mice following intranasal infection with influenza A (PR8). **P* > 0.05; * *P* > 0.01; ****P* > 0.001 (n=8 per group). (B-C) Enumeration of total CD45^{+} hematopoietic cells and leukocyte subsets in the BALF of influenza infected mice (n = 4 or 6 mice per group). **P* > 0.05, (*n* = 8 or 10 per group).

Interestingly, however, we found greater evidence of tissue pathology in lung sections of *Cd34*$^{-/-}$ animals (Fig. 3.9A). Although keratin 5 (Krt5) positive staining was restricted to the epithelial cells in the bronchioles of WT lung sections, Krt5-expressing clusters were more abundant, appearing in the peribronchial regions and in the distal airways of *Cd34*$^{-/-}$ lung tissues arguing for greater disease severity (Fig. 3.9B). In

summary, the loss of CD34 also results in more pronounced sensitivity to influenza-induced tissue injury as evidenced by unresolved tissue remodeling.

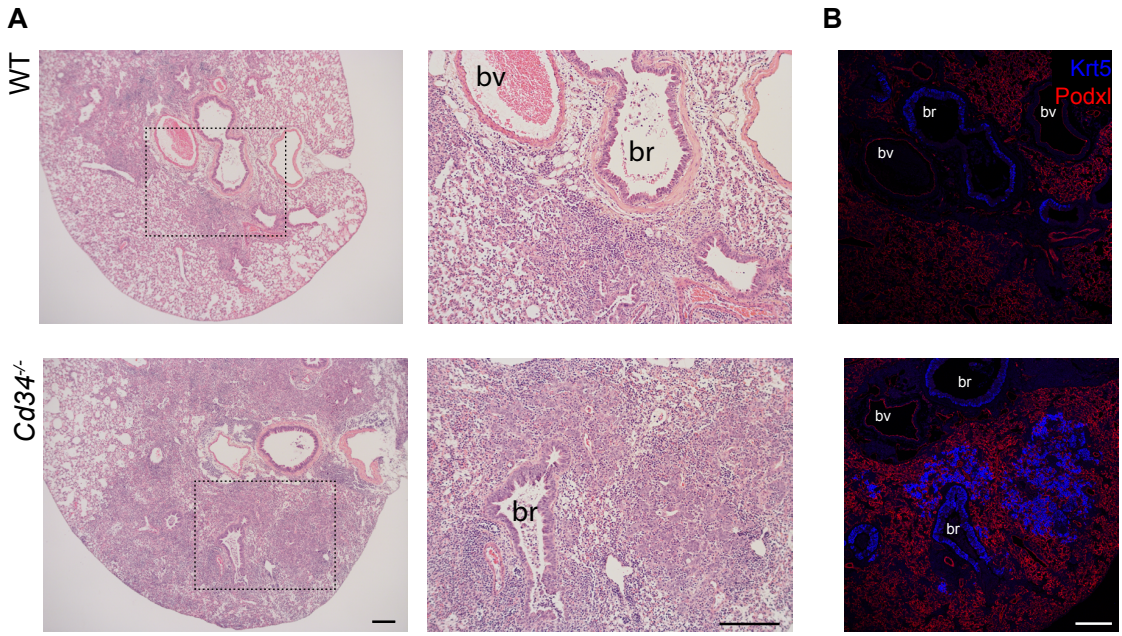

Figure 3.9. *Cd34*$^{-/-}$ mice display more pronounced tissue remodeling after influenza infection. (A) Representative hematoxylin and eosin stained lung sections of WT and *Cd34*$^{-/-}$ mice 12 days after infection. (B) Immunofluorescent images of lung sections as shown in (A) stained for podocalyxin (Podxl, red) and keratin 5 (Krt5, blue). Scale bar = 200 μm. Bv, blood vessel; br, bronchiole.

3.4 Discussion

Inflammatory mediators have a clear association with the development and progression of lung fibrosis, particularly in cases arising from exposure to environmental irritants, infection, or in patients afflicted with chronic inflammatory conditions such as graft-versus host disease, scleroderma or rheumatoid arthritis (*188*). Our previous work suggests that CD34 plays a key role in the recruitment of several inflammatory subsets during inflammation and that *Cd34*$^{-/-}$ mice exhibit attenuated pathological features of

lung or intestinal inflammatory diseases (*124-126, 178*). However, the relevance of CD34 in regulating responses to lung injury, remodeling, and fibrosis, to our knowledge, has not been examined.

Given the importance of CD34 in mast cell and eosinophil trafficking, we postulated a function in fibrotic disease (*115, 123, 125, 141*). The accumulation of eosinophils and mast cells in alveolar structures has previously been associated with a number of chronic interstitial lung disorders including idiopathic pulmonary fibrosis (IPF). Lung biopsies in IPF patients with dense fibrotic scarring appear eosinophilic (*189*) and elevated eosinophils in the BALF is associated with poor prognosis (*190*). Pathological contributions of eosinophils to IPF has been attributed to the cytotoxic factors they produce (eosinophil peroxidase, major basic protein, and eosinophil cationic protein) (*191, 192*) or, alternatively, to the release of eosinophil-derived pro-fibrogenic cytokines (IL-5, IL-13, and TGF-β1) that act directly on stromal cells and induce excessive tissue remodeling (*46, 193, 194*). Although we did indeed observe a reduced frequency of rare eosinophils recruited to the lung in *Cd34*$^{-/-}$ mice early after BLM treatment, this did not have a protective effect and the inflammatory response was unaltered. Thus, in the bleomycin model, eosinophils appear to be largely dispensable. Although eosinophilia and type 2 immune cytokines have previously been reported to be critical promoters of BLM-induced fibrosis (*193-195*), our findings are consistent with more recent studies demonstrating that fibrosis in this disease model is primarily Th17 driven and independent of IL-13 signaling (*196, 197*).

Instead of providing protection, we found that loss of CD34 renders mice extremely sensitive to BLM-induced mortality at early stages with animals displaying

severe pulmonary interstitial edema. More surprisingly, we found that nearly all incidences of morbidity and mortality occur prior to the appearance of scarring and lesions in the lungs and that the late phase fibrosis and tissue remodeling is equivalent in WT and *Cd34*$^{-/-}$ mice that survived the treatment. Because the single-dose BLM treatment model is often associated with a transient and self-limiting fibrotic disease we can not rule out a more subtle effect of CD34 loss in more robust chronic models of fibrosis (*85*). Nevertheless, our data suggest that CD34 is dispensable for the debilitating production of matrix in response to acute lung injury and that, instead, it plays a role during a transient window after the initial inflammatory response but before the remodeling and fibrotic response. This result was confirmed in a second, influenza-driven model of lung injury where tissue remodeling is a prominent feature. Here too, CD34 appears to be dispensable during the inflammatory response, but *Cd34*$^{-/-}$ mice displayed greater weight loss and their lungs displayed a more pronounced pathology, accompanied by the appearance of Krt5^{+} epithelial clusters in the areas surrounding the bronchioles and in the distal airways. While Krt5^{+} epithelial progenitors are necessary for regeneration to restore gas exchange, their accumulation may also be indicative of increased susceptibility to damage or unresolved tissue remodeling (*198, 199*).

Previously we have noted that loss of CD34 results in altered vascular integrity in a number of inflammatory settings including autoimmune arthritis (*187*), hypersensitivity pneumonitis (*124*), and tumour formation (*200*). Many pro-inflammatory mediators such as TNFα and are known to increase vascular permeability by altering adherens junction complexes and integrin-dependent adhesion to matrix proteins (*201*). Because we observed no major differences in the number of BALF infiltrates or transcript levels of

pro-inflammatory cytokines in *Cd34*$^{-/-}$ and WT animals our data suggest the exacerbated interstitial edema observed in *Cd34*$^{-/-}$ animals is a cell intrinsic defect of the endothelium. BM chimera experiments further support a non-hematopoietic origin of this phenotype as the mortality occurred in the absence of CD34 on hematopoietic cells. Vascular integrity can be modulated by changes in junctional proteins that alter cell-cell interactions and integrin-dependent cell-matrix interactions (*202*). Consistent with altered integrin dependent adhesion, but normal cell junctions, TEM evaluation of BLM-challenged *Cd34*$^{-/-}$ lungs revealed extensive interstitial edema and vascular leak yet the endothelial-endothelial junctional complexes remain intact. Thus, our data suggest that CD34 plays a role in maintaining the integrity of endothelial adhesion to the basal lamina.

In many ways, the decreased adhesion of *Cd34*$^{-/-}$ endothelia to basal lamina is counter-intuitive. Previously we have shown that CD34 and its close relative, podocalyxin (Podxl), are heavily-glycosylated and negatively-charged sialomucins that provide an anti-adhesive quality to hematopoietic cells, developing endothelia and epithelial tumor cells (*115, 121, 123, 203, 204*). It is noteworthy, however, that we and others have found that, on endothelial and epithelial cells, the anti-adhesive Podxl and active integrin signaling cooperate to facilitate the establishment of distinct integrin-linked basolateral/matrix bound surfaces and integrin-free, Podxl-rich, non-adhesive apical domains (*115, 203, 205, 206*). Thus, loss of CD34 or Podxl would be predicted to impede the sorting of integrins to the sites of cell-matrix interaction and weaken vessel integrity; an effect that we observe via TEM analyses of *Cd34*$^{-/-}$ endothelia after BLM treatment. Future studies aimed at detailed structure function analyses may provide mechanistic insights into the functional domains of CD34 required for modulating

integrin sorting and function.

CD34 is commonly used as a marker for progenitor subsets of multiple non-hematopoietic cell types including muscle satellite cells, hair follicle stem cells, and mesenchymal progenitors (*117, 118, 170, 171*). It has recently been postulated that its utility as an enrichment marker for undifferentiated cells could be extended to an epithelial stem cell population of the lung, namely bronchoalveolar stem cells (BASCs). These cells are proposed to exist at bronchoalveolar duct junctions (BADJs) and have the potential to give rise to terminal epithelial cells of both the large and distal airways (*172*). However, subsequent lung fractionation studies have reported that epithelial lineages lack CD34 expression (*184, 207, 208*). In the current study, we have used *Cd34*$^{-/-}$ mice, immunofluorescence staining of tissue sections, and spatial localization in lung to address this issue. By confocal analyses of naïve lung, we do not observe co-expression of CD34 and epithelial markers SFPC and E-cadherin in BADJ regions. This is corroborated by flow cytometric data suggesting the absence of CD34 expression by any EpCam^{+} epithelial fraction of lung derived cells, a subpopulation believed to contain epithelial progenitor cells (*207*). As epithelial cells are well known for their non-specific binding of macromolecules (such as antibodies), it is possible that earlier reports of specific staining were technical artifacts. Instead, our data suggest that CD34 is expressed by vascular endothelia and mesenchymal cells including vimentin^{+} fibroblasts and FAPs (phenotyped by PDGFRα^{+} Sca1^{+} expression). FAPs were previously characterized as stromal cells that support skeletal muscle regeneration, and were more recently described in the lung as desmin^{+} lipofibroblasts of the alveolar niche with an analogous function (*185, 186*). Previously we found that CD34 is dispensable for normal function of muscle

resident FAPs (*209*). This is consistent with our observations that lung FAPs, in an acute response to BLM, expanded in similar numbers and displayed similar rates of proliferation in WT and *Cd34*$^{-/-}$ animals.

In summary, our data suggest that vascular CD34 serves a protective function during acute lung injury by enhancing the endothelial/matrix interactions and thereby preventing delamination and reducing permeability. Future structural and functional studies designed to identify the requisite domains of the molecule could offer insights into how this function could be modulated to treat acute pulmonary edema.

Chapter 4.

Summary and future perspectives

4.1 Research summary and significance

The objective of this thesis was to characterize inflammatory modulators, which contribute to fibrotic scarring in mucosal tissues. Given the longstanding interest in type 2 immune responses associated with dysregulated wound healing and fibrosis (particularly in host defense tolerance strategies against parasitic infections), we focused on two components of this inflammatory pathway that could potentially be targeted for therapeutic applications: the transcription factor RORα, which is critical for ILC2 development and CD34, a cell surface sialomucin required for efficient migration of eosinophils and mast cells to peripheral sites.

The work presented in chapter 2 demonstrates that *Rora*$^{sg/sg}$ BMT animals were protected from *Salmonella*-induced intestinal fibrosis; surprisingly, this phenotype was due to a reduction in ILC3 and Th17 derived cytokines. Additional experiments with mixed *Rora*$^{sg/sg}$ and *Rag1*$^{-/-}$ BM transplanted animals indicate that ILC3s were sufficient to cause fibrosis in the absence of WT T cells. Further examination of *Rora*$^{sg/sg}$ ILC3s by whole transcriptome analyses revealed downregulation of key ILC3-defining transcripts (notably *Rorc*, *Il23r*, and *Il1r*), which suggests that RORα may be required for ILC3 lineage maintenance. Together, these results argue that RORα and ILC3s could be important participants in the IL-23/IL-17 axis as it relates to fibrosis and other inflammatory diseases (Fig. 4.1).

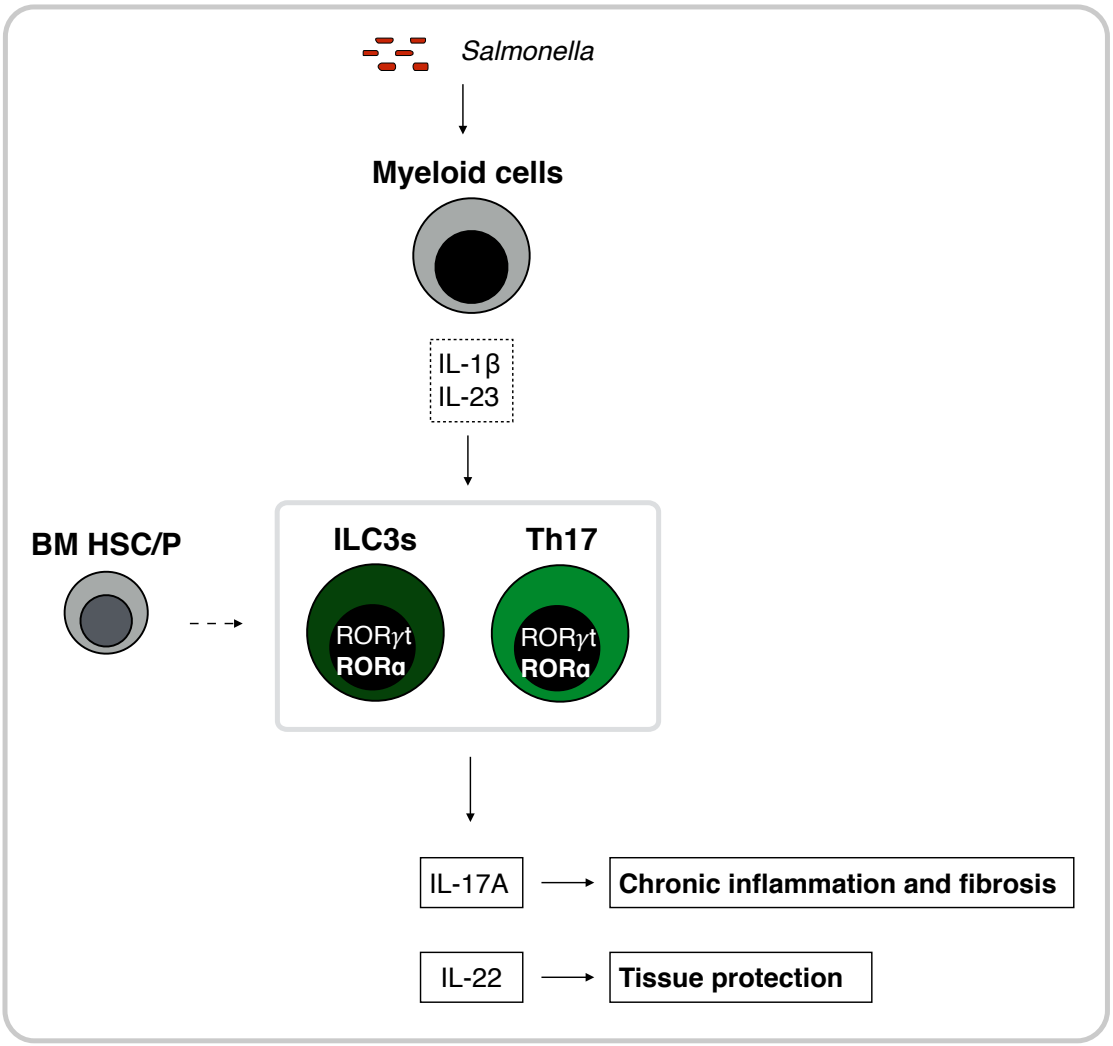

Figure 4.1. Summary of RORα and lymphoid cells in response to chronic *Salmonella* infection.

In chapter 3, we examined the role of CD34 in response to lung injury; we found that *Cd34*$^{-/-}$ mice were extremely sensitive to bleomycin-induced lung damage due to a vascular defect resulting in exacerbated edema. These findings were further supported by experiments demonstrating *Cd34*$^{-/-}$ animals reconstituted with WT BM were equally susceptible to bleomycin treatment. Furthermore, *Cd34*$^{-/-}$ mice infected with influenza virus also displayed greater weight loss and more pronounced evidence of excessive

epithelial remodeling. This work defines a protective role of CD34 in maintaining lung vascular integrity and restoring normal tissue architecture after injury and highlights the link between vascular defects and degenerative respiratory diseases.

4.2 Study limitations

The main caveats of the work presented in this thesis are associated with the fidelity of the genetic lesions in the mouse strains as they relate to the cellular functions we intended to investigate. Moreover, the clinical implications of these findings are limited by the fact that the animal disease models employed do not fully reproduce the complex features of multifactorial fibrotic diseases related to IBD and IPF.

In chapter 2, the work presented mainly relied on the selective hematopoietic deletion of RORα. This involved transplanting BM from germline knockout animals into lethally irradiated wild type recipients. In response to chronic *Salmonella* infection, we found that RORα was required for efficient cytokine production by both Th17 cells and ILC3s. We attempted to delineate the unique contributions of these two lymphoid lineages in intestinal fibrosis by co-transplanting *Rora*$^{sg/sg}$ and *Rag1*$^{-/-}$ BM. Functional ILCs in the absence of competent T cells were sufficient to restore IL-17A and IL-22 levels and a fibrotic phenotype; this suggests that ILC3s are important promoters of fibrosis. However, it is not clear if the reverse is true; whether Th17 cells can similarly cause fibrosis in the absence of ILC3s. Additional experiments employing mouse strains that are RORα-deficient specifically in ILC3s, or that lack ILC3s altogether would be necessary to definitively demonstrate that these cells are the critical mediators of intestinal fibrosis. Moreover, since RORα is well known to be required for ILC2

development, experiments with ILC3-specific perturbations could provide additional evidence that ILC2s are irrelevant in *Salmonella*-induced fibrosis.

The work described in chapter 3 indicates that vascular CD34 was required for survival following bleomycin-induced lung injury and resolution of excessive epithelial cell remodeling in response to influenza infection. Though the role of endothelial CD34 in maintaining vascular permeability has been well described in other inflammatory settings (*124, 187*), we attempted to exclude the possibility that hematopoietic CD34 may be important in lung injury responses by demonstrating similar susceptibility in *Cd34*$^{-/-}$ mice reconstituted with WT BM. However, CD34 is also highly expressed in pulmonary mesenchymal stromal cells, which have important functions in facilitating lung development and regenerative processes (*68, 76*). Although we found that fibroblast expansion and proliferation is unaltered in *Cd34*$^{-/-}$ mice in response to bleomycin-induced injury, the examination of endothelial-specific CD34-null animals in lung injury models would be necessary to definitively exclude the functional contributions of CD34^{+} stromal cells in this model.

4.3 Future perspectives

We demonstrate that ILC3s lacking RORα have a reduced capacity to produce IL-17A and IL-22 in response to chronic *Salmonella* infection. RNA sequencing of sorted bulk RORα-deficient ILC3s revealed downregulation of several key ILC3 signature transcripts and increased expression in the majority of "ex-RORγt" ILC3-defining transcripts previously reported (*156*). These observations may suggest that RORα is required for the preservation of the ILC3 lineage and that deletion of RORα results in

enhanced instability of this lineage and differentiation towards an ILC1-like phenotype. Similarly, $CD4^+$ Th cells lacking RORα have increased *Tbx21* transcript levels suggesting that RORα may play a role in repressing a Th1 program (*96*). Additional experiments would be necessary to test this hypothesis such as comparing the behaviour of WT and RORα-deficient ILC3s in response to Th1 or ILC1 inducing pathogens like influenza or in anti-tumor immunity. Although bulk cell whole transcriptome analysis is informative, recently described single-cell RNA sequencing (scRNA-seq) indicate that there is immense heterogeneity within each ILC subset. For instance, the scRNA-seq analyses of human tonsil ILC3s have revealed 3 distinct subsets including an effector NCR^+ ILC3, L-$selectin^+$ naïve-like ILC3, and an HLA^+ antigen-presenting ILC3 (*210*). In the small intestine of mice, five subsets of ILC3s (denoted as ILC3a-e) were identified by scRNA-seq (*211*). Although all ILC3 subgroups expressed comparable levels of *Rorc*, *Il22* expression was restricted to subgroup ILC3c (*211*). In contrast, the ILC3a subset expressed high levels of *Il17a*, *Ltb*, and *Ccr6* and was disproportionately affected by perturbations in the microbiota (*211*). Therefore, specific subsets of ILC3s may have contrasting pathogenic or protective functions in intestinal inflammation. The examination RORα-deficient ILC3s by scRNA-seq would therefore provide greater insight into the precise ILC3 lineage perturbations.

While we have shown an effect of RORα in mediating ILC3 cytokine production, it is not clear whether these RORα-deficient ILC3s possess additional deficiencies that alter their ability to interact with adaptive immune cells or other accessory cells during intestinal inflammation. ILC3s are known to express MHCII or co-stimulatory molecules enabling them to activate $CD4^+$ Th cells or mediate negative selection of commensal

bacteria-specific T cells (*21, 212*). Moreover, ILC3-derived GM-CSF can instruct DCs to promote intestinal homeostasis (*213*). The relevance of RORα in these ILC3-mediated cellular interactions as it relates to intestinal fibrosis is unknown. However, the analysis of competent T cells and DCs in ILC3-specific RORα null mice during infection may provide important insights into these questions. In addition, $CD1d^{+}$ ILC3s can present lipid antigens and activate iNKT cells; this engagement can in turn promote IL-22 production by ILC3s (*214*). Further experiments would be necessary to test whether these lipid antigen-dependent interactions are altered in RORα-deficient ILCs and to determine its impact on chronic inflammatory responses.

Numerous studies have implicated ILC3s in inflammation-driven pathologies including those associated with IBD and our own recent observations highlighting the importance of these cells in intestinal fibrosis: a severe and largely untreatable complication in a subset of Crohn's disease patients. Modulation of ILC3s to suppress pro-inflammatory responses is an attractive therapeutic strategy for the treatment of IBD. A major challenge in this approach may be the deleterious effects of depleting a major source of IL-22, which may serve critical functions in tissue protection. However, our findings suggest that selective inhibition of RORα may be beneficial in IBD-associated fibrosis and potentially other related autoimmune disorders. The comparison of RORα- or ILC3-deficient animals in alternate models of intestinal fibrosis such as chronic TNBS exposure would provide further justification for exploring the therapeutic potential of targeting RORα.

Our analysis of bulk $Rora^{sg/sg}$ ILC3s by flow cytometry indicate a profound defect in IL-17A production while IL-22 suppression was comparatively mild. Moreover,

when comparing host versus donor chimerism of all IL-17$^+$ inflammatory cells, there was a substantial increase in the contribution of endogenous radioresistant IL-17A$^+$ cells in *Salmonella* infected *Rora*$^{sg/sg}$ BMT mice. Meanwhile, IL-22 chimerism remained mostly unchanged in *Rora*$^{sg/sg}$ BMT mice when compared with WT controls possibly due to compensatory IL-22 producing cell types such as CD4$^+$ T cells or other myeloid cells. This suggests that RORα predominantly affects IL-17A expression while influencing IL-22 production to a lesser extent. Given the contrasting roles of IL-17A in driving fibrosis and the protective effects of IL-22 in epithelial barrier maintenance following chronic *Salmonella* infection, RORα may be disproportionately required for the maintenance of the pathogenic rather than the protective hematopoetic subsets.

Our work demonstrates that RORα functions as a key regulator of the expression of cytokine and chemokine receptor genes that modulate the ability of ILC3s to sense their inflammatory milieu and respond by activating downstream inflammatory cytokines including IL-17. However, the precise mechanisms of RORα-dependent gene regulation in ILC3s remains an open question and may provide important insights into the design of novel treatment strategies for inflammatory disorders. Recently, the potential therapeutic value of RORγt suppression in IBD was investigated in multiple mouse models; the pharmacological inhibition of Rorγt with compound GSK805 (or its inducible genetic deletion) can reduce the pathological features of colitis by attenuating pathogenic Th17 responses without altering ILC3 behaviour (*164*). This report revealed divergent requirements of Rorγt in the preservation of Th17 cells and ILC3s, suggesting that there are compensatory mechanisms in ILC3s that conserves their function after Rorγt ablation. Interestingly, RORα-specific binding motifs were found to be preferentially enriched in

RORE associated with pathological Th17 cell signature genes in addition to those targeted by drug-mediated RORγt suppression (*97*). This indicates that regulatory regions containing RORα binding motifs may be more pertinent to Th17 cell differentiation as it relates to disease states. Moreover, a similar RORE consensus sequence was highly enriched in the enhancer regions of ILC3s signature genes arguing that parallel ROR-mediated regulatory programs may exist within Th17 cells and ILC3s (*211*). Therefore, additional genome wide analyses would enhance our understating of downstream gene regulation of RORα inhibition during ILC3 modulation in immune-related diseases.

Bibliography

1. R. Medzhitov, Toll-like receptors and innate immunity. *Nat Rev Immunol* **1**, 135-145 (2001).

2. B. Beutler, Innate immunity: an overview. *Mol Immunol* **40**, 845-859 (2004).

3. M. A. Oettinger, D. G. Schatz, C. Gorka, D. Baltimore, RAG-1 and RAG-2, adjacent genes that synergistically activate V(D)J recombination. *Science* **248**, 1517-1523 (1990).

4. R. N. Germain, MHC-dependent antigen processing and peptide presentation: providing ligands for T lymphocyte activation. *Cell* **76**, 287-299 (1994).
5. J. Zhu, H. Yamane, W. E. Paul, Differentiation of effector CD4 T cell populations (*). *Annu Rev Immunol* **28**, 445-489 (2010).

6. T. W. LeBien, T. F. Tedder, B lymphocytes: how they develop and function. *Blood* **112**, 1570-1580 (2008).

7. G. Eberl, M. Colonna, J. P. Di Santo, A. N. McKenzie, Innate lymphoid cells. Innate lymphoid cells: a new paradigm in immunology. *Science* **348**, aaa6566 (2015).

8. X. Fan, A. Y. Rudensky, Hallmarks of Tissue-Resident Lymphocytes. *Cell* **164**, 1198-1211 (2016).

9. G. Gasteiger, X. Fan, S. Dikiy, S. Y. Lee, A. Y. Rudensky, Tissue residency of innate lymphoid cells in lymphoid and nonlymphoid organs. *Science* **350**, 981-985 (2015).

10. E. G. Perdiguero, F. Geissmann, The development and maintenance of resident macrophages. *Nat Immunol* **17**, 2-8 (2016).

11. C. Schulz, E. Gomez Perdiguero, L. Chorro, H. Szabo-Rogers, N. Cagnard, K. Kierdorf, M. Prinz, B. Wu, S. E. Jacobsen, J. W. Pollard, J. Frampton, K. J. Liu, F. Geissmann, A lineage of myeloid cells independent of Myb and hematopoietic stem cells. *Science* **336**, 86-90 (2012).

12. L. V. Hooper, Epithelial cell contributions to intestinal immunity. *Adv Immunol* **126**, 129-172 (2015).

13. M. Rescigno, M. Urbano, B. Valzasina, M. Francolini, G. Rotta, R. Bonasio, F. Granucci, J. P. Kraehenbuhl, P. Ricciardi-Castagnoli, Dendritic cells express tight junction proteins and penetrate gut epithelial monolayers to sample bacteria. *Nat Immunol* **2**, 361-367 (2001).

14. J. L. Coombes, F. Powrie, Dendritic cells in intestinal immune regulation. *Nat Rev Immunol* **8**, 435-446 (2008).

15. C. M. Sun, J. A. Hall, R. B. Blank, N. Bouladoux, M. Oukka, J. R. Mora, Y. Belkaid, Small intestine lamina propria dendritic cells promote de novo generation of Foxp3 T reg cells via retinoic acid. *J Exp Med* **204**, 1775-1785 (2007).

16. M. Kamanaka, S. T. Kim, Y. Y. Wan, F. S. Sutterwala, M. Lara-Tejero, J. E. Galan, E. Harhaj, R. A. Flavell, Expression of interleukin-10 in intestinal lymphocytes detected by an interleukin-10 reporter knockin tiger mouse. *Immunity* **25**, 941-952 (2006).

17. C. L. Maynard, C. T. Weaver, Intestinal effector T cells in health and disease. *Immunity* **31**, 389-400 (2009).

18. A. J. Macpherson, E. Slack, The functional interactions of commensal bacteria with intestinal secretory IgA. *Curr Opin Gastroenterol* **23**, 673-678 (2007).

19. G. Gasteiger, A. Y. Rudensky, Interactions between innate and adaptive lymphocytes. *Nat Rev Immunol* **14**, 631-639 (2014).

20. G. F. Sonnenberg, D. Artis, Innate lymphoid cells in the initiation, regulation and resolution of inflammation. *Nat. Med.* **21**, 698-708 (2015).

21. M. R. Hepworth, T. C. Fung, S. H. Masur, J. R. Kelsen, F. M. McConnell, J. Dubrot, D. R. Withers, S. Hugues, M. A. Farrar, W. Reith, G. Eberl, R. N. Baldassano, T. M. Laufer, C. O. Elson, G. F. Sonnenberg, Immune tolerance. Group 3 innate lymphoid cells mediate intestinal selection of commensal bacteria-specific CD4(+) T cells. *Science* **348**, 1031-1035 (2015).

22. T. Y. Halim, Y. Y. Hwang, S. T. Scanlon, H. Zaghouani, N. Garbi, P. G. Fallon, A. N. McKenzie, Group 2 innate lymphoid cells license dendritic cells to potentiate memory TH2 cell responses. *Nat Immunol* **17**, 57-64 (2016).

23. M. G. Constantinides, H. Gudjonson, B. D. McDonald, I. E. Ishizuka, P. A. Verhoef, A. R. Dinner, A. Bendelac, PLZF expression maps the early stages of ILC1 lineage development. *Proceedings of the National Academy of Sciences of the United States of America* **112**, 5123-5128 (2015).

24. M. Cherrier, S. Sawa, G. Eberl, Notch, Id2, and RORgammat sequentially orchestrate the fetal development of lymphoid tissue inducer cells. *The Journal of experimental medicine* **209**, 729-740 (2012).

25. C. Seillet, L. C. Rankin, J. R. Groom, L. A. Mielke, J. Tellier, M. Chopin, N. D. Huntington, G. T. Belz, S. Carotta, Nfil3 is required for the development of all

innate lymphoid cell subsets. *The Journal of experimental medicine* **211**, 1733-1740 (2014).

26. R. Yagi, C. Zhong, D. L. Northrup, F. Yu, N. Bouladoux, S. Spencer, G. Hu, L. Barron, S. Sharma, T. Nakayama, Y. Belkaid, K. Zhao, J. Zhu, The transcription factor GATA3 is critical for the development of all IL-7Ralpha-expressing innate lymphoid cells. *Immunity* **40**, 378-388 (2014).

27. M. Moser, K. M. Murphy, Dendritic cell regulation of TH1-TH2 development. *Nat Immunol* **1**, 199-205 (2000).

28. M. Cella, H. Miller, C. Song, Beyond NK cells: the expanding universe of innate lymphoid cells. *Front Immunol* **5**, 282 (2014).

29. W. E. Paul, J. Zhu, How are T(H)2-type immune responses initiated and amplified? *Nat Rev Immunol* **10**, 225-235 (2010).

30. H. Hammad, M. Plantinga, K. Deswarte, P. Pouliot, M. A. Willart, M. Kool, F. Muskens, B. N. Lambrecht, Inflammatory dendritic cells--not basophils--are necessary and sufficient for induction of Th2 immunity to inhaled house dust mite allergen. *The Journal of experimental medicine* **207**, 2097-2111 (2010).

31. T. Korn, E. Bettelli, M. Oukka, V. K. Kuchroo, IL-17 and Th17 Cells. *Annu Rev Immunol* **27**, 485-517 (2009).

32. S. Danese, C. Fiocchi, Ulcerative colitis. *N Engl J Med* **365**, 1713-1725 (2011).
33. D. C. Baumgart, W. J. Sandborn, Crohn's disease. *The Lancet* **380**, 1590-1605 (2012).

34. D. Knights, K. G. Lassen, R. J. Xavier, Advances in inflammatory bowel disease pathogenesis: linking host genetics and the microbiome. *Gut* **62**, 1505-1510 (2013).

35. R. J. Xavier, D. K. Podolsky, Unravelling the pathogenesis of inflammatory bowel disease. *Nature* **448**, 427-434 (2007).

36. J. H. Cho, The genetics and immunopathogenesis of inflammatory bowel disease. *Nat Rev Immunol* **8**, 458-466 (2008).

37. Y. Ogura, D. K. Bonen, N. Inohara, D. L. Nicolae, F. F. Chen, R. Ramos, H. Britton, T. Moran, R. Karaliuskas, R. H. Duerr, J. P. Achkar, S. R. Brant, T. M. Bayless, B. S. Kirschner, S. B. Hanauer, G. Nunez, J. H. Cho, A frameshift mutation in NOD2 associated with susceptibility to Crohn's disease. *Nature* **411**, 603-606 (2001).

38. L. Jostins, S. Ripke, R. K. Weersma, R. H. Duerr, D. P. McGovern, K. Y. Hui, J. C. Lee, L. P. Schumm, Y. Sharma, C. A. Anderson, J. Essers, M. Mitrovic, K. Ning, I. Cleynen, E. Theatre, S. L. Spain, S. Raychaudhuri, P. Goyette, Z. Wei, C. Abraham, J. P. Achkar, T. Ahmad, L. Amininejad, A. N. Ananthakrishnan, V. Andersen, J. M. Andrews, L. Baidoo, T. Balschun, P. A. Bampton, A. Bitton, G. Boucher, S. Brand, C. Buning, A. Cohain, S. Cichon, M. D'Amato, D. De Jong, K. L. Devaney, M. Dubinsky, C. Edwards, D. Ellinghaus, L. R. Ferguson, D. Franchimont, K. Fransen, R. Gearry, M. Georges, C. Gieger, J. Glas, T. Haritunians, A. Hart, C. Hawkey, M. Hedl, X. Hu, T. H. Karlsen, L. Kupcinskas, S. Kugathasan, A. Latiano, D. Laukens, I. C. Lawrance, C. W. Lees, E. Louis, G. Mahy, J. Mansfield, A. R. Morgan, C. Mowat, W. Newman, O. Palmieri, C. Y. Ponsioen, U. Potocnik, N. J. Prescott, M. Regueiro, J. I. Rotter, R. K. Russell, J. D. Sanderson, M. Sans, J. Satsangi, S. Schreiber, L. A. Simms, J. Sventoraityte, S. R. Targan, K. D. Taylor, M. Tremelling, H. W. Verspaget, M. De Vos, C. Wijmenga, D. C. Wilson, J. Winkelmann, R. J. Xavier, S. Zeissig, B. Zhang, C. K. Zhang, H. Zhao, I. B. D. G. C. International, M. S. Silverberg, V. Annese, H. Hakonarson, S. R. Brant, G. Radford-Smith, C. G. Mathew, J. D. Rioux, E. E. Schadt, M. J. Daly, A. Franke, M. Parkes, S. Vermeire, J. C. Barrett, J. H. Cho, Host-microbe interactions have shaped the genetic architecture of inflammatory bowel disease. *Nature* **491**, 119-124 (2012).

39. M. A. Rivas, M. Beaudoin, A. Gardet, C. Stevens, Y. Sharma, C. K. Zhang, G. Boucher, S. Ripke, D. Ellinghaus, N. Burtt, T. Fennell, A. Kirby, A. Latiano, P. Goyette, T. Green, J. Halfvarson, T. Haritunians, J. M. Korn, F. Kuruvilla, C. Lagace, B. Neale, K. S. Lo, P. Schumm, L. Torkvist, D. National Institute of, C. Digestive Kidney Diseases Inflammatory Bowel Disease Genetics, C. United Kingdom Inflammatory Bowel Disease Genetics, C. International Inflammatory Bowel Disease Genetics, M. C. Dubinsky, S. R. Brant, M. S. Silverberg, R. H. Duerr, D. Altshuler, S. Gabriel, G. Lettre, A. Franke, M. D'Amato, D. P. McGovern, J. H. Cho, J. D. Rioux, R. J. Xavier, M. J. Daly, Deep resequencing of GWAS loci identifies independent rare variants associated with inflammatory bowel disease. *Nat Genet* **43**, 1066-1073 (2011).

40. J. D. Rioux, R. J. Xavier, K. D. Taylor, M. S. Silverberg, P. Goyette, A. Huett, T. Green, P. Kuballa, M. M. Barmada, L. W. Datta, Y. Y. Shugart, A. M. Griffiths, S. R. Targan, A. F. Ippoliti, E. J. Bernard, L. Mei, D. L. Nicolae, M. Regueiro, L. P. Schumm, A. H. Steinhart, J. I. Rotter, R. H. Duerr, J. H. Cho, M. J. Daly, S. R. Brant, Genome-wide association study identifies new susceptibility loci for Crohn disease and implicates autophagy in disease pathogenesis. *Nat Genet* **39**, 596-604 (2007).

41. H. H. Uhlig, F. Powrie, Mouse models of intestinal inflammation as tools to understand the pathogenesis of inflammatory bowel disease. *Eur J Immunol* **39**, 2021-2026 (2009).

42. S. Nell, S. Suerbaum, C. Josenhans, The impact of the microbiota on the pathogenesis of IBD: lessons from mouse infection models. *Nat Rev Microbiol* **8**, 564-577 (2010).

43. J. B. Pucilowska, K. L. Williams, P. K. Lund, Fibrogenesis. IV. Fibrosis and inflammatory bowel disease: cellular mediators and animal models. *Am J Physiol Gastrointest Liver Physiol* **279**, G653-659 (2000).

44. S. Wirtz, C. Neufert, B. Weigmann, M. F. Neurath, Chemically induced mouse models of intestinal inflammation. *Nat Protoc* **2**, 541-546 (2007).

45. K. Suzuki, X. Sun, M. Nagata, T. Kawase, H. Yamaguchi, V. Sukumaran, Y. Kawauchi, H. Kawachi, T. Nishino, K. Watanabe, H. Yoneyama, H. Asakura, Analysis of intestinal fibrosis in chronic colitis in mice induced by dextran sulfate sodium. *Pathol Int* **61**, 228-238 (2011).

46. S. Fichtner-Feigl, I. J. Fuss, C. A. Young, T. Watanabe, E. K. Geissler, H. J. Schlitt, A. Kitani, W. Strober, Induction of IL-13 Triggers TGF- 1-Dependent Tissue Fibrosis in Chronic 2,4,6-Trinitrobenzene Sulfonic Acid Colitis. *The Journal of Immunology* **178**, 5859-5870 (2007).

47. B. A. Vallance, W. Deng, K. Jacobson, B. B. Finlay, Host susceptibility to the attaching and effacing bacterial pathogen Citrobacter rodentium. *Infect Immun* **71**, 3443-3453 (2003).

48. C. Song, J. S. Lee, S. Gilfillan, M. L. Robinette, R. D. Newberry, T. S. Stappenbeck, M. Mack, M. Cella, M. Colonna, Unique and redundant functions of NKp46+ ILC3s in models of intestinal inflammation. *The Journal of experimental medicine* **212**, 1869-1882 (2015).

49. M. Barthel, S. Hapfelmeier, L. Quintanilla-Martinez, M. Kremer, M. Rohde, M. Hogardt, K. Pfeffer, H. Russmann, W. D. Hardt, Pretreatment of mice with streptomycin provides a Salmonella enterica serovar Typhimurium colitis model that allows analysis of both pathogen and host. *Infect Immun* **71**, 2839-2858 (2003).

50. Y. Valdez, G. A. Grassl, J. A. Guttman, B. Coburn, P. Gros, B. A. Vallance, B. B. Finlay, Nramp1 drives an accelerated inflammatory response during Salmonella-induced colitis in mice. *Cellular microbiology* **11**, 351-362 (2009).

51. G. A. Grassl, Y. Valdez, K. Bergstrom, B. A. Vallance, B. B. Finlay, Chronic Enteric Salmonella Infection in Mice Leads to Severe and Persistent Intestinal Fibrosis. *Gastroenterol*. **134**, 768-780 (2008).

52. Y. Valdez, R. B. Ferreira, B. B. Finlay, Molecular mechanisms of Salmonella virulence and host resistance. *Curr Top Microbiol Immunol* **337**, 93-127 (2009).

53. C. S. Klose, E. A. Kiss, V. Schwierzeck, K. Ebert, T. Hoyler, Y. d'Hargues, N. Goppert, A. L. Croxford, A. Waisman, Y. Tanriver, A. Diefenbach, A T-bet gradient controls the fate and function of CCR6-RORgammat+ innate lymphoid cells. *Nature* **494**, 261-265 (2013).

54. C. L. Small, S. A. Reid-Yu, J. B. McPhee, B. K. Coombes, Persistent infection with Crohn's disease-associated adherent-invasive Escherichia coli leads to chronic inflammation and intestinal fibrosis. *Nat Commun* **4**, 1957 (2013).

55. S. Buonocore, P. P. Ahern, H. H. Uhlig, I. I. Ivanov, D. R. Littman, K. J. Maloy, F. Powrie, Innate lymphoid cells drive interleukin-23-dependent innate intestinal pathology. *Nature* **464**, 1371-1375 (2010).

56. M. C. Kullberg, J. M. Ward, P. L. Gorelick, P. Caspar, S. Hieny, A. Cheever, D. Jankovic, A. Sher, Helicobacter hepaticus triggers colitis in specific-pathogen-free interleukin-10 (IL-10)-deficient mice through an IL-12- and gamma interferon-dependent mechanism. *Infect Immun* **66**, 5157-5166 (1998).

57. S. Kirchberger, D. J. Royston, O. Boulard, E. Thornton, F. Franchini, R. L. Szabady, O. Harrison, F. Powrie, Innate lymphoid cells sustain colon cancer through production of interleukin-22 in a mouse model. *J. Exp. Med.* **210**, 917-931 (2013).

58. M. W. Leach, A. G. Bean, S. Mauze, R. L. Coffman, F. Powrie, Inflammatory bowel disease in C.B-17 scid mice reconstituted with the CD45RBhigh subset of CD4+ T cells. *The American journal of pathology* **148**, 1503-1515 (1996).

59. F. Powrie, R. Correa-Oliveira, S. Mauze, R. L. Coffman, Regulatory interactions between CD45RBhigh and CD45RBlow CD4+ T cells are important for the balance between protective and pathogenic cell-mediated immunity. *The Journal of experimental medicine* **179**, 589-600 (1994).

60. F. Powrie, M. W. Leach, S. Mauze, L. B. Caddle, R. L. Coffman, Phenotypically distinct subsets of CD4+ T cells induce or protect from chronic intestinal inflammation in C. B-17 scid mice. *Int Immunol* **5**, 1461-1471 (1993).

61. H. H. Uhlig, B. S. McKenzie, S. Hue, C. Thompson, B. Joyce-Shaikh, R. Stepankova, N. Robinson, S. Buonocore, H. Tlaskalova-Hogenova, D. J. Cua, F. Powrie, Differential activity of IL-12 and IL-23 in mucosal and systemic innate immune pathology. *Immunity* **25**, 309-318 (2006).

62. R. Kuhn, J. Lohler, D. Rennick, K. Rajewsky, W. Muller, Interleukin-10-deficient mice develop chronic enterocolitis. *Cell* **75**, 263-274 (1993).

63. D. J. Berg, N. Davidson, R. Kuhn, W. Muller, S. Menon, G. Holland, L. Thompson-Snipes, M. W. Leach, D. Rennick, Enterocolitis and colon cancer in

interleukin-10-deficient mice are associated with aberrant cytokine production and CD4(+) TH1-like responses. *The Journal of clinical investigation* **98**, 1010-1020 (1996).

64. R. K. Sellon, S. Tonkonogy, M. Schultz, L. A. Dieleman, W. Grenther, E. Balish, D. M. Rennick, R. B. Sartor, Resident enteric bacteria are necessary for development of spontaneous colitis and immune system activation in interleukin-10-deficient mice. *Infect Immun* **66**, 5224-5231 (1998).

65. B. A. Vallance, M. I. Gunawan, B. Hewlett, P. Bercik, C. Van Kampen, F. Galeazzi, P. J. Sime, J. Gauldie, S. M. Collins, TGF-beta1 gene transfer to the mouse colon leads to intestinal fibrosis. *Am J Physiol Gastrointest Liver Physiol* **289**, G116-128 (2005).

66. G. A. Grassl, B. B. Finlay, Pathogenesis of enteric Salmonella infections. *Curr Opin Gastroenterol* **24**, 22-26 (2008).

67. J. P. Burke, J. J. Mulsow, C. O'Keane, N. G. Docherty, R. W. Watson, P. R. O'Connell, Fibrogenesis in Crohn's disease. *Am J Gastroenterol* **102**, 439-448 (2007).

68. B. L. Hogan, C. E. Barkauskas, H. A. Chapman, J. A. Epstein, R. Jain, C. C. Hsia, L. Niklason, E. Calle, A. Le, S. H. Randell, J. Rock, M. Snitow, M. Krummel, B. R. Stripp, T. Vu, E. S. White, J. A. Whitsett, E. E. Morrisey, Repair and regeneration of the respiratory system: complexity, plasticity, and mechanisms of lung stem cell function. *Cell stem cell* **15**, 123-138 (2014).

69. C. Fiocchi, P. K. Lund, Themes in fibrosis and gastrointestinal inflammation. *Am J Physiol Gastrointest Liver Physiol* **300**, G677-683 (2011).

70. F. Rieder, C. Fiocchi, Intestinal fibrosis in IBD—a dynamic, multifactorial process. *Nat. Rev. Gastroenterol. Hepatol.* **6**, 228-235 (2009).

71. G. Bouguen, L. Peyrin-Biroulet, Surgery for adult Crohn's disease: what is the actual risk? *Gut* **60**, 1178-1181 (2011).

72. T. A. Wynn, Cellular and molecular mechanisms of fibrosis. *J. Pathol.* **214**, 199-210 (2008).

73. E. M. Zeisberg, O. Tarnavski, M. Zeisberg, A. L. Dorfman, J. R. McMullen, E. Gustafsson, A. Chandraker, X. Yuan, W. T. Pu, A. B. Roberts, E. G. Neilson, M. H. Sayegh, S. Izumo, R. Kalluri, Endothelial-to-mesenchymal transition contributes to cardiac fibrosis. *Nature medicine* **13**, 952-961 (2007).

74. F. Bataille, C. Rohrmeier, R. Bates, A. Weber, F. Rieder, J. Brenmoehl, U. Strauch, S. Farkas, A. Furst, F. Hofstadter, J. Scholmerich, H. Herfarth, G.

Rogler, Evidence for a role of epithelial mesenchymal transition during pathogenesis of fistulae in Crohn's disease. *Inflamm Bowel Dis* **14**, 1514-1527 (2008).

75. S. L. Friedman, D. Sheppard, J. S. Duffield, S. Violette, Therapy for fibrotic diseases: nearing the starting line. *Sci Transl Med* **5**, 167sr161 (2013).

76. L. Barron, S. A. Gharib, J. S. Duffield, Lung Pericytes and Resident Fibroblasts: Busy Multitaskers. *The American journal of pathology*, (2016).

77. T. A. Wynn, Cellular and molecular mechanisms of fibrosis. *J Pathol* **214**, 199-210 (2008).

78. T. A. Wynn, T. R. Ramalingam, Mechanisms of fibrosis: therapeutic translation for fibrotic disease. *Nature medicine* **18**, 1028-1040 (2012).

79. M. F. Neurath, Cytokines in inflammatory bowel disease. *Nat Rev Immunol* **14**, 329-342 (2014).

80. P. Biancheri, S. L. Pender, F. Ammoscato, P. Giuffrida, G. Sampietro, S. Ardizzone, A. Ghanbari, R. Curciarello, A. Pasini, G. Monteleone, G. R. Corazza, T. T. Macdonald, A. Di Sabatino, The role of interleukin 17 in Crohn's disease-associated intestinal fibrosis. *Fibrogenesis Tissue Repair* **6**, 13 (2013).

81. T. E. King, Jr., A. Pardo, M. Selman, Idiopathic pulmonary fibrosis. *Lancet* **378**, 1949-1961 (2011).

82. S. R. Duncan, in *Idiopathic Pulmonary Fibrosis: A Comprehensive Clinical Guide,* K. C. Meyer, S. D. Nathan, Eds. (Humana Press, Totowa, NJ, 2014), pp. 123-159.

83. A. Q. Thomas, K. Lane, J. Phillips, 3rd, M. Prince, C. Markin, M. Speer, D. A. Schwartz, R. Gaddipati, A. Marney, J. Johnson, R. Roberts, J. Haines, M. Stahlman, J. E. Loyd, Heterozygosity for a surfactant protein C gene mutation associated with usual interstitial pneumonitis and cellular nonspecific interstitial pneumonitis in one kindred. *American journal of respiratory and critical care medicine* **165**, 1322-1328 (2002).

84. M. A. Seibold, A. L. Wise, M. C. Speer, M. P. Steele, K. K. Brown, J. E. Loyd, T. E. Fingerlin, W. Zhang, G. Gudmundsson, S. D. Groshong, C. M. Evans, S. Garantziotis, K. B. Adler, B. F. Dickey, R. M. du Bois, I. V. Yang, A. Herron, D. Kervitsky, J. L. Talbert, C. Markin, J. Park, A. L. Crews, S. H. Slifer, S. Auerbach, M. G. Roy, J. Lin, C. E. Hennessy, M. I. Schwarz, D. A. Schwartz, A common MUC5B promoter polymorphism and pulmonary fibrosis. *N Engl J Med* **364**, 1503-1512 (2011).

85. B. B. Moore, C. M. Hogaboam, Murine models of pulmonary fibrosis. *American journal of physiology. Lung cellular and molecular physiology* **294**, L152-160 (2008).

86. F. Chua, J. Gauldie, G. J. Laurent, Pulmonary fibrosis: searching for model answers. *American journal of respiratory cell and molecular biology* **33**, 9-13 (2005).

87. J. Gauldie, M. Kolb, Animal models of pulmonary fibrosis: how far from effective reality? *American journal of physiology. Lung cellular and molecular physiology* **294**, L151 (2008).

88. H. Umezawa, M. Ishizuka, K. Maeda, T. Takeuchi, Studies on bleomycin. *Cancer* **20**, 891-895 (1967).

89. J. Usuki, Y. Fukuda, Evolution of three patterns of intra-alveolar fibrosis produced by bleomycin in rats. *Pathol Int* **45**, 552-564 (1995).

90. J. R. Rock, C. E. Barkauskas, M. J. Cronce, Y. Xue, J. R. Harris, J. Liang, P. W. Noble, B. L. Hogan, Multiple stromal populations contribute to pulmonary fibrosis without evidence for epithelial to mesenchymal transition. *Proceedings of the National Academy of Sciences of the United States of America* **108**, E1475-1483 (2011).

91. D. N. Cook, H. S. Kang, A. M. Jetten, Retinoic Acid-Related Orphan Receptors (RORs): Regulatory Functions in Immunity, Development, Circadian Rhythm, and Metabolism. *Nucl Receptor Res* **2**, (2015).

92. Ivanov, II, B. S. McKenzie, L. Zhou, C. E. Tadokoro, A. Lepelley, J. J. Lafaille, D. J. Cua, D. R. Littman, The orphan nuclear receptor RORgammat directs the differentiation program of proinflammatory IL-17+ T helper cells. *Cell* **126**, 1121-1133 (2006).

93. G. Eberl, S. Marmon, M. J. Sunshine, P. D. Rennert, Y. Choi, D. R. Littman, An essential function for the nuclear receptor RORgamma(t) in the generation of fetal lymphoid tissue inducer cells. *Nat Immunol* **5**, 64-73 (2004).

94. C. Luci, A. Reynders, Ivanov, II, C. Cognet, L. Chiche, L. Chasson, J. Hardwigsen, E. Anguiano, J. Banchereau, D. Chaussabel, M. Dalod, D. R. Littman, E. Vivier, E. Tomasello, Influence of the transcription factor RORgammat on the development of NKp46+ cell populations in gut and skin. *Nat. Immunol.* **10**, 75-82 (2009).

95. N. Satoh-Takayama, C. Vosshenrich, S. Lesjean-Pottier, S. Sawa, M. Lochner, F. Rattis, J.-J. Mention, K. Thiam, N. Cerf-Bensussan, O. Mandelboim, G. Eberl, J. P. Santo, Microbial Flora Drives Interleukin 22 Production in Intestinal NKp46+

Cells that Provide Innate Mucosal Immune Defense. *Immunity* **29**, 958-970 (2008).

96. X. O. Yang, B. P. Pappu, R. Nurieva, A. Akimzhanov, H. S. Kang, Y. Chung, L. Ma, B. Shah, A. D. Panopoulos, K. S. Schluns, S. S. Watowich, Q. Tian, A. M. Jetten, C. Dong, T helper 17 lineage differentiation is programmed by orphan nuclear receptors ROR alpha and ROR gamma. *Immunity* **28**, 29-39 (2008).

97. S. Xiao, N. Yosef, J. Yang, Y. Wang, L. Zhou, C. Zhu, C. Wu, E. Baloglu, D. Schmidt, R. Ramesh, M. Lobera, M. S. Sundrud, P. Y. Tsai, Z. Xiang, J. Wang, Y. Xu, X. Lin, K. Kretschmer, P. B. Rahl, R. A. Young, Z. Zhong, D. A. Hafler, A. Regev, S. Ghosh, A. Marson, V. K. Kuchroo, Small-molecule RORgammat antagonists inhibit T helper 17 cell transcriptional network by divergent mechanisms. *Immunity* **40**, 477-489 (2014).

98. J. Du, C. Huang, B. Zhou, S. F. Ziegler, Isoform-specific inhibition of ROR alpha-mediated transcriptional activation by human FOXP3. *Journal of immunology* **180**, 4785-4792 (2008).

99. L. Zhou, J. E. Lopes, M. M. Chong, Ivanov, II, R. Min, G. D. Victora, Y. Shen, J. Du, Y. P. Rubtsov, A. Y. Rudensky, S. F. Ziegler, D. R. Littman, TGF-beta-induced Foxp3 inhibits T(H)17 cell differentiation by antagonizing RORgammat function. *Nature* **453**, 236-240 (2008).

100. C. Ohnmacht, J. H. Park, S. Cording, J. B. Wing, K. Atarashi, Y. Obata, V. Gaboriau-Routhiau, R. Marques, S. Dulauroy, M. Fedoseeva, M. Busslinger, N. Cerf-Bensussan, I. G. Boneca, D. Voehringer, K. Hase, K. Honda, S. Sakaguchi, G. Eberl, The microbiota regulates type 2 immunity through RORgammat(+) T cells. *Science* **349**, 989-993 (2015).

101. S. H. Wong, J. A. Walker, H. E. Jolin, L. F. Drynan, E. Hams, A. Camelo, J. L. Barlow, D. R. Neill, V. Panova, U. Koch, F. Radtke, C. S. Hardman, Y. Y. Hwang, P. G. Fallon, A. N. McKenzie, Transcription factor RORalpha is critical for nuocyte development. *Nat. Immunol.* **13**, 229-236 (2012).

102. T. Halim, A. MacLaren, M. T. Romanish, M. J. Gold, K. M. McNagny, F. Takei, Retinoic-Acid-Receptor-Related Orphan Nuclear Receptor Alpha Is Required for Natural Helper Cell Development and Allergic Inflammation. *Immunity* **37**, 463-474 (2012).

103. D. A. Gold, P. M. Gent, B. A. Hamilton, ROR alpha in genetic control of cerebellum development: 50 staggering years. *Brain Res* **1140**, 19-25 (2007).

104. M. J. Gold, F. Antignano, T. Y. Halim, J. A. Hirota, M. R. Blanchet, C. Zaph, F. Takei, K. M. McNagny, Group 2 innate lymphoid cells facilitate sensitization to

local, but not systemic, TH2-inducing allergen exposures. *The Journal of allergy and clinical immunology* **133**, 1142-1148 (2014).

105. R. H. Duerr, K. D. Taylor, S. R. Brant, J. D. Rioux, M. S. Silverberg, M. J. Daly, A. H. Steinhart, C. Abraham, M. Regueiro, A. Griffiths, T. Dassopoulos, A. Bitton, H. Yang, S. Targan, L. W. Datta, E. O. Kistner, L. P. Schumm, A. T. Lee, P. K. Gregersen, M. M. Barmada, J. I. Rotter, D. L. Nicolae, J. H. Cho, A genome-wide association study identifies IL23R as an inflammatory bowel disease gene. *Science* **314**, 1461-1463 (2006).

106. S. Fujino, A. Andoh, S. Bamba, A. Ogawa, K. Hata, Y. Araki, T. Bamba, Y. Fujiyama, Increased expression of interleukin 17 in inflammatory bowel disease. *Gut* **52**, 65-70 (2003).

107. A. Dige, S. Stoy, T. K. Rasmussen, J. Kelsen, C. L. Hvas, T. D. Sandahl, J. F. Dahlerup, B. Deleuran, J. Agnholt, Increased levels of circulating Th17 cells in quiescent versus active Crohn's disease. *J Crohns Colitis* **7**, 248-255 (2013).

108. A. Geremia, C. V. Arancibia-Cárcamo, M. Fleming, N. Rust, B. Singh, N. J. Mortensen, S. Travis, F. Powrie, IL-23–responsive innate lymphoid cells are increased in inflammatory bowel disease. *J. Exp. Med.* **208**, 1127-1133 (2011).

109. W. J. Sandborn, C. Gasink, L. L. Gao, M. A. Blank, J. Johanns, C. Guzzo, B. E. Sands, S. B. Hanauer, S. Targan, P. Rutgeerts, S. Ghosh, W. J. de Villiers, R. Panaccione, G. Greenberg, S. Schreiber, S. Lichtiger, B. G. Feagan, C. S. Group, Ustekinumab induction and maintenance therapy in refractory Crohn's disease. *N Engl J Med* **367**, 1519-1528 (2012).

110. S. Huber, N. Gagliani, L. A. Zenewicz, F. J. Huber, L. Bosurgi, B. Hu, M. Hedl, W. Zhang, W. O'Connor, Jr., A. J. Murphy, D. M. Valenzuela, G. D. Yancopoulos, C. J. Booth, J. H. Cho, W. Ouyang, C. Abraham, R. A. Flavell, IL-22BP is regulated by the inflammasome and modulates tumorigenesis in the intestine. *Nature* **491**, 259-263 (2012).

111. W. Hueber, D. D. Patel, T. Dryja, A. M. Wright, I. Koroleva, G. Bruin, C. Antoni, Z. Draelos, M. H. Gold, G. Psoriasis Study, P. Durez, P. P. Tak, J. J. Gomez-Reino, G. Rheumatoid Arthritis Study, C. S. Foster, R. Y. Kim, C. M. Samson, N. S. Falk, D. S. Chu, D. Callanan, Q. D. Nguyen, G. Uveitis Study, K. Rose, A. Haider, F. Di Padova, Effects of AIN457, a fully human antibody to interleukin-17A, on psoriasis, rheumatoid arthritis, and uveitis. *Sci Transl Med* **2**, 52ra72 (2010).

112. D. D. Patel, D. M. Lee, F. Kolbinger, C. Antoni, Effect of IL-17A blockade with secukinumab in autoimmune diseases. *Ann Rheum Dis* **72 Suppl 2**, ii116-123 (2013).

113. J. R. Huh, D. R. Littman, Small molecule inhibitors of RORgammat: targeting Th17 cells and other applications. *Eur J Immunol* **42**, 2232-2237 (2012).

114. L. A. Solt, N. Kumar, P. Nuhant, Y. Wang, J. L. Lauer, J. Liu, M. A. Istrate, T. M. Kamenecka, W. R. Roush, D. Vidovic, S. C. Schurer, J. Xu, G. Wagoner, P. D. Drew, P. R. Griffin, T. P. Burris, Suppression of TH17 differentiation and autoimmunity by a synthetic ROR ligand. *Nature* **472**, 491-494 (2011).

115. J. S. Nielsen, K. M. McNagny, Novel functions of the CD34 family. *Journal of cell science* **121**, 3683-3692 (2008).

116. D. S. Krause, M. J. Fackler, C. I. Civin, W. S. May, CD34: structure, biology, and clinical utility. *Blood* **87**, 1-13 (1996).

117. C. S. Trempus, R. J. Morris, C. D. Bortner, G. Cotsarelis, R. S. Faircloth, J. M. Reece, R. W. Tennant, Enrichment for living murine keratinocytes from the hair follicle bulge with the cell surface marker CD34. *The Journal of investigative dermatology* **120**, 501-511 (2003).

118. J. R. Beauchamp, L. Heslop, D. S. Yu, S. Tajbakhsh, R. G. Kelly, A. Wernig, M. E. Buckingham, T. A. Partridge, P. S. Zammit, Expression of CD34 and Myf5 defines the majority of quiescent adult skeletal muscle satellite cells. *The Journal of cell biology* **151**, 1221-1234 (2000).

119. A. Somasiri, J. S. Nielsen, N. Makretsov, M. L. McCoy, L. Prentice, C. B. Gilks, S. K. Chia, K. A. Gelmon, D. B. Kershaw, D. G. Huntsman, K. M. McNagny, C. D. Roskelley, Overexpression of the anti-adhesin podocalyxin is an independent predictor of breast cancer progression. *Cancer Res* **64**, 5068-5073 (2004).

120. K. A. Snyder, M. R. Hughes, B. Hedberg, J. Brandon, D. C. Hernaez, P. Bergqvist, F. Cruz, K. Po, M. L. Graves, M. E. Turvey, J. S. Nielsen, J. A. Wilkins, S. R. McColl, J. S. Babcook, C. D. Roskelley, K. M. McNagny, Podocalyxin enhances breast tumor growth and metastasis and is a target for monoclonal antibody therapy. *Breast Cancer Res* **17**, 46 (2015).

121. J. S. Nielsen, M. L. Graves, S. Chelliah, A. W. Vogl, C. D. Roskelley, K. M. McNagny, The CD34-related molecule podocalyxin is a potent inducer of microvillus formation. *PloS one* **2**, e237 (2007).

122. S. Baumheter, M. S. Singer, W. Henzel, S. Hemmerich, M. Renz, S. D. Rosen, L. A. Lasky, Binding of L-selectin to the vascular sialomucin CD34. *Science* **262**, 436-438 (1993).

123. E. Drew, J. S. Merzaban, W. Seo, H. J. Ziltener, K. M. McNagny, CD34 and CD43 inhibit mast cell adhesion and are required for optimal mast cell reconstitution. *Immunity* **22**, 43-57 (2005).

124. M. R. Blanchet, J. L. Bennett, M. J. Gold, E. Levantini, D. G. Tenen, M. Girard, Y. Cormier, K. M. McNagny, CD34 is required for dendritic cell trafficking and pathology in murine hypersensitivity pneumonitis. *American journal of respiratory and critical care medicine* **184**, 687-698 (2011).

125. M. R. Blanchet, S. Maltby, D. J. Haddon, H. Merkens, L. Zbytnuik, K. M. McNagny, CD34 facilitates the development of allergic asthma. *Blood* **110**, 2005-2012 (2007).

126. S. Maltby, C. Wohlfarth, M. Gold, L. Zbytnuik, M. R. Hughes, K. M. McNagny, CD34 is required for infiltration of eosinophils into the colon and pathology associated with DSS-induced ulcerative colitis. *The American journal of pathology* **177**, 1244-1254 (2010).

127. M. G. Chiaramonte, D. D. Donaldson, A. W. Cheever, T. A. Wynn, An IL-13 inhibitor blocks the development of hepatic fibrosis during a T-helper type 2-dominated inflammatory response. *The Journal of clinical investigation* **104**, 777-785 (1999).

128. R. Medzhitov, D. S. Schneider, M. P. Soares, Disease tolerance as a defense strategy. *Science* **335**, 936-941 (2012).

129. G. Han, H. Zhang, C. H. Xie, Y. F. Zhou, Th2-like immune response in radiation-induced lung fibrosis. *Oncol Rep* **26**, 383-388 (2011).

130. F. Heller, I. J. Fuss, E. E. Nieuwenhuis, R. S. Blumberg, W. Strober, Oxazolone colitis, a Th2 colitis model resembling ulcerative colitis, is mediated by IL-13-producing NK-T cells. *Immunity* **17**, 629-638 (2002).

131. M. H. Oh, S. Y. Oh, J. Yu, A. C. Myers, W. J. Leonard, Y. J. Liu, Z. Zhu, T. Zheng, IL-13 induces skin fibrosis in atopic dermatitis by thymic stromal lymphopoietin. *Journal of immunology* **186**, 7232-7242 (2011).

132. R. Fattouh, M. Jordana, TGF-beta, eosinophils and IL-13 in allergic airway remodeling: a critical appraisal with therapeutic considerations. *Inflamm Allergy Drug Targets* **7**, 224-236 (2008).

133. G. Yang, A. Volk, T. Petley, E. Emmell, J. Giles-Komar, X. Shang, J. Li, A. M. Das, D. Shealy, D. E. Griswold, L. Li, Anti-IL-13 monoclonal antibody inhibits airway hyperresponsiveness, inflammation and airway remodeling. *Cytokine* **28**, 224-232 (2004).

134. L. A. Murray, R. L. Argentieri, F. X. Farrell, M. Bracht, H. Sheng, B. Whitaker, H. Beck, P. Tsui, K. Cochlin, H. L. Evanoff, C. M. Hogaboam, A. M. Das, Hyper-responsiveness of IPF/UIP fibroblasts: interplay between TGFbeta1, IL-13 and CCL2. *Int J Biochem Cell Biol* **40**, 2174-2182 (2008).

135. E. Hams, M. E. Armstrong, J. L. Barlow, S. P. Saunders, C. Schwartz, G. Cooke, R. J. Fahy, T. B. Crotty, N. Hirani, R. J. Flynn, D. Voehringer, A. N. J. McKenzie, S. C. Donnelly, P. G. Fallon, IL-25 and type 2 innate lymphoid cells induce pulmonary fibrosis. *Proc. Natl. Acad. Sci. USA* **111**, 367-372 (2014).

136. J. R. Bailey, P. W. Bland, J. F. Tarlton, I. Peters, M. Moorghen, P. A. Sylvester, C. S. J. Probert, C. V. Whiting, IL-13 Promotes Collagen Accumulation in Crohn's Disease Fibrosis by Down-Regulation of Fibroblast MMP Synthesis: A Role for Innate Lymphoid Cells? *PLoS ONE* **7**, e52332 (2012).

137. C. G. Lee, R. J. Homer, Z. Zhu, S. Lanone, X. Wang, V. Koteliansky, J. M. Shipley, P. Gotwals, P. Noble, Q. Chen, R. M. Senior, J. A. Elias, Interleukin-13 induces tissue fibrosis by selectively stimulating and activating transforming growth factor beta(1). *The Journal of experimental medicine* **194**, 809-821 (2001).

138. M. Kaviratne, M. Hesse, M. Leusink, A. W. Cheever, S. J. Davies, J. H. McKerrow, L. M. Wakefield, J. J. Letterio, T. A. Wynn, IL-13 activates a mechanism of tissue fibrosis that is completely TGF-beta independent. *Journal of immunology* **173**, 4020-4029 (2004).

139. T. R. Ramalingam, J. T. Pesce, F. Sheikh, A. W. Cheever, M. M. Mentink-Kane, M. S. Wilson, S. Stevens, D. M. Valenzuela, A. J. Murphy, G. D. Yancopoulos, J. F. Urban, Jr., R. P. Donnelly, T. A. Wynn, Unique functions of the type II interleukin 4 receptor identified in mice lacking the interleukin 13 receptor alpha1 chain. *Nat Immunol* **9**, 25-33 (2008).

140. M. G. Chiaramonte, M. Mentink-Kane, B. A. Jacobson, A. W. Cheever, M. J. Whitters, M. E. Goad, A. Wong, M. Collins, D. D. Donaldson, M. J. Grusby, T. A. Wynn, Regulation and function of the interleukin 13 receptor alpha 2 during a T helper cell type 2-dominant immune response. *The Journal of experimental medicine* **197**, 687-701 (2003).

141. A. Suzuki, D. P. Andrew, J. A. Gonzalo, M. Fukumoto, J. Spellberg, M. Hashiyama, H. Takimoto, N. Gerwin, I. Webb, G. Molineux, R. Amakawa, Y. Tada, A. Wakeham, J. Brown, I. McNiece, K. Ley, E. C. Butcher, T. Suda, J. C. Gutierrez-Ramos, T. W. Mak, CD34-deficient mice have reduced eosinophil accumulation after allergen exposure and show a novel crossreactive 90-kD protein. *Blood* **87**, 3550-3562 (1996).

142. M. R. Blanchet, M. J. Gold, K. M. McNagny, Mouse models to evaluate the function of genes associated with allergic airway disease. *Curr Opin Allergy Clin Immunol* **12**, 467-474 (2012).

143. P. G. Fallon, E. J. Richardson, G. J. McKenzie, A. N. McKenzie, Schistosome infection of transgenic mice defines distinct and contrasting pathogenic roles for IL-4 and IL-13: IL-13 is a profibrotic agent. *J. Immunol.* **164**, 2585-2591 (2000).

144. S. Fichtner-Feigl, I. J. Fuss, C. A. Young, T. Watanabe, E. K. Geissler, H.-J. J. Schlitt, A. Kitani, W. Strober, Induction of IL-13 triggers TGF-beta1-dependent tissue fibrosis in chronic 2,4,6-trinitrobenzene sulfonic acid colitis. *J. Immunol.* **178**, 5859-5870 (2007).

145. L. A. Monticelli, G. F. Sonnenberg, M. C. Abt, T. Alenghat, C. G. K. Ziegler, T. A. Doering, J. M. Angelosanto, B. J. Laidlaw, C. Y. Yang, T. Sathaliyawala, M. Kubota, D. Turner, J. M. Diamond, A. W. Goldrath, D. L. Farber, R. G. Collman, J. E. Wherry, D. Artis, Innate lymphoid cells promote lung-tissue homeostasis after infection with influenza virus. *Nat. Immunol.* **12**, 1045-1054 (2011).

146. L. A. Monticelli, L. C. Osborne, M. Noti, S. V. Tran, D. M. W. Zaiss, D. Artis, IL-33 promotes an innate immune pathway of intestinal tissue protection dependent on amphiregulin–EGFR interactions. *Proc. Natl. Acad. Sci. USA* **112**, 10762-10767 (2015).

147. A. Gladiator, N. Wangler, K. Trautwein-Weidner, S. LeibundGut-Landmann, Cutting edge: IL-17-secreting innate lymphoid cells are essential for host defense against fungal infection. *J. Immunol.* **190**, 521-525 (2013).

148. P. Aparicio-Domingo, M. Romera-Hernandez, J. J. Karrich, F. Cornelissen, N. Papazian, D. J. Lindenbergh-Kortleve, J. A. Butler, L. Boon, M. C. Coles, J. N. Samsom, T. Cupedo, Type 3 innate lymphoid cells maintain intestinal epithelial stem cells after tissue damage. *J. Exp. Med.* **212**, 1783-1791 (2015).

149. S. Mizuno, Y. Mikami, N. Kamada, T. Handa, A. Hayashi, T. Sato, K. Matsuoka, M. Matano, Y. Ohta, A. Sugita, K. Koganei, R. Sahara, M. Takazoe, T. Hisamatsu, T. Kanai, Cross-talk between RORγt+ innate lymphoid cells and intestinal macrophages induces mucosal IL-22 production in Crohn's disease. *Inflamm. Bowel Dis.* **20**, 1426-1434 (2014).

150. J. C. Masterson, K. E. Capocelli, L. Hosford, K. Biette, E. N. McNamee, E. F. de Zoeten, R. Harris, S. D. Fernando, P. Jedlicka, C. Protheroe, J. J. Lee, G. T. Furuta, Eosinophils and IL-33 Perpetuate Chronic Inflammation and Fibrosis in a Pediatric Population with Stricturing Crohn's Ileitis. *Inflamm. Bowel Dis.* **21**, 2429 (2015).

151. S. L. Sanos, V. L. Bui, A. Mortha, K. Oberle, C. Heners, C. Johner, A. Diefenbach, RORgammat and commensal microflora are required for the differentiation of mucosal interleukin 22-producing NKp46+ cells. *Nat. Immunol.* **10**, 83-91 (2009).

152. S. Sawa, M. Cherrier, M. Lochner, N. Satoh-Takayama, H. J. Fehling, F. Langa, J. P. Di Santo, G. Eberl, Lineage relationship analysis of RORgammat+ innate lymphoid cells. *Science* **330**, 665-669 (2010).

153. M. J. Gold, F. Antignano, T. Halim, J. A. Hirota, M.-R. Blanchet, C. Zaph, F. Takei, K. M. McNagny, Group 2 innate lymphoid cells facilitate sensitization to local, but not systemic, TH2-inducing allergen exposures. *J. Allergy Clin. Immunol.* **133**, 1142-1148 (2014).

154. T. Y. Halim, C. A. Steer, L. Matha, M. J. Gold, I. Martinez-Gonzalez, K. M. McNagny, A. N. McKenzie, F. Takei, Group 2 innate lymphoid cells are critical for the initiation of adaptive T helper 2 cell-mediated allergic lung inflammation. *Immunity* **40**, 425-435 (2014).

155. T. Hoyler, C. Klose, A. Souabni, A. Turqueti-Neves, D. Pfeifer, E. L. Rawlins, D. Voehringer, M. Busslinger, A. Diefenbach, The Transcription Factor GATA-3 Controls Cell Fate and Maintenance of Type 2 Innate Lymphoid Cells. *Immunity* **37**, 634-648 (2012).

156. M. L. Robinette, A. Fuchs, V. S. Cortez, J. S. Lee, Y. Wang, S. K. Durum, S. Gilfillan, M. Colonna, L. Shaw, B. Yu, A. Goldrath, S. Mostafavi, A. Regev, E. Y. Kim, D. F. Dwyer, M. B. Brenner, F. K. Austen, A. Rhoads, D. Moodley, H. Yoshida, D. Mathis, C. Benoist, T. Nabekura, V. Lam, L. L. Lanier, B. Brown, M. Merad, V. Cremasco, S. Turley, P. Monach, M. L. Dustin, Y. Li, S. A. Shinton, R. R. Hardy, T. Shay, Y. Qi, K. Sylvia, J. Kang, K. Fairfax, G. J. Randolph, M. L. Robinette, A. Fuchs, M. Colonna, Transcriptional programs define molecular characteristics of innate lymphoid cell classes and subsets. *Nat. Immunol.* **16**, 306-317 (2015).

157. D. S. J. Allan, C. L. Kirkham, O. A. Aguilar, L. C. Qu, P. Chen, J. H. Fine, P. Serra, G. Awong, J. L. Gommerman, J. C. Zúñiga-Pflücker, J. R. Carlyle, An in vitro model of innate lymphoid cell function and differentiation. *Mucosal Immunology* **8**, 340-351 (2015).

158. C. Vonarbourg, A. Mortha, V. L. Bui, P. P. Hernandez, E. A. Kiss, T. Hoyler, M. Flach, B. Bengsch, R. Thimme, C. Holscher, M. Honig, U. Pannicke, K. Schwarz, C. F. Ware, D. Finke, A. Diefenbach, Regulated expression of nuclear receptor RORgammat confers distinct functional fates to NK cell receptor-expressing RORgammat(+) innate lymphocytes. *Immunity* **33**, 736-751 (2010).

159. L. E. Månsson, M. Montero, M. Zarepour, K. S. Bergstrom, C. Ma, T. Huang, C. Man, G. A. Grassl, B. A. Vallance, MyD88 signaling promotes both mucosal homeostatic and fibrotic responses during Salmonella-induced colitis. *Am. J. Physiol. Gastrointest. Liver Physiol.* **303**, (2012).

160. L. A. Johnson, A. Luke, K. Sauder, D. S. Moons, J. C. Horowitz, P. D. Higgins, Intestinal fibrosis is reduced by early elimination of inflammation in a mouse model of IBD: impact of a "Top-Down" approach to intestinal fibrosis in mice. *Inflamm. Bowel. Dis.* **18**, 460-471 (2012).

161. Y. Imai, K. Yasuda, Y. Sakaguchi, T. Haneda, H. Mizutani, T. Yoshimoto, K. Nakanishi, K. Yamanishi, Skin-specific expression of IL-33 activates group 2 innate lymphoid cells and elicits atopic dermatitis-like inflammation in mice. *Proc. Natl. Acad. Sci. USA.* **110**, 13921-13926 (2013).

162. W. Hueber, B. E. Sands, S. Lewitzky, M. Vandemeulebroecke, W. Reinisch, P. D. Higgins, J. Wehkamp, B. G. Feagan, M. D. Yao, M. Karczewski, J. Karczewski, N. Pezous, S. Bek, G. Bruin, B. Mellgard, C. Berger, M. Londei, A. P. Bertolino, G. Tougas, S. P. Travis, G. Secukinumab in Crohn's Disease Study, Secukinumab, a human anti-IL-17A monoclonal antibody, for moderate to severe Crohn's disease: unexpected results of a randomised, double-blind placebo-controlled trial. *Gut* **61**, 1693-1700 (2012).

163. J. de Wit, M. H. Al-Mossawi, M. H. Huhn, C. V. Arancibia-Carcamo, K. Doig, B. Kendrick, R. Gundle, P. Taylor, T. McClanahan, E. Murphy, H. Zhang, K. Barr, J. R. Miller, X. Hu, T. D. Aicher, R. W. Morgan, G. D. Glick, D. Zaller, C. Correll, F. Powrie, P. Bowness, RORgammat inhibitors suppress TH17 responses in inflammatory arthritis and inflammatory bowel disease. *J. Allergy Clin. Immunol.* **137**, 960-963 (2016).

164. D. R. Withers, M. R. Hepworth, X. Wang, E. C. Mackley, E. E. Halford, E. E. Dutton, C. L. Marriott, V. Brucklacher-Waldert, M. Veldhoen, J. Kelsen, R. N. Baldassano, G. F. Sonnenberg, Transient inhibition of ROR-gammat therapeutically limits intestinal inflammation by reducing TH17 cells and preserving group 3 innate lymphoid cells. *Nat. Med.* **22**, 319-323 (2016).

165. E. Sefik, N. Geva-Zatorsky, S. Oh, L. Konnikova, D. Zemmour, A. M. McGuire, D. Burzyn, A. Ortiz-Lopez, M. Lobera, J. Yang, S. Ghosh, A. Earl, S. B. Snapper, R. Jupp, D. Kasper, D. Mathis, C. Benoist, Individual intestinal symbionts induce a distinct population of RORgamma(+) regulatory T cells. *Science* **349**, 993-997 (2015).

166. E. Ueda, S. Kurebayashi, M. Sakaue, M. Backlund, B. Koller, A. M. Jetten, High incidence of T-cell lymphomas in mice deficient in the retinoid-related orphan receptor RORgamma. *Cancer Res.* **62**, 901-909 (2002).

167. C. Wansleeben, C. E. Barkauskas, J. R. Rock, B. L. Hogan, Stem cells of the adult lung: their development and role in homeostasis, regeneration, and disease. *Wiley interdisciplinary reviews. Developmental biology* **2**, 131-148 (2013).

168. R. J. Berenson, R. G. Andrews, W. I. Bensinger, D. Kalamasz, G. Knitter, C. D. Buckner, I. D. Bernstein, Antigen CD34+ marrow cells engraft lethally irradiated baboons. *The Journal of clinical investigation* **81**, 951-955 (1988).

169. R. J. Berenson, W. I. Bensinger, R. S. Hill, R. G. Andrews, J. Garcia-Lopez, D. F. Kalamasz, B. J. Still, G. Spitzer, C. D. Buckner, I. D. Bernstein, et al.,

Engraftment after infusion of CD34+ marrow cells in patients with breast cancer or neuroblastoma. *Blood* **77**, 1717-1722 (1991).

170. A. Scherberich, N. D. Di Maggio, K. M. McNagny, A familiar stranger: CD34 expression and putative functions in SVF cells of adipose tissue. *World journal of stem cells* **5**, 1-8 (2013).

171. D. O. Traktuev, S. Merfeld-Clauss, J. Li, M. Kolonin, W. Arap, R. Pasqualini, B. H. Johnstone, K. L. March, A population of multipotent CD34-positive adipose stromal cells share pericyte and mesenchymal surface markers, reside in a periendothelial location, and stabilize endothelial networks. *Circulation research* **102**, 77-85 (2008).

172. C. F. Kim, E. L. Jackson, A. E. Woolfenden, S. Lawrence, I. Babar, S. Vogel, D. Crowley, R. T. Bronson, T. Jacks, Identification of bronchioalveolar stem cells in normal lung and lung cancer. *Cell* **121**, 823-835 (2005).

173. S. Yanagi, H. Kishimoto, K. Kawahara, T. Sasaki, M. Sasaki, M. Nishio, N. Yajima, K. Hamada, Y. Horie, H. Kubo, J. A. Whitsett, T. W. Mak, T. Nakano, M. Nakazato, A. Suzuki, Pten controls lung morphogenesis, bronchioalveolar stem cells, and onset of lung adenocarcinomas in mice. *The Journal of clinical investigation* **117**, 2929-2940 (2007).

174. T. Kawasaki, T. Nishiwaki, A. Sekine, R. Nishimura, R. Suda, T. Urushibara, T. Suzuki, S. Takayanagi, J. Terada, S. Sakao, K. Tatsumi, Vascular Repair by Tissue-resident Endothelial Progenitor Cells in Endotoxin-induced Lung Injury. *American journal of respiratory cell and molecular biology*, (2015).

175. E. Drew, H. Merkens, S. Chelliah, R. Doyonnas, K. M. McNagny, CD34 is a specific marker of mature murine mast cells. *Experimental hematology* **30**, 1211-1218 (2002).

176. T. Asahara, T. Murohara, A. Sullivan, M. Silver, R. van der Zee, T. Li, B. Witzenbichler, G. Schatteman, J. M. Isner, Isolation of putative progenitor endothelial cells for angiogenesis. *Science* **275**, 964-967 (1997).

177. K. Chamoto, B. C. Gibney, G. S. Lee, M. Lin, D. Collings-Simpson, R. Voswinckel, M. A. Konerding, A. Tsuda, S. J. Mentzer, CD34+ progenitor to endothelial cell transition in post-pneumonectomy angiogenesis. *American journal of respiratory cell and molecular biology* **46**, 283-289 (2012).

178. G. A. Grassl, M. Faustmann, N. Gill, L. Zbytnuik, H. Merkens, L. So, F. M. Rossi, K. M. McNagny, B. B. Finlay, CD34 mediates intestinal inflammation in Salmonella-infected mice. *Cellular microbiology* **12**, 1562-1575 (2010).

179. I. Y. Adamson, D. H. Bowden, The pathogenesis of bleomycin-induced pulmonary fibrosis in mice. *The American journal of pathology* **77**, 185-197 (1974).

180. J. A. Vanoirbeek, M. Rinaldi, V. De Vooght, S. Haenen, S. Bobic, G. Gayan-Ramirez, P. H. Hoet, E. Verbeken, M. Decramer, B. Nemery, W. Janssens, Noninvasive and invasive pulmonary function in mouse models of obstructive and restrictive respiratory diseases. *American journal of respiratory cell and molecular biology* **42**, 96-104 (2010).

181. D. B. Yap, D. C. Walker, L. M. Prentice, S. McKinney, G. Turashvili, K. Mooslehner-Allen, T. R. de Algara, J. Fee, X. de Tassigny, W. H. Colledge, S. Aparicio, Mll5 is required for normal spermatogenesis. *PloS one* **6**, e27127 (2011).

182. I. Y. Adamson, Drug-induced pulmonary fibrosis. *Environmental health perspectives* **55**, 25-36 (1984).

183. H. Chen, K. Matsumoto, B. L. Brockway, C. R. Rackley, J. Liang, J. H. Lee, D. Jiang, P. W. Noble, S. H. Randell, C. F. Kim, B. R. Stripp, Airway epithelial progenitors are region specific and show differential responses to bleomycin-induced lung injury. *Stem cells* **30**, 1948-1960 (2012).

184. R. M. Teisanu, H. Chen, K. Matsumoto, J. L. McQualter, E. Potts, W. M. Foster, I. Bertoncello, B. R. Stripp, Functional analysis of two distinct bronchiolar progenitors during lung injury and repair. *American journal of respiratory cell and molecular biology* **44**, 794-803 (2011).

185. A. W. Joe, L. Yi, A. Natarajan, F. Le Grand, L. So, J. Wang, M. A. Rudnicki, F. M. Rossi, Muscle injury activates resident fibro/adipogenic progenitors that facilitate myogenesis. *Nature cell biology* **12**, 153-163 (2010).

186. C. E. Barkauskas, M. J. Cronce, C. R. Rackley, E. J. Bowie, D. R. Keene, B. R. Stripp, S. H. Randell, P. W. Noble, B. L. Hogan, Type 2 alveolar cells are stem cells in adult lung. *The Journal of clinical investigation* **123**, 3025-3036 (2013).

187. M. R. Blanchet, M. Gold, S. Maltby, J. Bennett, B. Petri, P. Kubes, D. M. Lee, K. M. McNagny, Loss of CD34 leads to exacerbated autoimmune arthritis through increased vascular permeability. *Journal of immunology* **184**, 1292-1299 (2010).

188. T. A. Wynn, Integrating mechanisms of pulmonary fibrosis. *The Journal of experimental medicine* **208**, 1339-1350 (2011).

189. A. L. Katzenstein, J. L. Myers, Idiopathic pulmonary fibrosis: clinical relevance of pathologic classification. *American journal of respiratory and critical care medicine* **157**, 1301-1315 (1998).

190. D. A. Schwartz, D. S. Van Fossen, C. S. Davis, R. A. Helmers, C. S. Dayton, L. F. Burmeister, G. W. Hunninghake, Determinants of progression in idiopathic pulmonary fibrosis. *American journal of respiratory and critical care medicine* **149**, 444-449 (1994).

191. R. Hallgren, L. Bjermer, R. Lundgren, P. Venge, The eosinophil component of the alveolitis in idiopathic pulmonary fibrosis. Signs of eosinophil activation in the lung are related to impaired lung function. *The American review of respiratory disease* **139**, 373-377 (1989).

192. M. W. Peterson, M. Monick, G. W. Hunninghake, Prognostic role of eosinophils in pulmonary fibrosis. *Chest* **92**, 51-56 (1987).

193. M. Gharaee-Kermani, B. McGarry, N. Lukacs, G. Huffnagle, R. W. Egan, S. H. Phan, The role of IL-5 in bleomycin-induced pulmonary fibrosis. *Journal of leukocyte biology* **64**, 657-666 (1998).

194. F. Huaux, T. Liu, B. McGarry, M. Ullenbruch, Z. Xing, S. H. Phan, Eosinophils and T Lymphocytes Possess Distinct Roles in Bleomycin-Induced Lung Injury and Fibrosis. *The Journal of Immunology* **171**, 5470-5481 (2003).

195. M. Gharaee-Kermani, Y. Nozaki, K. Hatano, S. H. Phan, Lung interleukin-4 gene expression in a murine model of bleomycin-induced pulmonary fibrosis. *Cytokine* **15**, 138-147 (2001).

196. G. F. Sonnenberg, M. G. Nair, T. J. Kirn, C. Zaph, L. A. Fouser, D. Artis, Pathological versus protective functions of IL-22 in airway inflammation are regulated by IL-17A. *J Exp Med* **207**, 1293-1305 (2010).

197. M. S. Wilson, S. K. Madala, T. R. Ramalingam, B. R. Gochuico, I. O. Rosas, A. W. Cheever, T. A. Wynn, Bleomycin and IL-1beta-mediated pulmonary fibrosis is IL-17A dependent. *J Exp Med* **207**, 535-552 (2010).

198. P. A. Kumar, Y. Hu, Y. Yamamoto, N. B. Hoe, T. S. Wei, D. Mu, Y. Sun, L. S. Joo, R. Dagher, E. M. Zielonka, Y. Wang de, B. Lim, V. T. Chow, C. P. Crum, W. Xian, F. McKeon, Distal airway stem cells yield alveoli in vitro and during lung regeneration following H1N1 influenza infection. *Cell* **147**, 525-538 (2011).

199. W. Zuo, T. Zhang, D. Z. Wu, S. P. Guan, A. A. Liew, Y. Yamamoto, X. Wang, S. J. Lim, M. Vincent, M. Lessard, C. P. Crum, W. Xian, F. McKeon, p63(+)Krt5(+) distal airway stem cells are essential for lung regeneration. *Nature* **517**, 616-620 (2015).

200. S. Maltby, S. Freeman, M. J. Gold, J. H. Baker, A. I. Minchinton, M. R. Gold, C. D. Roskelley, K. M. McNagny, Opposing roles for CD34 in B16 melanoma tumor

growth alter early stage vasculature and late stage immune cell infiltration. *PloS one* **6**, e18160 (2011).

201. R. F. Rotundo, T. M. Curtis, M. D. Shah, B. Gao, A. Mastrangelo, S. E. LaFlamme, T. M. Saba, TNF-alpha disruption of lung endothelial integrity: reduced integrin mediated adhesion to fibronectin. *American journal of physiology. Lung cellular and molecular physiology* **282**, L316-329 (2002).

202. L. M. Goddard, M. L. Iruela-Arispe, Cellular and molecular regulation of vascular permeability. *Thrombosis and haemostasis* **109**, 407-415 (2013).

203. B. Strilic, T. Kucera, J. Eglinger, M. R. Hughes, K. M. McNagny, S. Tsukita, E. Dejana, N. Ferrara, E. Lammert, The molecular basis of vascular lumen formation in the developing mouse aorta. *Dev Cell* **17**, 505-515 (2009).

204. M. J. Siemerink, M. R. Hughes, M. G. Dallinga, T. Gora, J. Cait, I. M. Vogels, B. Yetin-Arik, C. J. Van Noorden, I. Klaassen, K. M. McNagny, R. O. Schlingemann, CD34 Promotes Pathological Epi-Retinal Neovascularization in a Mouse Model of Oxygen-Induced Retinopathy. *PloS one* **11**, e0157902 (2016).

205. D. M. Bryant, J. Roignot, A. Datta, A. W. Overeem, M. Kim, W. Yu, X. Peng, D. J. Eastburn, A. J. Ewald, Z. Werb, K. E. Mostov, A molecular switch for the orientation of epithelial cell polarization. *Dev Cell* **31**, 171-187 (2014).

206. E. J. Debruin, M. R. Hughes, C. Sina, A. Liu, J. Cait, Z. Jian, M. Lopez, B. Lo, T. Abraham, K. M. McNagny, Podocalyxin regulates murine lung vascular permeability by altering endothelial cell adhesion. *PloS one* **9**, e108881 (2014).

207. J. L. McQualter, K. Yuen, B. Williams, I. Bertoncello, Evidence of an epithelial stem/progenitor cell hierarchy in the adult mouse lung. *Proceedings of the National Academy of Sciences of the United States of America* **107**, 1414-1419 (2010).

208. R. M. Teisanu, E. Lagasse, J. F. Whitesides, B. R. Stripp, Prospective isolation of bronchiolar stem cells based upon immunophenotypic and autofluorescence characteristics. *Stem cells* **27**, 612-622 (2009).

209. L. A. Alfaro, S. A. Dick, A. L. Siegel, A. S. Anonuevo, K. M. McNagny, L. A. Megeney, D. D. Cornelison, F. M. Rossi, CD34 promotes satellite cell motility and entry into proliferation to facilitate efficient skeletal muscle regeneration. *Stem cells* **29**, 2030-2041 (2011).

210. A. K. Bjorklund, M. Forkel, S. Picelli, V. Konya, J. Theorell, D. Friberg, R. Sandberg, J. Mjosberg, The heterogeneity of human CD127(+) innate lymphoid cells revealed by single-cell RNA sequencing. *Nat Immunol* **17**, 451-460 (2016).

211. M. Gury-BenAri, C. A. Thaiss, N. Serafini, D. R. Winter, A. Giladi, D. Lara-Astiaso, M. Levy, T. M. Salame, A. Weiner, E. David, H. Shapiro, M. Dori-Bachash, M. Pevsner-Fischer, E. Lorenzo-Vivas, H. Keren-Shaul, F. Paul, A. Harmelin, G. Eberl, S. Itzkovitz, A. Tanay, J. P. Di Santo, E. Elinav, I. Amit, The Spectrum and Regulatory Landscape of Intestinal Innate Lymphoid Cells Are Shaped by the Microbiome. *Cell* **166**, 1231-1246 e1213 (2016).

212. N. von Burg, S. Chappaz, A. Baerenwaldt, E. Horvath, S. Bose Dasgupta, D. Ashok, J. Pieters, F. Tacchini-Cottier, A. Rolink, H. Acha-Orbea, D. Finke, Activated group 3 innate lymphoid cells promote T-cell-mediated immune responses. *Proceedings of the National Academy of Sciences of the United States of America* **111**, 12835-12840 (2014).

213. A. Mortha, A. Chudnovskiy, D. Hashimoto, M. Bogunovic, S. P. Spencer, Y. Belkaid, M. Merad, Microbiota-dependent crosstalk between macrophages and ILC3 promotes intestinal homeostasis. *Science* **343**, 1249288 (2014).

214. J. Saez de Guinoa, R. Jimeno, N. Farhadi, P. J. Jervis, L. R. Cox, G. S. Besra, P. Barral, CD1d-mediated activation of group 3 innate lymphoid cells drives IL-22 production. *EMBO Rep* **18**, 39-47 (2017).

Appendices.

Appendix 1. Primer sequences (5'-3') used for transcript detection by quantitative RT-PCR.

Gapdh-fwd	ATTGTCAGCAATGCATCCTG
Gapdh-rev	ATGGACTGTGGTCATGAGCC
Tnfa-fwd	CATCTTCTCAAAATTCGAGTGACAA
Tnfa-rev	TGGGAGTAGACAAGGTACAACCC
Il6-fwd	TAGTCCTTCCTACCCCAATTTCC
Il6-rev	TTGGTCCTTAGCCACTCCTTC
Col1a2-fwd	TGTTGGCCCATCTGGTAAAGA
Col1a2-rev	CAGGGAATCCGATGTTGCC
Tgfb1-fwd	TGACGTCACTGGAGTTGTACGG
Tgfb1-rev	GGTTCATGTCATGGATGGTGC
Epx-fwd	CTCACCCAACACGCTGAAG
Epx-rev	TTTTCTGTGTGTGATTGTAGG CA
Il17a-fwd	TTTAACTCCCTTGGCGCAAAA
Il17a-rev	CTTTCCCTCCGCATTGACAC
Il22-fwd	ATGAGTTTTTCCCTTATGGGGAC
Il22-rev	GCTGGAAGTTGGACACCTCAA
Il5-fwd	GATGAGGCTTCCTGTCCCTACTC
Il5-rev	TCGCCACACTTCTCTTTTTGG
Il13-fwd	CCTGGCTCTTGCTTGCCTT
Il13-rev	GGTCTTGTGTGATGTTGCTCA

Appendix 2. Gating strategy for ILC3 and T cell analysis by flow cytometry. (A) Sorting parameters for ILC2s, ILC3s and T cells restimulated with PMA and ionomycin in the presence of BFA and stained for intracellular IL-17A and IL-22. (B) Negative isotype controls for IL-17A and IL-22 staining in ILCs and CD3e^{+} T cells.

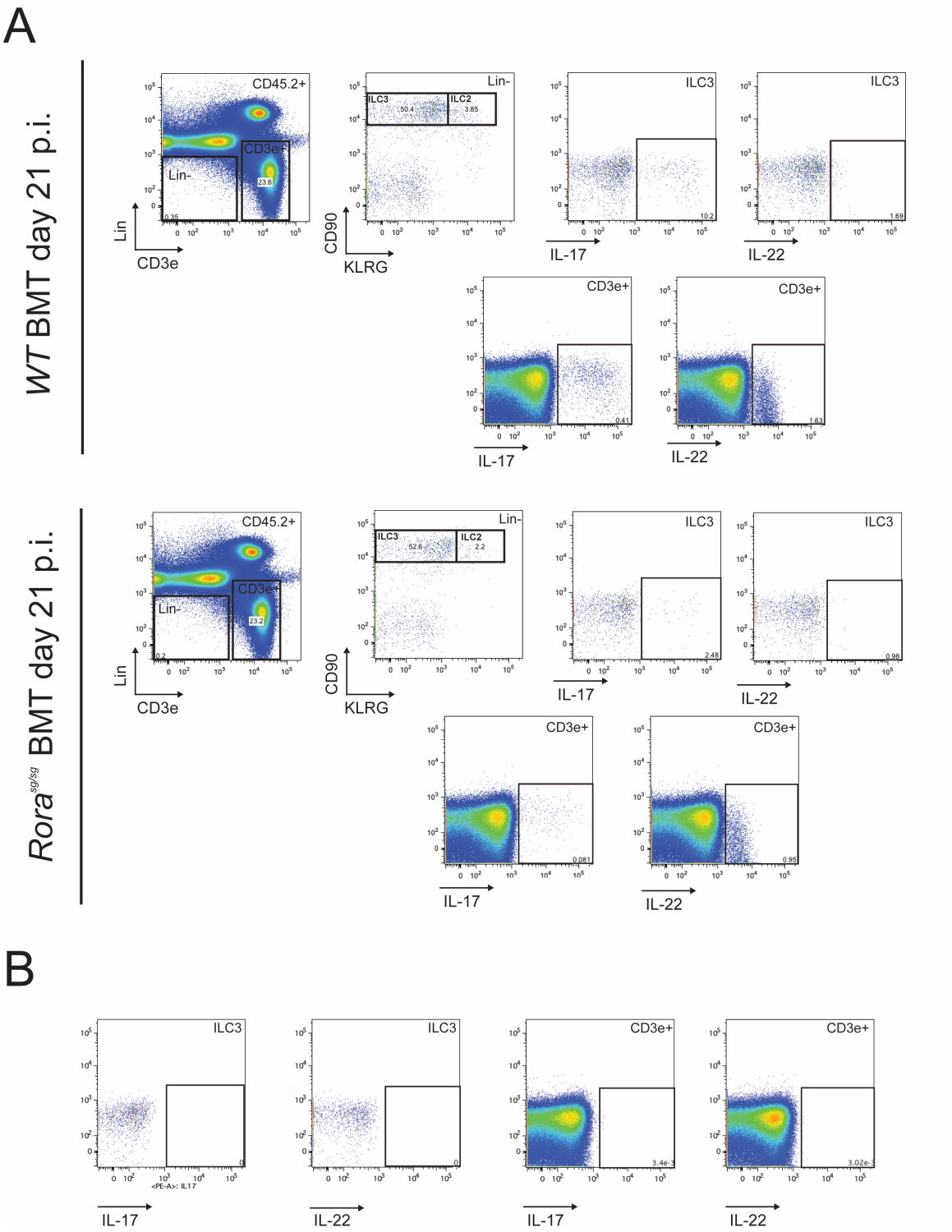

Appendix 3. Fibrotic responses in WT and *Cd34*$^{-/-}$ mice following low dose bleomycin treatment. Mice were treated endotracheally with bleomycin at a dose of 1.25 U/kg and euthanized 18 days post treatment for tissue collection. (A) Quantification of areas displaying fibrotic scarring in lung tissues. (B) Bright field micrographs of Masson's trichrome stained lung sections.

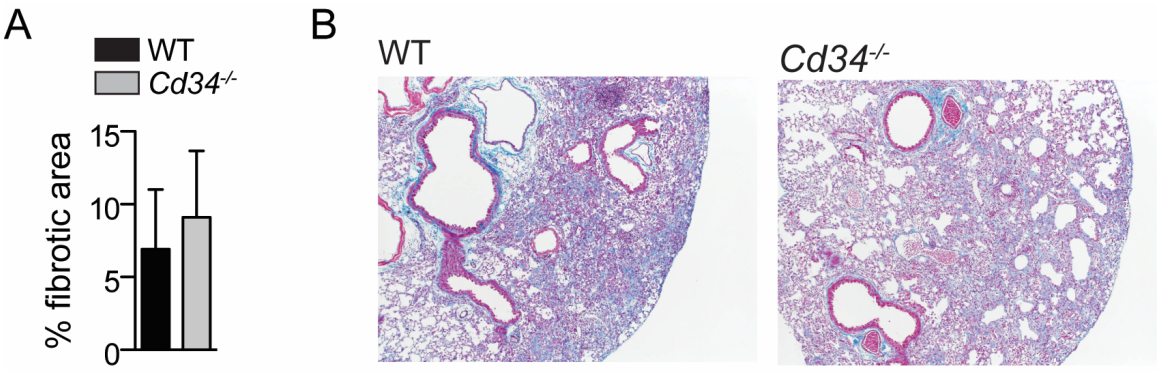

Appendix 4. Ultrastructural analysis of WT and *Cd34*$^{-/-}$ lung specimens by transmission electron microscopy. Representative WT (A-C) and *Cd34*$^{-/-}$ (D-F) lung micrographs are shown. AL, alveolus; EN, endothelial cell; T1, type 1 alveolar epithelial cell (AEC); T2, type 2 AEC; CL, capillary lumen; RBC, erythrocyte.

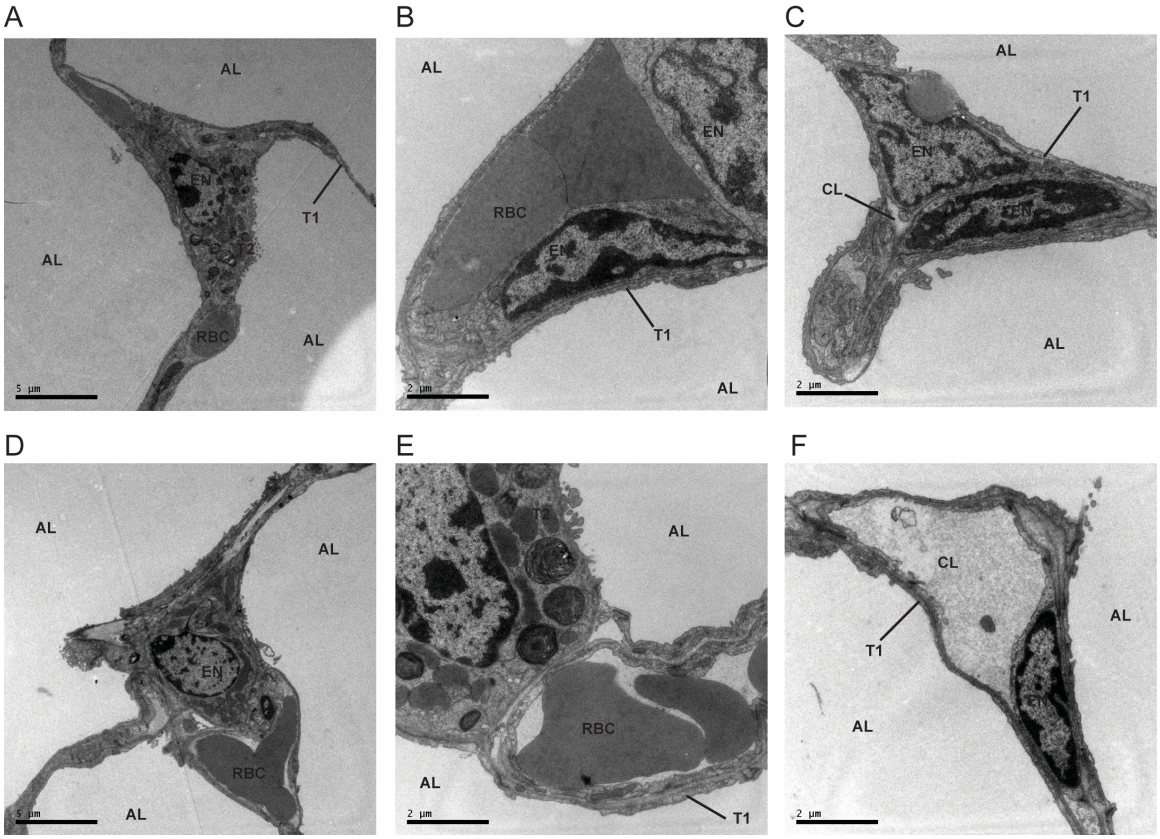

Appendix 5. CD34 expression in naïve mouse lung. CD34 expression was assessed in naïve WT and *Cd34*$^{-/-}$ mouse lung using an anti-CD34 antibody (RAM34, eBiosciences) and visualized by 3,3'-diaminobenzidine (DAB) chromogenic detection and counterstained with hematoxylin (Vector). CD34 expression is detected in cells of the distal airway and blood vessel, but excluded by large airway epithelia and alveolar macrophages.